HARD-HARD AND SOFT-SOFT COORDINATION IN COMPLEXES OF GROUP 6 AND GROUP 10 & 11 METALS RESPECTIVELY

by

ADELÉ LE ROUX

THESIS

submitted in fulfilment of the requirement
for the degree of

MASTERS

in

CHEMISTRY

in the

FACULTY OF SCIENCE

at the

UNIVERSITY OF STELLENBOSCH

SUPERVISOR: DR. R.C. LUCKAY
CO-SUPERVISOR: PROF. H.G. RAUBENHEIMER

MARCH 2008

Declaration

I, the undersigned, hereby declare that the work contained in this thesis is my own original work and that I have not previously in its entirety or in part submitted it at any university for a degree.

Signature: …….

Date: …….

Summary

In this study, the coordination of certain Group 6 and Group 10 & 11 metals to O-donor and S-donor ligands were investigated. For the most part, this involved the isolation of new Mo(VI) and W(VI) complexes. By using a distribution diagram that shows the dependence of the type of species in solution with pH, we attempted to crystallize new polyoxoanion species of the two metals. It was found that the products that crystallize are not necessarily dependant upon the relative concentrations of the species in solution, but rather on the effective packing of the crystal types that are prepared. During this study a unique W(VI) polyanion, $[(CH_3CH_2)_4N]_2[W_6O_{19}]$ (**4**), was isolated. The Mo(VI) analogue of this compound as well as the dinuclear Mo(VI)-W(VI) complex have been reported previously, but a pure W(VI) compound of this type has not been successfully isolated yet. A new polymorph of a known dimolybdate, $K_2Mo_2O_7{\cdot}H_2O$ (**1**), was also crystallized, even though dimolybdate species do not generally occur in solution. This structure, although previously reported, shows some differences with the one in the literature, in particular large deviations in unit cell dimensions. Subsequently, as a second component of this study, a variety of carboxylates were coordinated to Mo(VI) and W(VI) species in an acidic medium. Two new complexes of Mo(VI) with these carboxylate ligands were isolated: $[(CH_3CH_2)_4N][MoO_3(mal)]{\cdot}H_2O$ (**5**) (mal = malate) and $Na_6[Mo_2O_5(cit)_2]$ (**6**) (cit = citrate). The ligands are two- and threefold deprotonated respectively and coordinate in a polydentate manner to the metal centra. The formation of compound **5** in solution has been known for many years, but the structure of this complex has not been determined in the solid state until now. Also, the tungsten analogue of compound **6** was reported years ago, but the Mo(VI) complex has not been crystallized before. Compounds **5** and **6** exhibit a 1:1 and 2:2 metal to ligand ratio respectively, and these ratios are quite rare in Mo(VI) crystal chemistry. Finally, the dimolybdate complex, $[CH_3)_3N(CH_2)_6N(CH_3)_3][Mo_2O_7(cit)]$ (**7**), was isolated, and its structure determined and compared to the one in the literature.

In the third part of this study, our attention shifted to the group 10 and 11 metals, platinum and gold. Attempts were made to coordinate unusual ligands with donor atoms P, Se and/or S to these metal centers. During this investigation, we isolated a unique Pt(IV) complex, $PtCl_2(S_3C_8H_7)_2$ (**9**). The structure of this compound that was determined crystallographically involves the coordination of two identical R-SCS_2 fragments to the metal ion forming four-membered chelate rings. No compounds of Pt and Au with the P-Se ligand, $P_3Se_3(C(C_6H_5)_3)_3$, could be isolated. However, a mixed valence compound of Au(I,III), $[Au(I)Cl(S(CH_2C_6H_5)_2)][Au(III)Cl_3(S(CH_2C_6H_5)_2]$ (**8**), could be isolated and characterized. In this compound Au exhibits two oxidation states, +1 and +3. Although the complex has been reported previously, the structure was not described fully, and we now unequivocally determined its crystal structure. The extended structure shows the formation of chains of alternating Au(I) and Au(III) centers with a separation of 5.610 Å.

Opsomming

In hierdie ondersoek is die koördinasie-chemie van sekere Groep 6 en Groep 10 en 11 metale met onderskeidelik O-donor en S-donor ligande ondersoek. ’n Belangrike deel hiervan het die isolasie en kristallisasie van nuwe Mo(VI) en W(VI) komplekse behels. Deur gebruik te maak van ’n pH-distribusie diagram wat die afhanklikheid van die tipe spesies in oplossing van pH waardes aandui, is gepoog om nuwe polioksi-anioon spesies van hierdie twee metale te kristalliseer. Daar is gevind dat die kristallisasie van die uiteindelike produk in meeste gevalle gedryf word deur effektiewe kristalpakking eerder as deur die relatiewe konsentrasie van die spesies wat in oplossing teenwoordig is. Tydens hierdie ondersoek is een nuwe W(VI) polianioon, $[(CH_3CH_2)_4N]_2[W_6O_{19}]$ (**4**), geisoleer. Die Mo(VI) analoog van hierdie verbinding is reeds bekend, sowel as die dikernige Mo(VI)-W(VI) kompleks, maar tot dusver is ‘n suiwer W(VI) verbinding van hierdie tipe nog nie geïsoleer nie. ‘n Nuwe polimorf van ’n bekende dimolibdaat, $K_2Mo_2O_7{\cdot}H_2O$ (**1**), is ook gekristalliseer, ten spyte van die feit dat dimolibdaat spesies oor die algemeen nie voorkom in oplossing nie. Hierdie verbinding, hoewel reeds gerapporteer, toon verskille met dié in die literatuur, soos byvoorbeeld die groot afwykings in eenheidsel dimensies. Vervolgens, as ’n tweede aspek van die ondersoek, is ’n verskeidenheid karboksilate in suurmedium aan Mo(VI) en W(VI) spesies gekoördineer. Twee nuwe komplekse van Mo(VI) is sodoende geïsoleer: $[(CH_3CH_2)_4N][MoO_3(mal)]{\cdot}H_2O$ (**5**) (mal = malaat oftewel gedeprotoneerde appelsuur) en $Na_6[Mo_2O_5(cit)_2]$ (**6**) (cit = sitraat oftewel gedeprotoneerde sitroensuur). Die ligande is onderskeidelik twee- en drievoudig gedeprotoneer en koördineer op toepaslike polidentate wyse aan die metaalsentra. Die teenwoordigheid van verbinding **5** in oplossing is lank reeds voorspel, maar nog nie as enkelkristalle geïsoleer nie. Die wolfram analoog van verbinding **6** is reeds tevore gerapporteer, maar die Mo(VI) kompleks was nog onbekend in die vaste toestand. Verbinding 5 en 6 toon onderskeidelik die 1:1 en 2:2 verhouding van metaal tot ligand, wat raar is in Mo(VI) kristalchemie. Verder is die bekende Mo(VI) kompleks, $[CH_3)_3N(CH_2)_6N(CH_3)_3][Mo_2O_7(cit)]$ (**7**), gekristalliseer en die struktuur daarvan ondersoek en vergelyk met dié in die literatuur.

In die derde deel van hierdie studie is die aandag toegespits op die groep 10 en 11 metale platinum en goud. Pogings is aangewend om ongewone en unieke ligande wat P, Se en/of S bevat aan die metaalsentra te koördineer. Gedurende hierdie ondersoek is ’n unieke Pt(IV) kompleks, $PtCl_2(S_3C_8H_7)_2$ (**9**), geïsoleer. Die struktuur behels die koördinasie van twee identiese $R\text{-}SCS_2$ fragmente aan die metaalioon en is kristallografies bepaal om die vierlid-chelaatringe wat vorm te toon. Geen verbindings van Pt en Au kon met die heterosikliese P-Se ligand, $P_3Se_3(C(C_6H_5)_3)_3$, geïsoleer word nie. ’n Goudverbinding, $[Au(I)Cl(S(CH_2C_6H_5)_2)][Au(III)Cl_3(S(CH_2C_6H_5)_2]$ (**8**), is gesintetiseer waarin goud in beide die +1 en +3 oksidasietoestande voorkom. Alhoewel hierdie verbinding reeds tevore gerapporteer is, is die kristalstruktuur daarvan onvolledig en swak beskryf. Die ongewone kompleks is derhalwe eenduidig kristallografies gekarakteriseer en toon dat die uitgebreide struktuur saamgestel is uit kettings op ’n afstand van 5.610 Å vanaf mekaar, bestaande uit afwisselende Au(I)- en Au(III)-kerne.

Acknowledgements

Firstly and most importantly I would like to thank my supervisors, Dr. Robbie Luckay and Prof. Helgard Raubenheimer, for their hard work, support and willingness to assist me in writing this thesis, and also Prof. J.J. Cruywagen for all his advice.

Secondly, I want to thank every single person in the Inorganic research group for their help, support and guidance. A special word of thanks to Elzet Stander, Leigh-Anne De Jongh and Christoph Strasser for your friendship and support in the laboratory.

I am also very much in debt to Dr. Jan Gertenbach and Christoph Strasser for their endless patience in helping me solve the crystal structures. I really could not have done this without them.

Finally, I thank the NRF for funding this research.

Different aspects of the work in this thesis have been presented and published in the form of:

- Poster presentations by the author at two South African Chemical Institute (SACI) conferences: in December 2006, Durban, South Africa, entitled “Synthesis, coordination chemistry and structural analysis of Mo, W and Pt complexes”, and in July 2007, Langebaan (Club Mykonos), South Africa, entitled “Synthesis and structural analysis of new Mo, W, Pt and Au complexes”.

CONTENTS

CHAPTER 3

Synthesis and structural study of new Au(I,III) and Pt(IV) complexes

ABBREVIATIONS

Å	Ångstrom (10^{-10} m)
Bu	Butyl
cit	citrate
COD	(1,5)-cyclooctadiene
DMF	*N*,*N*'-dimethylformamide
DMSO	Dimethylsulfoxide
Et	Ethyl
mal	malate
Me	Methyl
NMR	Nuclear Magnetic Resonance
Ph	Phenyl
Pr	Propyl
THF	Tetrahydrofuran
tht	Tetrahydrothiophene
e.s.d.s	Estimated Standard Deviations

The most exciting phrase to hear in science, the one that heralds new discoveries, is not 'Eureka!' but 'That's funny...'

Isaac Asimov

Chapter 1

Introduction

1.1 General introduction

1.1.1 Molybdenum

The solution and solid state chemistry of molybdenum is amongst the most complex of all the transition metals. Not only does it exhibit a variety of oxidation states, but also a wide range of stereochemistries. The main use of molybdenum for many years was in different grades of steel, whereas the oxides and sulphides have found applications as industrial catalysts. In fact, molybdenum is one of the only metals in the second and third transition series that has an important role as a trace metal in enzymes, and several aspects of this metal have been investigated to gain a better understanding of its biological role.[1]

Metallic molybdenum does not react with oxygen or water at room temperature, but at very high temperatures it forms MoO_3 according to the reaction: $2Mo + 3O_2 \rightarrow 2MoO_3$. Molybdenum forms complexes with various organic molecules in any of its oxidation states (-2 to +6), but in solution at pH > 6, the tetrahedral molybdate ion $[MoO_4]^{2-}$ predominates. (Fig. 1.1). Decrease of the pH leads to the formation of other species, which will be explained later.[2]

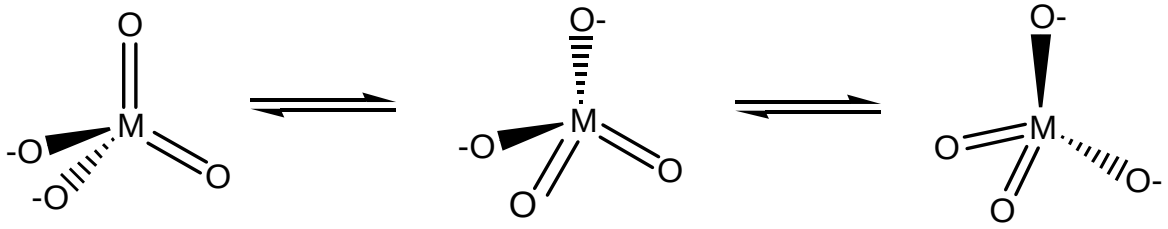

Figure 1.1 Three resonance forms of the molybdate ion, $[MO_4]^{2-}$, with M = Mo.

The molybdates which we are concerned with in this study are the oxoanions of molybdenum in its highest oxidation state of 6. Molybdenum(VI) is known to form a broad range of these oxoanions, of which the larger species belong to the polyoxometalate family.[3] At low molybdate concentration (less than 10^{-4} mol.dm^{-3}), neutral mononuclear species (MoO_2) predominate in solution. At higher acid concentrations, and also at higher ionic strength, molybdenum(VI) shows a tendency to dimerise and form the cationic dimolybdate $[Mo_2O_5]^+$ moiety, which has been isolated in the solid state with a few ligands such as citric and malic acid (Fig. 1.2). These complexes have 2 *cis*-oxygens for each octahedral six-coordinate Mo atom, and a single oxygen bridge between them.[4]

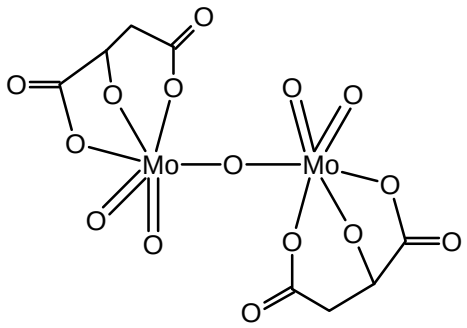

Figure 1.2 The dimeric complex of Mo(VI) with malic acid, $[Mo_2O_5(mal)_2]^{4-}$.

The type of molybdate anion that forms depends on the counter ion which is present during the reaction. Thus a dimolybdate, $[Mo_2O_7^{2-}]$, has been isolated as the tetrabutyl-ammonium salt,[5] a hexamolybdate $[Mo_6O_{19}^{2-}]$ as the tetramethylammonium salt,[6] and a heptamolybdate $[Mo_7O_{24}^{6-}]$ as the ammonium salt,[7] to name but a few. Smaller oxoanions such as $[MoO_4]^{2-}$ and $[Mo_2O_7]^{2-}$ usually contain only four coordinate Mo atoms, with $[MoO_4]^{2-}$ being tetrahedral, whereas the $[Mo_2O_7]^{2-}$ species normally consists of two tetrahedra sharing a corner (a single bridging oxygen atom).[3] On the other hand, the larger oxoanions generally contain six-coordinate molybdenum. In particular the $[Mo_8O_{26}]^{4-}$ unit consists of both octahedral and tetrahedral molybdenum atoms, and has been isolated in three isomeric forms, namely alpha (α), beta (β) and gamma (γ).[4]

The mechanism for the formation of these polyoxoanions is not quite clear, but it is assumed that the process is driven by the tendency of $[MoO_4]^{2-}$ to increase its coordination sphere from four to six. There exists a favorable enthalpy change for this reaction due to the extra bond energy that results from the increase in the coordination number of molybdenum. Therefore the polyanions usually, but not always, consist of MoO_6 octahedra sharing edges and vertices. [4]

1.1.2 Tungsten

Tungsten is a complicated metal to study, not only because of its ability to form complexes with a large number of different coordination numbers and geometries, but also since it has a tendency to form clusters and polynuclear complexes with a variety of metal ions. The most common oxidation state of tungsten is +6, however it has been known to exist in any state from -1 to +6. Since it has such a high melting point, its primary application for many years was as a filament for incandescent lamps. Nowadays the interest has shifted towards alloys containing tungsten, for use in high temperature applications.[8] In aqueous chemistry, tungsten is most often used as the well known tungstate ion, $[WO_4]^{2-}$ (see Fig. 1.1 with M = W). [4]

The solution chemistry of tungsten(VI) is more difficult to investigate than that of molybdenum(VI). The reason for this is firstly that the reactions which occur on acidification are very slow and, secondly, due to the formation of kinetic intermediates. In the same way as molybdenum, tungsten also forms polyoxoanions in both acidic and neutral aqueous solutions. Upon treatment of these tungstate solutions with acid, $[W_7O_{24}]^{6-}$ (better known as paratungstate A) forms. After a few days or even hours, this compound is converted to $[H_2W_{12}O_{42}]^{10-}$ (paratungstate B). Addition of more acid then leads to the formation of the lesser known metatungstate, $[H_2W_{12}O_{40}]^{6-}$ at equilibrium. Paratungstate A and B exist at a pH range between 5 and 8. Notably, up to date no tungsten analogue of the $[Mo_8O_{26}]^{4-}$ complex has been isolated, yet many other polyanions of tungsten have been crystallized. Unlike the molybdenum(VI) and vanadium(V) complexes, which both have metal ions occuring in an “other-than-octahedral” environment of oxygen atoms, all the known structures of tungsten(VI) are

built from WO_6 octahedra. Except for a few of these, all the octahedra share edges so as to form structures which have only single-terminal oxygens. This differs from molybdenum(VI), where most of the polyoxomolybdates have *cis*-dioxo-terminal oxygens. This phenomenon is yet to be explained, but it is suspected that this is the result of the possibly better overlap of the oxygen atoms with the more extended 5d orbitals of tungsten(VI). [4]

1.1.3 Molybdenum and tungsten as polyoxometalates

Polyoxometalates are oligomeric aggregates of metal cations (mostly d^0 species like Mo(VI) and W(VI)) bridged by oxide anions that form through self-assembly processes.[9] They form a unique class of clusters that have unusual structural and electronic properties. In fact, a few of these species possess cavities that may incorporate a range of organic cations. In addition to functioning as structure directing cations or counter ions, these organic molecules can act as ligands forming an important part of the covalent or non-covalent scheme of the solid, or participate in the complex network of hydrogen bonding. Moreover counter ions are believed to direct the self-assembly of the cluster formation.[10]

Two generic families of polyoxometalates exist: the isopoly-compounds that contain only the metal ions and the oxide anions, and the heteropoly-compounds that may contain, in addition to the metal and oxygen atoms, one or more *p*-, *d*-, or *f*-block heteroatoms in its structure. In fact more than half the elements in the periodic table have been known to act as heteroatoms in these compounds.[9]

Polyoxometalates and their derivatives form a family of complexes that combine chemical and structural diversity, with the possibility of extensive modification of their physicochemical properties. Over the last couple of years, the structural chemistry of these compounds have experienced a large growth, which was assisted by the implementation of new synthetic routes.[11] In particular the structure of the isopolyanion, $[Mo_7O_{24}]^{6-}$, is well established, and has been analyzed by X-ray crystallography with different counter ions, most commonly ammonium and some potassium derivatives.

Counter ions play an important role in the isolation of polyoxoanions. In fact, even ions existing in negligible amounts in solution can be precipitated from aqueous solution with the right cations, while other major species remain in solution. Different ions can be isolated at the same pH by adding different cations. Moreover it has been found through extensive research that the careful manipulation of both pH and temperature, as well as the addition of the right counter ion, can result in a great variety of molybdenum and tungsten oxoanion species precipitating and/or crystallizing, even those that were thought not to exist in solution. [4, 11]

1.1.4 Molybdenum and tungsten with carboxylic acids as ligands

Hydroxycarboxylic acids have the ability to act as ligands toward various metals, which is an important property in a variety of fields in chemistry and other sciences. For instance, hydroxy acids are very often used in analytical chemistry as masking agents. Some hydroxy acids show potential in pharmacology, a property that can be directly linked to their ability to coordinate to metal ions. There is also a great increase in the interest in these acids in electroplating baths for improving surface quality and other aspects of this process.[12] Malic acid has the ability to form complexes with metal ions quite easily, and thus has many uses including the prevention of oxidation of vegetable oils, a process which is catalyzed by the presence of trace metals. On the other hand, citric acid has been studied extensively the last couple of decades because of its biological activity, such as the transport of inorganic ions in biofluids and natural waters.[12]

Tungsten and molybdenum are chemically analogous and very similar in most aspects. Intensive research has been carried out previously regarding the complex formation of tungsten and molybdenum with carboxylate and hydroxycarboxylate ligands (Fig. 1.3). The research has focused on the identification and characterization of the various compounds in terms of structure, thermodynamic quantities and stability. However, the study of these complexes was difficult due to the tendency of tungsten(VI) and molybdenum(VI) to form polyoxoanions; still, a better picture of their coordination has emerged.[13]

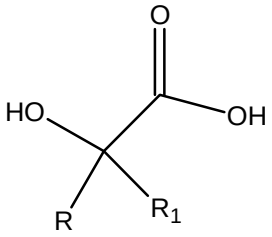

Figure 1.3 Structure of an α-hydroxycarboxylic acid.

It is known that mono-, di- and tetra-nuclear complexes of these acids exist in solution, some in minor amounts, and all protonated to various extents. Until now only a select few of these complexes have been isolated in the solid state and characterized by X-ray diffraction techniques. Typically, α-hydroxycarboxylic acids (Fig. 1.4) tend to form very stable 1:2 complexes with tungsten(VI) and molybdenum(VI), rather than 1:1 and 2:2 complexes. Still, a great variety of tungstate-malate complexes occur between pH 1.5 and 7.5, showing stoichiometries such as 1:1, 1:2, 2:1 and 2:2 respectively. Previous studies regarding the complexation of molybdate with malate have revealed the existence of a number of complexes with this metal in solution. Typical stoichiometries such as 1:1, 1:2 and 2:1 (molybdate to malate ratios) have been proposed, but the stability and composition of most of these complexes remain uncertain. Nonetheless, salts of a few of these complexes have been crystallized and structurally characterized by X-ray analysis. The tungsten complexes with citrate are more stable than the molybdenum complexes, and this difference is mainly caused by the enthalpy change for complexation, which is associated with the greater tendency of tungstate to increase its coordination from 4 to 6.[14,13,15] However, more complexes of molybdenum with citrate are known than with tungsten.[15] The complexes mentioned above will be discussed in greater detail in Chapter 2.

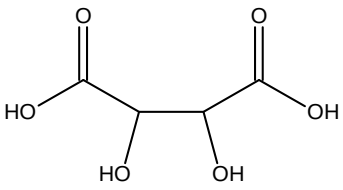

Figure 1.4a Tartaric acid

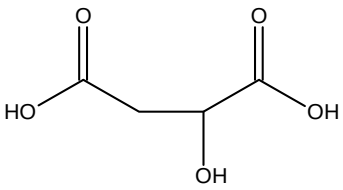

Figure 1.4b Malic acid

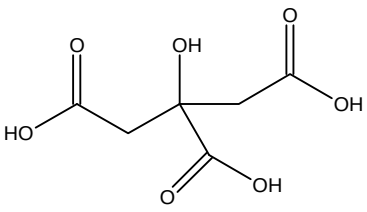

Figure 1.4c Citric acid

1.1.5 Uses and applications of molybdenum and tungsten complexes

The most outstanding quality of molybdenum and tungsten is their chemical versatility, not only the large range of oxidation states and coordination numbers they can exhibit, but also their varied stereochemistry and the ability to form complexes with most organic and inorganic ligands. Its these properties that make the applications and uses of these metals many and varied. For instance, molybdates are often used in paints and corrosion inhibitors as well as flame retardants, and also in agriculture. However one of its most important roles is in catalysis.[16] The reason for this interest is because the polyoxoanions of molybdenum can be considered as analogous to some metal oxide surfaces, which could be useful in catalytic applications. Furthermore, monomeric chelates of W(VI) with diols were also found to be useful in catalysis.[17]

Molybdenum plays an important role in biology as molybdoenzymes.[17] In fact, it forms a necessary part of at least 15 enzymes,[18] for example xanthine oxidase, aldehyde oxidase, nitrate reductase and nitrogenase. A decade ago it was discovered that tungsten competes with molybdenum for the binding site of the molybdoenzymes in living organisms, and it is present in a few microbial enzymes, e.g. the formate hydrogenase from *Clostridium thermoaceticum*. This discovery led to a renewed interest in reactions of tungsten with biological ligands in the field of biochemistry.[19]

What makes molybdenum so suited for its biological function? It has been speculated that it is because of the following qualities: its wide range of oxidation states in aqueous solution, the formation of oxo-compounds and their sulphur analogues, the ability of molybdenum to take part in atom-transfer reactions, and lastly because of the possibility of higher coordination numbers. In some cases, replacing molybdenum with tungsten has shown increased activity, like in the case of formate hydrogenase, as mentioned earlier.[18] Also, when used in combination with β-lactam antibiotics, polyoxotungstates increase the effectiveness of the antibiotics against otherwise resistant strains of bacteria.[9]

Molybdenum and tungsten compounds have been successfully used in the determination of antihistamines, alkaloids, antibiotics and some pharmacologically active substances. Nevertheless the mechanism of the reactions that take place in the above mentioned applications are still far from being completely understood. It is known, however, that a large number of the incompletely defined isopoly- and heteropoly-compounds are formed as a result of the above reactions. Excluding the compounds with simple structures, bioactivities of molybdenum and tungsten can be mostly attributed to their isopoly- and heteropoly-compounds.[2]

In particular, polyoxomolybdates are used as imaging agents for electron microscopy, and as spectroanalytical reagents,[20] as well as electron microscope *stains*, super ionic proton conductors, fuel cells, and more recently as precursors of nanoporous materials.[2] Some molybdenum compounds are also involved in hydro-desulphurization, which is an important process for the purification of petroleum products.[21]

Polyoxometalate complexes of both tungsten and molybdenum have applications in a variety of fields, such as the ones mentioned above. However, there is more to these complicated compounds than meets the eye: they are often used in the field of medicine.[11] More specifically, a number of these compounds have been reported as having the ability to inhibit the replication of several viruses, including HIV, herpes simplex virus, the influenza virus, and respiratory syncytial virus. Polyoxomolybdates in particular show promising potential for the treatment of cancers that are usually difficult to treat. In particular, a heptamolybdate polyanion, $[NH_3Pr^i]_6[Mo_7O_{24}]\cdot 3H_2O$, has been known to exhibit strong antitumour potential, by inhibiting the cell growth of human pancreatic cells.[22]

Certain attributes of polyoxometalates make them very suited for applications in medicine. The feature that is most advantageous would be the fact that almost every molecular property that has an effect on the recognition and reactivity of polyoxometalates with target biological macromolecules can be altered. Such properties include redox potential, shape, acidity, polarity, and surface charge distribution. In

addition to this, rational and reproducible synthetic methods are known to replace one or more of the skeletal early transition metal ions in the structure with *d*- or *p*-block ions. Synthetic routes are also known for the covalent attachment of organic groups to the polyoxometalates by means of linkages that are compatible with physiological conditions. These two modifications to the structure greatly increase the number of polyoxometalates that are potentially available. By incorporating pendant organic and/or biological groups into their structure, the polyoxometalates could be used to modulate bioavailabilities, increase selective binding of important substructures in target biomacromolecules, and also enhance the facility of drug formulation. The one disadvantage of the use of polyoxometalates in medicine is the fact that they are not organic species. To date, low molecular weight organic compounds dominate the pharmaceutical industry, in both drug discovery and synthesis. However, polyoxometalate-based pharmaceuticals are a lot less expensive than their organic counterparts, thus the development of these compounds might have a positive impact on this growing market.[9]

1.1.6 Platinum

Platinum is a precious metal that exists mostly in the +2 and +4 oxidation states in its compounds, although the +1 and +3 states do exist. It has many applications, most of which include catalysis, jewellery and electrical applications. Furthermore, it has shown electrical conductivity and potential as a chemotherapeutic agent. The study of platinum complexes has been pivotal for the development of coordination chemistry. Most research up to date has involved Pt(II) and Pt(IV) complexes.[23]

1.1.7 Platinum in cancer treatment

Most pharmaceutical agents for cancer treatment contain several examples of metal compounds which are currently being used clinically. New areas for the applications of these compounds are emerging fast. Platinum(II) complexes are some of the most widely used metal containing drugs for the treatment of cancer. Up until now, only a few injectable platinum(II) diamine compounds have been approved for clinical use, such as cisplatin (Fig. 1.5a), oxaliplatin (Fig. 1.5b) and carboplatin (Fig. 1.5c).

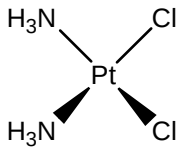

Figure 1.5a Cisplatin

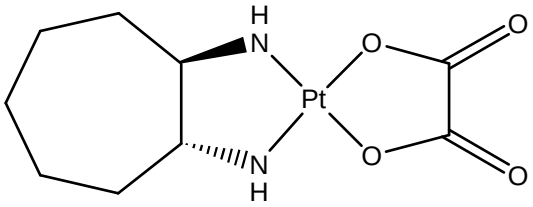

Figure 1.5b Oxaliplatin

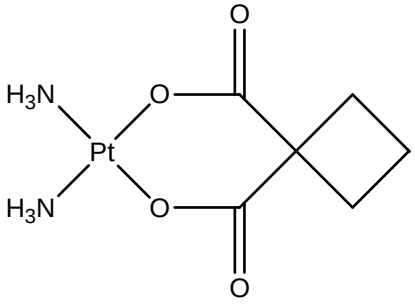

Figure 1.5c Carboplatin

A number of other cis-diamine complexes are currently in clinical trials, but cisplatin is still one of the most effective drugs currently used for the treatment of ovarian, testicular, bladder and cervical cancer. However, even with its high effectiveness, there are still many clinical problems and severe side-effects regarding its use, such as extreme normal tissue toxicity, which causes vomiting and nausea, as well as initial and acquired resistance to the treatment. One of the biggest side effects of cisplatin is its nephrotoxicity, a result from injury to the renal tubular epithelial cells, which may lead to acute renal failure. These adverse effects on the renal function are correlated to platinum binding and the inactivation of thiol-containing enzymes. Huge efforts are constantly being made to reduce the toxicity of these anticancer platinum complexes towards normal cells. Sulphur-containing compounds have been administered as antidotes, with some success.[24]

New Pt(II), Pt(IV) and Pd(II) complexes have been synthesized with the aim of lowering the toxic side effects but still provide anticancer activity. More than 3000 platinum complexes have been tested in the past, both *in vitro* and *in vivo*, but still only a handful of these show any promising results that suggest suitability for clinical trials. A few of these, e.g. carboplatin and oxaliplatin, are well known, but they are less active than

cisplatin and have the same negative side effects. The renal toxicity caused by platinum drugs is the result of the high affinity of Pt(II) for protein-sulphur sites. In the past, dithiocarbamate was used as ligand, coordinating to the platinum by means of 2 sulphur atoms, thereby preventing the reaction of the metal with proteins.[25] It has been reported that dialkyl dithiocarbamates, when administered with cisplatin, reduces its nephrotoxicity.[26] Thus sulphur complexes of platinum is a promising field of inorganic chemistry. Interesting new disulphide ligands such as the ones shown in Figure 1.6a & b, that can be readily prepared as described in Section 3.4.2.5, have not been coordinated with platinum to date.[27]

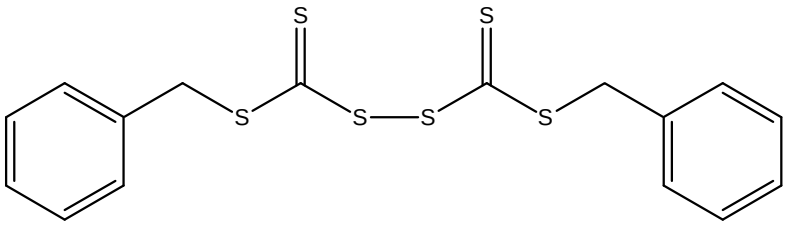

Figure 1.6a Structure of the ligand **I**, $S_6C_{16}H_{14}$.

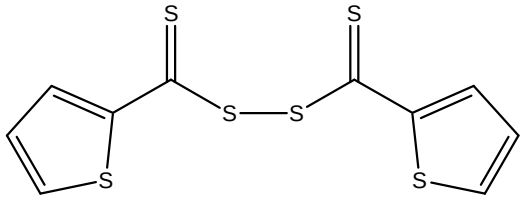

Figure 1.6b Structure of the ligand **II**, $S_6C_{10}H_8$.

Metal sulphides are important because they have applications in geochemistry, analytical and structural chemistry, biochemistry (where they act as electron transfer systems) and also as catalysts in the industry.[28] Thiocarbonyl thio compounds are currently widely used in free radical polymerization as agents that allow one to control the polydispersity and, more importantly, the molecular weight of the polymer in question. They also provide chemists with a very simple method for the synthesis of reverse addition-fragmentation chain transfer (RAFT) agents with tertiary leaving groups, by reaction of these sulphur compounds with azo compounds that form tertiary radicals upon

decomposition. Trithiocarbonate disulfides, however, have had more restricted uses in the past. Only a few examples of such compounds have been recorded in the literature.[27]

1.1.8 Gold

Throughout ancient history, gold has been known to have certain medicinal properties.[29] It can exist in a variety of oxidation states, ranging from -1 to 5. Of these states, only Au(0), Au(I) and Au(III) are stable in aqueous biological environments. Au(I) is thermodynamically more stable than Au(III). Furthermore, since many Au(III) complexes are oxidizing agents and are reduced to Au(I), they are generally toxic.[30] Au(I) compounds are typically linear, and react well with soft donor ligands such as sulphur.[29] Au(III), on the other hand, prefers hard donor ligands such as nitrogen and oxygen.[31] Most gold-based medical drugs are Au(I) derivatives. However, Au(III) is the most common oxidation state found.[29] Many ligands form stable complexes with Au(III), thus leading to a range of complexes with a variety of chemical and physical properties.[32] Au(III) has 8 electrons in the valence 5d subshell, thus making it a closed shell, low spin, diamagnetic species,[33] which coordinates with ligands to form mostly four-coordinate square-planar complexes.[29] Both Au(I) and Au(III) are soft metal ions, but Au(III) forms complexes more readily with harder ligands than Au(I).[34]

Au(III) complexes are isoelectronic and isostructural to platinum(II) complexes, and thus also hold promise as possible antitumour agents. Yet only a few cases in the literature [35] can be found describing the *in vivo* antitumour effects and cytotoxic properties of these compounds.[35] It is speculated that Au(III) might have a similar antitumour activity to that of cisplatin, although Au(III) complexes are generally much more reactive than Pt(II) complexes and also, as mentioned earlier, mostly toxic.[30] Preliminary data suggests that there exists a direct interaction of the Au(III) complexes with the DNA, forming the basis for their cytotoxic abilities. Unfortunately, pharmacological investigation of these compounds' antitumour properties are usually hindered by their poor kinetic and redox stabilities under physiological conditions, making them difficult to use for pharmaceutical purposes.[35]

Gold organometallic chemistry is a wide field that has received increasing attention over the last few years, mostly regarding bioinorganic chemistry and its antimicrobial and antitumour properties, as mentioned above. But more recently, much of the focus has shifted towards the synthesis of gold derivatives containing sulphur and/or phosphorous donor ligands. Dithiocarbamate compounds have been studied extensively because of their applications as vulcanization accelerators, flotation agents and pesticides, as well as their antimicrobial activity and protection against metal poisoning.[36] Potential ligands such as those seen in Figure 1.7 have not yet been coordinated with Au(III) to date.

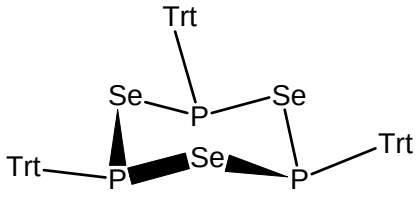

Figure 1.7a Structure of the heterocyclic ligand **III**, $P_3Se_3(C_{19}H_{15})_3$

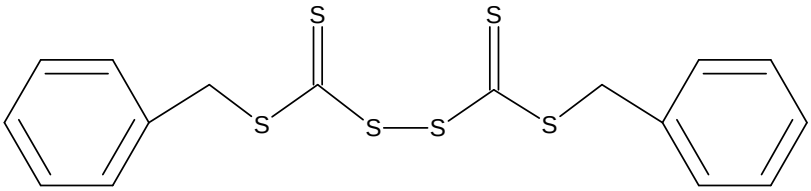

Figure 1.7b Structure of the ligand **I**, $S_6C_{16}H_{14}$

Previous uses of the sulphur ligand shown in Figure 1.7b have been discussed earlier. Thio-and seleno-phosphates are still a relatively small family of compounds, compared to the large range of oxophosphates that exist. Where oxophosphates can play an important role in catalysis, ceramics and molecular sieves, the thio- and seleno-phosphates have rather unique properties, such as intercalation chemistry and ion-exchange, as well as optical and magnetic phenomena.[37] The chemistry of organophosphorus-sulphur and selenium heterocycles is a rich and wide field. Most common ring sizes that exist are 4- to 5-membered, but larger and smaller ring sizes have been found. Cyclophosphanes with aromatic substituents are often studied because of their ability to stabilize compounds against undesired oxidation and/or hydrolysis.[38]

1.2 Research goals and thesis outline

The general aim of the research decribed in this thesis is the coordination of both hard and soft donor ligands to the chosen metal atoms. More specifically, it involves the investigation of the complicated chemistry that is Mo(VI) and W(VI) solution and solid state chemistry, and the filling in of the gaps that exist in this area of research. This is a structural study, and it does for the most part involve the analysis of crystal structures obtained throughout our research, and the interpretation of these results. Where does each new complex fit into the chemistry of Mo and W as we know it? And why do some complexes just not crystallize, even though the conditions are favorable according to the species distribution diagram? These are just some of the questions that exist regarding these metals' reactions, and some more which arose during this research.

As a second part to this thesis, we planned to study the coordination of the metal atoms Pt(II) and Au(III) to new and potentially useful ligands containing the soft donor atoms P, S and Se. We investigated the reaction and coordination of two new trithiocarbonyl disulfide ligands with these two metals, and how it differs for the Au(III) and Pt(II) metal centers. Also, we planned to coordinate an interesting new Se-P heterocycle to Au(III), and study the way the ligand chooses to coordinate to the metal centre.

In **Chapter 2**, we will investigate the complex nature of Mo and W chemistry. The questions mentioned above will be studied and new structures of these two metals will be analyzed and discussed. The complexes of these two metals with α-hydroxycarboxylic acids will be investigated, and the new complexes of the metal atoms with these acids will be structurally analyzed. The polyoxoanion complexes of Mo(VI) and W(VI) will also be discussed and any new behaviour will be highlighted.

In **Chapter 3**, we will discuss the general features of Pt(II) and Au(III) chemistry. The focus of the research will be on the new ligands used in the syntheses of our compounds, and the products obtained upon reaction of these ligands with the above-mentioned metal ions will be analysed and the structures discussed in detail.

1. Sykes AG. Molybdenum: The Element and Aqueous Solution Chemistry. **In**: Wilkinson G (ed.), *Comprehensive Coordination Chemistry: The Synthesis, Reactions, Properties & Applications of Coordination Compounds*, Vol. 3, Pergamon Press, Oxford, 1987; 1229-1261.
2. Jelikic-Stankov M, Uskokovic-Markovic S, Holclajtner-Antunovic I, Todorovic M, Djurdjevic P. *J. Trace Elem. Med. Bio.* 2007; **21**: 8-16.
3. Greenwood NN, Earnshaw A. *Chemistry of the Elements*. Oxford:Butterworth-Heinemann, 1997; 1167-1207
4. Cruywagen JJ. *Adv. Inorg. Chem.* 2000; **49**: 127-182.
5. Day VW, Fredrich MF, Klemperer WG, Shum W. *J. Am. Chem. Soc.* 1977; **18**: 6146.
6. Ghammami S. *Cryst. Res. Technol.* 2003; **38**: 913.
7. Evans HT. *J. Chem. Soc. Dalton Trans.* 1975: 505-514.
8. Dori Z. Tungsten. **In**: Wilkinson G (ed.), *Comprehensive Coordination Chemistry: The Synthesis, Reactions, Properties & Applications of Coordination Compounds,* Vol. 3, Pergamon Press, Oxford, 1987; 973-981.
9. Rhule JT, Hill CL, Judd DA. *Chem. Rev.* 1998; **98**: 327-357.
10. Duraisamy T, Ramanan A, Vittal JJ. *J. Mater. Chem.* 1999; **9**: 763-767.
11. Cruywagen JJ, Esterhuysen MW, Heyns JBB. *Inorg. Chim. Acta* 2003; **348**: 205-211.
12. PedrosaDeJesus JD. *Comprehensive Coordination Chemistry: The Synthesis, Reactions, Properties & Applications of Coordination Compounds,* Vol. 2, Pergamon Press, Oxford, 1987; 461-483
13. Cruywagen JJ, Kruger L, Rohwer EA. *J. Chem. Soc. Dalton Trans.* 1997: 1925-1929.
14. Cruywagen JJ, Rohwer EA, Van de Water RF. *Polyhedron* 1997; **16**: 243-251.
15. Cruywagen JJ, Saayman LJ, Niven ML. *J. Cryst. Spectrosc.* 1992; **22**: 737-740.
16. Mitchell PCH. *J. Less-Common Metals* 1974; **36**: 3-11.
17. Hlaibi M, Chapelle S, Benaissa M, Verchere J. *J. Inorg. Chem.* 1995; **34**: 4434-4440.
18. *Comprehensive Coordination Chemistry: The Synthesis, Reactions, Properties & Applications of Coordination Compounds*, Vol. 6, Pergamon Press, Oxford, 1987; 657-667.
19. Spence JT. *Coord. Chem. Rev.* 1969; **4**: 475-498.
20. Niven ML, Cruywagen JJ, Heyns JBB. *J. Chem. Soc. Dalton Trans.* 1991: 2007-2011.
21. Young CG, Minelli M, Enemark JH et al. *Polyhedron* 1986; **5**: 407-413.
22. Ogata A, Mitsui S, Yanagie H et al. *Biomed. Pharmacother.* 2005; **59**: 240-244.
23. Roundhill DM. *Comprehensive Coordination Chemistry: The Synthesis, Reactions, Properties & Applications of Coordination Compounds*, Vol. 5, Pergamon Press, Oxford, 1987; 353
24. Fregona D, Giovagnini L, Ronconi L, Marzano C, Trevisan A, Sitran S, Biondi B, Bordin F. *J. Inorg. Biochem.* 2003; **93**: 181-189.
25. Marzano C, Trevisan A, Giovagnini L, Fregona D. *Toxicol. in Vitro* 2002; **16**: 413-419.
26. Manav N, Mishra AK, Kaushik NK. *Spectrochim. Acta, Part A* 2006; **65**: 32-35.
27. Weber WG, McLeary JB, Sanderson RD. *Tetrahedron Lett.* 2006; **47**: 4771-4774.
28. Cras JA, Willemes J. *Comprehensive Coordination Chemistry: The Synthesis, Reactions, Properties & Applications of Coordination Compounds*, Vol 2, Pergamon Press, Oxford, 1987; 517-591
29. Shaw III CF. *Chem. Rev.* 1999; **99**: 2589-2600.
30. Fricker SP. Medicinal chemistry of gold compounds. **In**: Patai S, Rappoport Z (eds.), *The chemistry of organic derivates of gold and silver*. John Wiley & Sons, Ltd, 1999; 641-659.
31. Tiekink ERT. *Crit. Rev. Oncol. Hematol.* 2002; **42**: 225-248.
32. Shaw III CF. The Biochemistry of Gold. **In**: Schmidbaur H (ed.), *Progress in Chemistry, Biochemistry and Technology*. John Wiley & Sons, Ltd, 1999; 260-298.
33. Barakat K, Cundari TR. *Chem. Phys.* 2005; **311**: 3-11.
34. Puddephatt RJ. *Comprehensive Coordination Chemistry: The Synthesis, Reactions, Properties & Applications of Coordination Compounds*, Vol. 5, Pergamon Press, Oxford, 1987; 863-897
35. Messori L, Abbate F, Marcon G, Orioli P, Fontani M, Mini E, Mazzei T, Carotti S, O'Connell T, Zanello P. *J. Med. Chem* 2000; **43**: 3541-3548.
36. Ronconi L, Maccata C, Barreca D, Saini R, Zancato M, Fregona D. *Polyhedron* 2005; **24**: 521-531.
37. Canlas CG, Muthukumaran RB, Kanatzidis MG, Weliky DP. *Solid State Nucl. Mag.* 2003; **24**: 110-122.
38. Kilian P, Bhattacharyya P, Slawin AMZ, Woollins JD. *Eur. J. Inorg. Chem.* 2003: 1461-1467.

Chapter 2

Synthesis and structural study of new Mo(VI) and W(VI) complexes

Abstract

The polyanion chemistry of Mo(VI) and W(VI) was investigated by reacting sodium molybdate or sodium tungstate with a range of counter ions in various metal to ligand ratios, and also at different pH values and concentrations. A completely new polyanion of W(VI) with tetraethylammonium cations acting as counter ions in the structure was isolated, $[(CH_3CH_2)_4N]_2[W_6O_{19}]$ (**4**). A new polymorph of the potassium salt of a known dimolybdate species was crystallized, $K_2[Mo_2O_7]\cdot H_2O$ (**1**), and differences with the known complex was emphasized. Also, two polyanionic species that had been isolated before, $K_6[Mo_7O_{24}]\cdot 4H_2O$ (**2**) and $[(CH_3)_3N(CH_2)_6N(CH_3)_3]_2[Mo_8O_{26}]\cdot 2H_2O$ (**3**), have been crystallized and any differences in the structures were studied.

To synthesize the complexes of Mo(VI) and W(VI) with deprotonated carboxylic acids, sodium molybdate or sodium tungstate was reacted with a range of carboxylic acids and counter ions in various metal to ligand ratios, a range of pH values as well as different concentrations. Two new compounds of Mo(VI) with these acids have been isolated, one with malate and one with citrate: $[(CH_3CH_2)_4N][MoO_3(mal)]\cdot H_2O$ (**5**) and $Na_6[Mo_2O_5(cit)_2]$ (**6**). Also, a known dimer of dimolybdates has been crystallized again, $[(CH_3)_3N(CH_2)_6N(CH_3)_3][Mo_2O_7(cit)]$ (**7**), and any differences with the known complex has been studied.

2.1 Introduction and aim of this study

2.1.1 Background

Polyoxometalates

The solution chemistry of molybdenum(VI) has been an area of intense research activity for many years and it is dominated by the heteropoly- and isopolymolybdate forms. Heteropolyanions are polyoxometalate species containing heteroatoms such as P or transition metals in its structure, whereas isopolyanions comprise only molybdenum or tungsten in its structure, along with oxygen and hydrogen.[1] The aqueous chemistry of tungsten(VI) is more difficult to investigate than that of molybdenum(VI) owing to the slow reactions which occur upon acidification as well as the formation of kinetic intermediates. Molybdenum and tungsten in their highest oxidation state of +6 form the previously mentioned stable anions $[MoO_4]^{2-}$ and $[WO_4]^{2-}$. In aqueous solution these anions can easily be protonated, and they show a tendency to condense into polyoxoanions by the release of water molecules effecting oxygen bridge formation. The mechanisms for these reactions are not known with certainty, but it is believed that the process is driven by the ability of $[MO_4]^{2-}$ (M = Mo, W) to expand its coordination sphere from four to six. A large variety of ions may form depending on the pH and concentration of the ions in solution.[2]

The protonation equilibria of the mononuclear species of Mo(VI) in dilute solutions can be represented by the following equations: [2]

$$[MoO_4]^{2-} + H^+ \xrightarrow{K_1} [HMoO_4]^- \qquad \text{(I)}$$

$$[HMoO_4]^- + H^+ + 2H_2O \xrightarrow{K_2} MoO_3(H_2O)_3 \qquad \text{(II)}$$

Reactions I and II are only the beginning of the formation of the polyanions. One would expect the formation of the dimolybdate species to be the next step in the process according to reaction III: [3]

$$2[HMoO_4]^- \rightarrow [Mo_2O_7]^{2-} + H_2O \qquad \text{(III)}$$

However, this reaction does not generally take place, which may account for the fact that no detectable polynuclear species between the mononuclear ones and $[Mo_7O_{24}]^{6-}$ occur in

solution. The species forming upon further acidification of solutions containing the mononuclear molybdates is firstly the heptamolybdate and then the octamolybdate ion: [3]

$$7[MoO_4]^{2-} + 8H^+ \rightarrow [Mo_7O_{24}]^{6-} + 4H_2O \quad (IV)$$

$$[Mo_7O_{24}]^{6-} + [HMoO_4]^- + 3H^+ \rightarrow [Mo_8O_{26}]^{4-} + 2H_2O \quad (V)$$

The reason for the absence of the dimolybdate species in these equilibria is the polymerization reactions (shown below) which compete effectively with reaction III to rather form the heptamolybdate and other species.[3]

$$MoO_3(H_2O)_3 + [HMoO_4]^- \rightarrow [(HO)_5MoOMoO_3]^- + H_2O$$

$$[(HO)_5MoOMoO_3]^- + [HMoO_4]^- \rightarrow [(HO)_4Mo(OMoO_3)_2]^{2-} + H_2O$$

.

.

.

$$[(HO)Mo(OMoO_3)_5]^{5-} + [HMoO_4]^- \rightarrow [Mo(OMoO_3)_6]^{6-} + H_2O$$

$$[Mo(OMoO_3)_6]^{6-} \equiv [Mo_7O_{24}]^{6-}$$

The anion $[Mo(OMoO_3)_6]^{6-}$ consists of one central Mo atom and six MoO_4 octahedra which each are attached to the central Mo through an oxygen atom. It is suspected that the anion may rearrange its internal structure to yield the final heptamolybdate unit as we know it.[3]

Counter ions play a significant role in the isolation of polyoxometalates by precipitating ions that occur only in negligible amounts in solution, such as $[Mo_6O_{19}]^{2-}$, while other major anions still remain in solution. By adding different cations to the same solution at a chosen pH value, a large range of polyoxoanions can be isolated. The polyanions generally consists of only MO_6 (M = Mo, W) octahedra sharing vertices and edges. The metal atoms do not occur at the center of the octahedron, as would be expected, but rather at a corner and/or an edge of the structure due to M-O π-bonding. The resulting shorter M-O bonds are directed towards the exterior of the polyoxoanion.[2]

At pH > 7, Mo(VI) exists as the monomeric tetrahedral $[MoO_4]^{2-}$ species.[4] Certain forms of Mo(VI) are amphoteric and in H^+-concentrations between 0.2 and 3.0 mol.dm^{-3}, it forms, amongst others, cationic species such as $[HMoO_3]^+$, $[MoO_2]^{2+}$ and $[Mo_2O_5]^{2+}$, all of which are based on six-coordinate molybdenum. At molybdate concentrations greater than 10^{-3} mol.dm^{-3}, the acidification of aqueous solutions of Na_2MoO_4 leads to the formation of a variety of polyanions in solution, of which $[Mo_7O_{24}]^{6-}$ and β-$[Mo_8O_{26}]^{4-}$ are the most common. Many other polyanion species are thought to exist, but not all of these have been isolated.[1]

The heptamolybdate polyanion and its protonated forms, $[H_nMo_7O_{24}]^{(6-n)-}$ (n = 1-3), predominate in solutions of pH 3 to 5, depending on the concentration of the molybdate. The structures of the heptamolybdate compounds have been determined as their sodium, potassium and ammonium salts, to name but a few. They involve an arrangement of octahedra with *cis*-MoO_2 stereochemistry for each octahedral metal atom. The β-$[Mo_8O_{26}]^{4-}$ salts crystallize from a lower pH value of *ca* 2 to 3. The $[Mo_6O_{19}]^{2-}$ anion has also been isolated in the solid state, though many of the salts were prepared by serendipitous routes.[1]

Polyoxomolybdates are usually crystallized at the pH values mentioned above in the presence of an appropriate cation, either from an acidified sodium molybdate solution or from a neutralized molybdenum trioxide solution. Cruywagen *et al.* [5] made an interesting discovery in 2003. The species distribution diagram (Fig. 2.1) of a 2.0 mol.dm^{-3} solution of sodium molybdate in the pH range 3.5 to 8.0 indicates that the $[Mo_7O_{24}]^{6-}$ ion reaches its maximum concentration at pH 5.6. When they attempted crystallization of the $[Mo_{10}O_{35}]^{10-}$ ion at pH 6.9, which according to the species diagram would afford the maximum concentration for this species, the resulting crystal found was in fact $[Mo_7O_{24}]^{6-}$. The conditions for this crystallization were not favorable for the isolation of the heptamolybdate species. It was then proposed that the polyanion occurring in solution at pH 6.9 converts to $[Mo_7O_{24}]^{6-}$ during crystallization, due to the stability of the heptamolybdate ion within the complex network of ion-dipole and hydrogen bonding interactions in the crystal.[5]

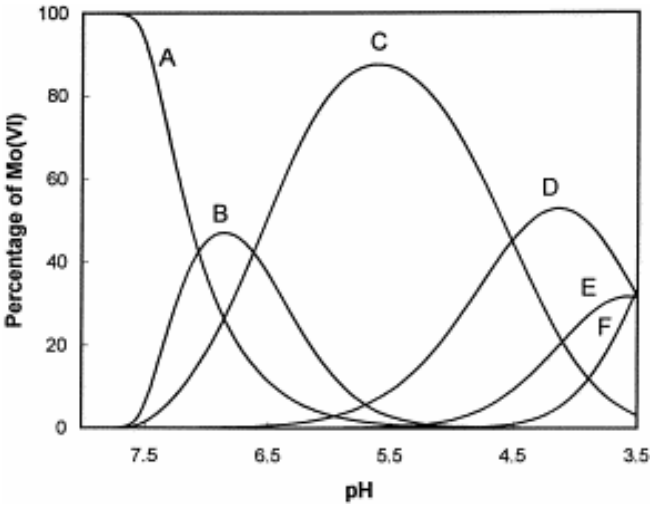

Figure 2.1 Distribution of molybdenum(VI) species in a 2.0 mol.dm^{-3} Na_2MoO_4 solution as a function of pH: A=$[MoO_4]^{2-}$; B=$[Mo_{10}O_{35}]^{10-}$; C=$[Mo_7O_{24}]^{6-}$; D=$[HMo_7O_{24}]^{5-}$; E=$[H_3Mo_8O_{28}]^{5-}$; F=$[Mo_8O_{26}]^{4-}$ [5]

This phenomenon leads to further complications in the synthesis and isolation of new polyoxomolybdate (and also tungstate) species. It is in principle possible to isolate a different polyanion at a specific pH by adding a different counter ion, but the extreme stability of the heptamolybdate species complicates this process significantly.

An intriguing molybdenum compound is the octamolybdate, $[Mo_8O_{26}]^{4-}$ which up until 1991 was only observed in the α and β isomer forms. It was later discovered to have a third isomer, the γ form.[6] The α and γ structures differ from the β isomer in that they do not contain only octahedral, but four coordinate (α) and five coordinate (γ) molybdenum atoms as well.[2] These isomers can each be viewed as distorted arrays of cubic close-packed oxygen atoms with molybdenum atoms occupying interstitial sites.[6] Of the three different structural types of octamolybdates, only the β isomer is known with certainty to be a major species in solution. This isomer has been crystallized with a variety of cations. The degree of distortion of the octahedra that makes up this anion, increases with the size of the cation and probably leads to the formation of the α structure. The latter structure has been obtained with only a few large cations such as tetrabutylammonium and propyl triphenylphosphonium.[2] The α form has approximate D_{3d} symmetry and consists of a ring

made up of six MoO_6 octahedra linked to one MoO_4 tetrahedron above and one below its octahedral cavity. Since a large variation in Mo-O distances occurs, the structure can be viewed as a loose addition compound between two MoO_4 units and a Mo_6O_{18} ring consisting of distorted MoO_4 tetrahedra that share corners. The β isomer, made up of 8 edge-sharing MoO_6 octahedra, has been observed for many compounds, such as $[NH_4]_4[Mo_8O_{26}]\cdot 4H_2O$ and $[NBu_4]_3K[Mo_8O_{26}]\cdot 2H_2O$. It has been proposed that the α and β forms can be interconverted *via* a facile isomerization process, during which an intermediate γ isomer, which contains six MoO_6 octahedra and two MoO_5 trigonal bipyramids, forms. The first isolation of this γ isomer was reported by Niven and co-workers.[6] The γ form has been isolated by addition of the hexamethonium cation as counter ion at pH 6, which is much higher than the pH range of 2 to 3 at which the α and β isomers generally crystallize. However the type of isomer also strongly depends on the cation used.[2]

Dimeric anions such as $[Mo_2O_7]^{2-}$ do not normally occur in aqueous solution but have been isolated in the solid state with bulky substituents, and also in non-aqueous solutions. This anion consists of two MoO_4 tetrahedra sharing a vertex. Generally the dimolybdate species is only stable with specific, large cations as counter ions; otherwise the heptamolybdate species is isolated.[2]

Many isopolytungstates have been isolated by crystallization from solution, though many more are thought to still remain uncharacterized. Analysis of aqueous polytungstate equilibria is complicated by the extreme range of rates involved: many of these polytungstates may appear stable, but are in fact kinetic intermediates.[1] The best known polytungstates are the paratungstates and metatungstates. Two paratungstate species are known, namely paratungstate A and B. Paratungstate A forms readily upon acidification of solutions of sodium tungstate, and has the empirical formula $[W_7O_{24}]^{6-}$, whereas paratungstate B has the composition $[H_2W_{12}O_{42}]^{10-}$.[1] Again, all the known structures of polyoxotungstates consist of WO_6 octahedra. In almost all cases, these octahedra share edges in such a way that only structures with single terminal oxygen atoms are formed. In this regard polyoxomolybdates differ from the tungstates: the majority of

polyoxomolybdates have *cis*-dioxo-terminal oxygens. A reason given for this observation is possibly the better overlap of the extended tungsten 5d orbitals with the oxygen orbitals.[2] Oxo-ligands form strong bonds with W(VI) by utilizing both σ and π donation, resulting in short W-O bond lengths.[7] The structures of $[W_7O_{24}]^{6-}$ and $[W_6O_{19}]^{2-}$ are the same as their molybdenum analogues.[2]

Molybdenum(VI) and tungsten(VI), although similar in many respects, behave differently under certain conditions. Equilibria involving $[MoO_4]^{2-}$ and polyoxomolybdates in aqueous solution are established very quickly; they are mostly completed in minutes. However, with tungsten, the same conversions may need several weeks. Structurally, the polyanions in one series do not always have their precise counterparts in the other.[4]

The relative ease with which early transition metals form polyoxoanions could be attributed to the size of the $M^{5/6+}$ cations and their π-acceptor properties. The larger effective ionic radii of Mo^{6+} and W^{6+} (0.77 Å and 0.74 Å respectively) are consistent with the observation that these metal ions can adopt four, five and six-fold coordination by oxygen atoms, whereas Cr^{6+}, which has a smaller ionic radius of 0.58 Å, can only form oxide complexes with a maximum coordination number of four. Only a few polyanions of Mo(VI) and W(VI) known at present are other than six-coordinate.[1]

Complexes with α -hydroxycarboxylic acids

α-Hydroxy acids all possess one hydroxyl group in a position α to a carboxyl group, and possibly other hydroxyl and carboxyl groups as well (Fig. 2.2). These acids, when acting as ligands, can form a large variety of complexes using several possible sites of chelation in which the donating oxygen atoms may be either from the hydroxyl and/or carboxylic groups. Most major complexes of tungsten and molybdenum with these acids are 1:2 species.[8]

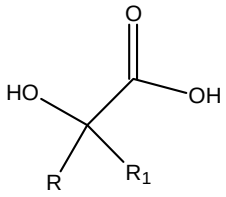

Figure 2.2 Structure of an α-hydroxy acid with R, R_1 = H, alkyl, aryl

The aliphatic hydroxy acids which have been most studied as ligands, are the low molecular mass 2-hydroxyalkanoic acids, namely glycolic, mandelic, lactic, malic, tartaric and citric acid. The more complex of these acids such as malic, tartaric and citric acid, show a range of bonding modes towards inorganic ions, depending on their deprotonation. A characteristic feature of such ligands is the co-planarity, or near co-planarity, of the 2-hydroxy and carboxyl groups observed in their crystal structures (Fig. 2.3a). The conjugated bases of these acids all have one property in common: they form very stable five-membered chelate rings (Fig. 2.3b). Uniquely, the metal-ionized-hydroxyl bond length is usually shorter than the corresponding metal-protonated-hydroxyl bond distance.[9]

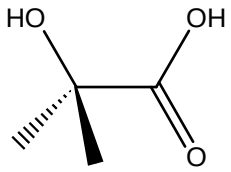

Figure 2.3a The co-planarity of the 2-hydroxy and carboxyl-groups.

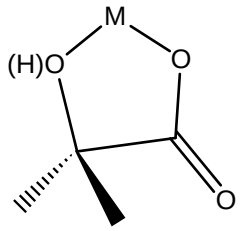

Figure 2.3b The five-membered chelate ring deprotonated α-hydroxyacids form when coordinated to a metal.

The addition of metal ions to solutions of malate, results in the formation of a range of complex species owing to the ability of malate to act in various ways as a multidentate ligand and thus having the capability of binding inorganic ions in different manners. The most common coordinating mode is bidentate, but tridentate chelation is also observed quite often, which involves the deprotonated hydroxy and two carboxyl groups, thus furnishing five and six-membered chelate rings, as illustrated by the compounds in Figure 2.4. Bridging *via* carboxyl oxygens is also possible.[9]

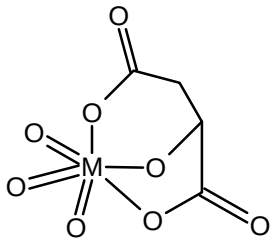

Figure 2.4a Structure of $[MO_3(mal)]^{3-}$.

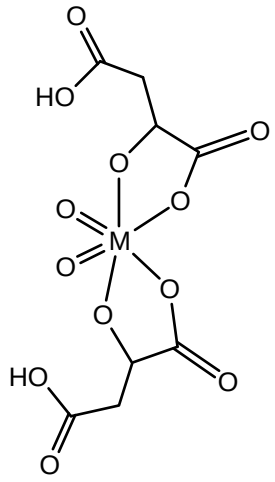

Figure 2.4b Structure of $[MO_2(mal)_2]^{4-}$.

Tridentate coordination has a stabilizing effect on the complexes, and the typical behaviour of α-hydroxycarboxylic acids towards the group 6 metals, Mo(VI) and W(VI) is, as mentioned before, to form very stable 1:2 complexes. This higher stability could structurally be attributed to the fact that in 1:1 complexes, one five-membered and one six-membered ring is formed (Fig. 2.4a), whereas in the 1:2 complexes, two preferred five-membered rings are present (Fig. 2.4b).[10]

The crystal structures of quite a few complexes of malic acid have been solved to date. Bidentate malate occurs very often in these structures. The chelate ring which forms is the result of the coordination of one oxygen atom of the deprotonated hydroxy group of the carboxyl, and a hydroxy group oxygen. Sometimes the malate ion binds through the hydroxy group and the two carboxyl groups in two manners: it may have the β-carboxyl group binding to the same metal centre as the α-hydroxycarboxylate group when the ligand is tridentate (Fig. 2.5), or it can act bidentately towards one metal and then use the β-carboxyl group to bind to another metal.[9]

A number of complexes of particularly molybdenum with malate ions have been reported, some of which have been isolated in crystalline form, such as $[NH_4]_4[Mo_4O_{11}(mal)_2]\cdot H_2O$.[10] A favourable enthalpy change for the 1:2 coordination of malate to molybdenum is exhibited by its complexes, explaining its greater stability in comparison to other complexes also occurring in solution at the same pH.[10]

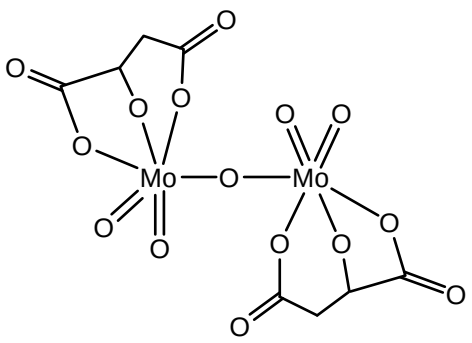

Figure 2.5 The dimeric complex of Mo(VI), $[Mo_2O_5(mal)_2]^{4-}$ (mal = malate)

For complexes of tungsten(VI) with malate, the tungstate:malate stoichiometry is typical of that previously observed for other comparable tungsten and molybdenum ligand systems such as W(VI) with citrate. It is particularly similar to the complexes of molybdenum with malate as ligand. Once again, tridentate coordination is expected to yield more stable tungsten-malate complexes. Depending on the concentration of tungstate and malate in solution, several complexes could occur simultaneously in the pH range of 1.5 to 7.5.[9] The tungsten-malate complexes are more stable than those with molybdenum. Although both molybdenum and tungsten experience an increase in coordination number upon complexation with malate, the enthalpy change is much more favourable in the case of tungsten, illustrating the greater tendency of tungsten(VI) to expand its coordination number from four to six.[11]

Citric acid has a tendency to form monomeric species when it coordinates to a metal ion through the two terminal carboxyl groups and the hydroxy group as a threefold deprotonated tridentate ligand (Fig. 2.6). It has been suggested that citrate may also act as a bidentate ligand, through the deprotonated carboxyl and hydroxy groups, forming a five-membered chelate ring. Therefore, citrate is also a ligand that is very versatile in its binding mode to metal ions. An even greater variety of coordination modes are apparent from solid state studies.[9]

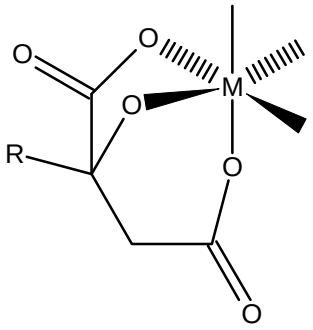

Figure 2.6 Tridentate coordination of citrate to a metal center.

The molybdenum-citrate stoichiometry of the complexes is typical of those observed for molybdenum(VI)-malate complexes. The citrate complexes are in general more stable than their malate analogues. If tridentate coordination of citrate occurs similar to that of malate, five- and six-membered rings can be formed (Fig. 2.6).[10]

Complexes between tungsten and citrate show much the same coordination as the corresponding tungsten-malate complexes. The citrate ligand can coordinate in 3 ways, but usually prefers coordinating tridentately to the tungsten atom, through the deprotonated α-alkoxy, α-carboxyl and one β-carboxyl group, making each metal atom six-coordinate (when including the other ligands present). This type of coordination can be divided into two groups: one wherein the ratio of tungsten to ligand is 1:1, and a second group wherein the ratio is 2:2 with an oxygen bridge between the two metal atoms. Citrate can also coordinate bidentately, where the tungsten is coordinated to the deprotonated central OH-group and the oxygen of the vicinal carboxylate group, to form a five-membered ring with the metal (Fig. 2.7).[12]

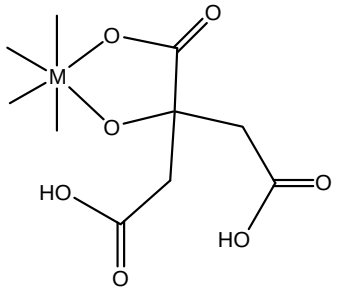

Figure 2.7 Bidentate coordination of citrate.

Tartaric acid (Fig. 2.8) is an α-hydroxy acid that has been intensely studied. It occurs as various stereo isomers, and this could be one reason for the complexity of its coordination chemistry.

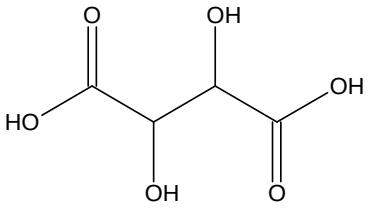

Figure 2.8 Structure of tartaric acid.

Tartrate coordinates bidentately to a metal center by means of one of the carboxylic oxygens and the adjacent hydroxyl oxygen to form a five-membered ring with the metal (Fig. 2.9).

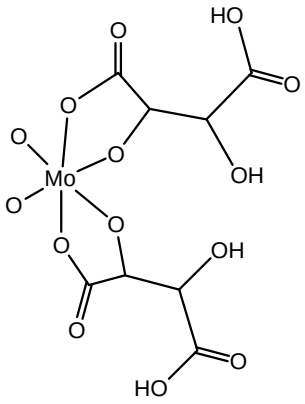

Figure 2.9 Tartrate coordinated bidentately to Mo

Studies have proved the existence of monomeric, dimeric and tetrameric species of Mo with tartrate in solution, though not many of these have been isolated as single crystals.[13] The more uncommon binding modes of tartaric acid are monodentate and tridentate.[9] The tetradentate coordination of one tartrate moiety to two Mo centers may also occur (Fig. 2.10), which leads to the formation of the above-mentioned dimeric and tetrameric species. The monomeric species (Fig. 2.9) with a 2:1 and tetrameric species (Fig. 2.11) with a 4:2 metal to ligand ratio have proved to be most stable in solution.[13]

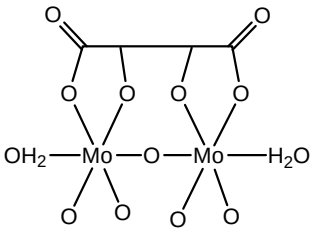

Figure 2.10 Tetradentate coordination of tartrate to 2 Mo atoms

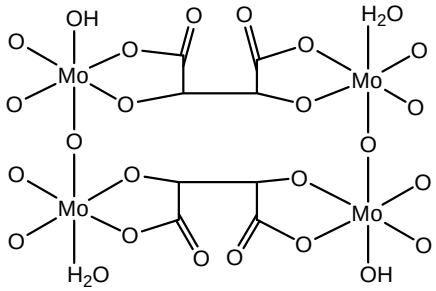

Figure 2.11 Tetradentate coordination of 2 tartrate moieties to 4 Mo atoms

2.1.2 Particular aims of the study

We firstly planned to structurally investigate aspects of the polyoxoanion chemistry of Mo(VI) and W(VI) by varying the reaction conditions systematically and attempting to isolate and characterize the species present. Working at a range of pH values, we varied the concentrations of Mo(VI) and W(VI) in the solutions, added different counter ions and altered the temperature and cooling rate of the solutions. As part of this investigation we also hoped to isolate some of the elusive species that are known to exist in solution, but are not yet unequivocally structurally characterized.

Secondly, we planned to study a number of α-hydroxy acids and their coordination modes toward Mo(VI) and W(VI) species in aqueous solution by again isolating product complexes and determining their crystal and molecular structure. We investigated this by varying the pH, the concentration of the solutions and the type of hydroxy acid; in certain instances different counter ions were utilized.

2.2 Results and discussion

2.2.1 Polyoxoanion complexes of Mo(VI) and W(VI)

Since the polyoxoanion chemistry of Mo(VI) and W(VI) is so unpredictable, we attempted just about all possible combinations of starting reagent, pH, concentration, temperature and counter ion to try and isolate new polyoxoanion complexes of these metals. The species diagram in Figure 2.1 proved to be only a starting point in this investigation, since the species that exist in solution (as represented by Figure 2.1) are rarely the complexes isolated in crystalline form. Most of the new complexes formed in this part of the study are unexpected for the reaction conditions we used. Still, one new W(VI) polyanion complex was isolated in the solid state, and a new polymorph of a known dimolybdate species was crystallized. We were also interested in crystallizing some of the elusive polyoxoanion species existing in solution, but unfortunately, none of these could be isolated. The new complexes will be structurally analyzed in the next section. Also, two structures that have been isolated before will be included and differences with those in the literature will be discussed.

2.2.1.1 Isolation and structural analysis of $K_2[Mo_2O_7]\cdot H_2O$ (1)

With this synthesis we attempted to isolate the evasive $[Mo_{10}O_{35}]^{10-}$ complex with $[N(CH_3)_4]^+$ as counter ion. The species distribution diagram in Figure 2.1 indicates that this species should be present at its maximum concentration at a pH of 7.0. We expected that, as previously mentioned, $[Mo_7O_{24}]^{6-}$ salts could possibly crystallize during this reaction. Instead a dimolybdate(VI) unit with potassium, $[K_2Mo_2O_7]\cdot H_2O$ (**1**), was isolated and there was no indication of the fate of the counter ions. Although the dimolybdate species does not appear in the distribution diagram in Figure 2.1 since it does not generally occur in aqueous solution, this pH value is clearly favourable for the crystallization of this rare species.

Compound **1** was synthesized by reacting MoO_3 with KOH, $(CH_3)_4NCl$ and HCl at a pH of 7.05 The solution was left at room temperature, and clear, hexagonal crystals of compound **1** formed after ten days.

The molecular structure of compound **1** is represented in Figure 2.12, and selected bond lengths and angles are given in Table 2.1. The structure was solved in the triclinic spacegroup Pī.

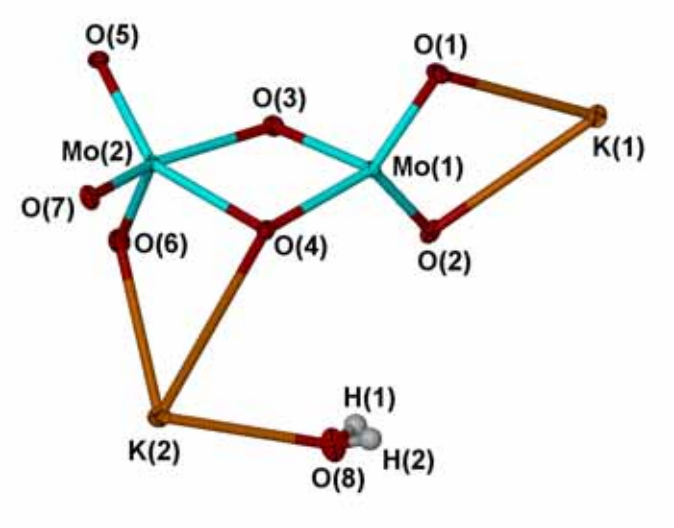

Figure 2.12 Molecular structure of compound **1,** showing the atom numbering scheme. Ellipsoids enclose 65 % of the electron density.

In its simplest repeatable unit, this compound is seen to consist of a dimolybdate moiety ($[Mo_2O_7]^{2-}$) coordinated to two potassium atoms, with one water of crystallization present in the structure. The two Mo(VI) atoms have different coordination environments: Mo(1) is coordinated tetrahedrally to its surrounding oxygens, whereas Mo(2) is coordinated to five oxygens in a distorted trigonal bipyramidal geometry. The potassium cations, although seemingly two- and three-coordinated, are in fact six-coordinated to the oxygen atoms of the surrounding dimolybdate units in the extended structure.

Potassium dimolybdate has been isolated before,[14] but compound **1** shows some differences with the one in the literature, the biggest difference between them being the significant deviations in the unit cell parameters, indicating that this is a different polymorph of the species. Also, a zinc dimolybdate, $\underline{ZnMo_2O_7{\cdot}5H_2O}$, has been isolated by Grzywa and coworkers,[15] and its structure shows some similarities to compound **1**. The zinc dimolybdate forms infinite chains in a similar manner as **1**, but where the five-coordinated molybdenum atoms of **1** exist in a trigonal bipyramidal environment, the

same molybdenum atoms in the zinc complex tend to prefer square-pyramidal coordination geometry.[15]

In the dimeric building blocks, Mo(1) exists in a tetrahedral environment. As seen in Table 1, the Mo(1)-O(4) bond distance is the longer side of the tetrahedron. There is a significant increase in bond length from Mo(1)-O(3) to Mo(1)-O(4): the Mo(1)-O(3) bond distance is 1.803(3) Å, whereas Mo(1)-O(4) is 2.023(3) Å. This phenomenon could possibly be explained by the coordination of K(2) to O(4), causing an increase in the separation of Mo(1) and O(4). The separation between Mo(2) and O(6) is typical of a Mo-O bond, 1.738 Å.[16] For double bonded oxygens, a typical bond length for the two terminal oxygens, O(7) and O(5), would be 1.693Å.[16] This is indeed the case for O(7), showing a bond length of 1.731(3) Å, however, the Mo(2)-O(5) bond length is significantly larger, 1.818(3) Å. Although not shown in Figure 2.12, both O(7) and O(5) are coordinated to nearby potassium atoms.

Mo(2) occurs in an approximate trigonal bipyramidal coordination. O(4), O(5) and O(6) form the equatorial plane, and O(3) and O(7) are axially placed. The separation between Mo(2) and O(3) is 2.220(3) Å, significantly longer than the normal 1.920 bond length.[16] On the other hand, the distance between O(3) and Mo(1) is much shorter, 1.803(3) Å, forcing the trigonal bipyramidal environment surrounding Mo(2) to distort.

The O(2)-Mo(1)-O(1) angle is 106.4(1)°, which is smaller than the expected 109.5° angles of an ideal tetrahedron, possibly because of the coordination of K(1) to these oxygens, forcing them to distort the tetrahedral geometry, and the O(3)-Mo(1)-O(4) angle is then only 77.23(11)°.

The O(7)-Mo(2)-O(3) angle should ideally be 180°, but it is in fact appreciably less obtuse at 158.1(1)°. Also, severe distortions of the O(4), O(5) and O(6) equatorial plane geometry are found: the O(6)-Mo(2)-O(5) and O(6)-Mo(2)-O(4) angles are 101.6(1)° and 97.8(1)° respectively, and the O(5)-Mo(2)-O(4) angle is 149.5(1)°, which deviates greatly from the expected 120°.

The crystal structure of **1** consists of layers that are built by infinite Mo_2O_7 chains containing MoO_6 octahedra and MoO_5 trigonal bipyramids. Separate chains are then linked together by K^+ cations. The dimers that build this infinite chain are connected in two ways: by edge-sharing of two dimolybdate units, and by sharing a mutual MoO_6 octahedron involving Mo(1) that has now extended its coordination sphere to six. The chain formation is illustrated in Figure 2.13.

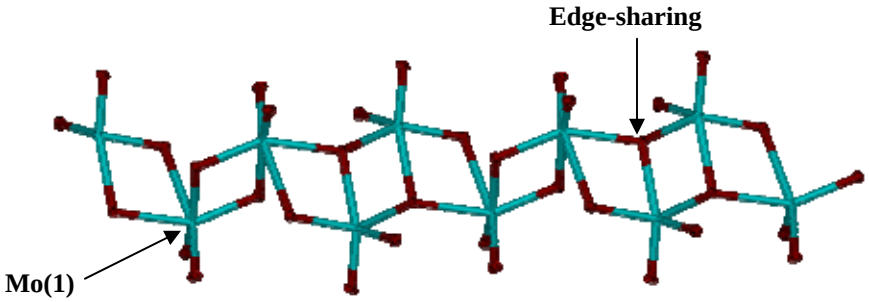

Figure 2.13 The chain-formation of the dimolybdate units of **1.**

Figures 2.14a & b show a presentation of the packing pattern of complex **1** along the b- and c-axis respectively, with the K atoms omitted for clarity to indicate the hydrogen bond formation. As described earlier, the complex forms infinite Mo_2O_7 chains, linked together by K^+ cations. The waters of crystallization all lie in the chambers created by the potassium atoms. Of particular interest are the two hydrogen bonds observed between O(8) and O(6), and between O(8) and O(5). These bonds are strong enough to introduce molecular recognition and self-assembly in the solid state. The hydrogen bonds can be classified as intermediate (2.52–2.95 Å),[17] with O(8)-H(1)···O(6) and O(8)-H(2)···O(5) being 2.857 Å and 2.723 Å respectively. Figure 2.14c illustrates the unit cell packing along the b-axis with the inclusion of the counter ions. No other significant intermolecular distances are noted.

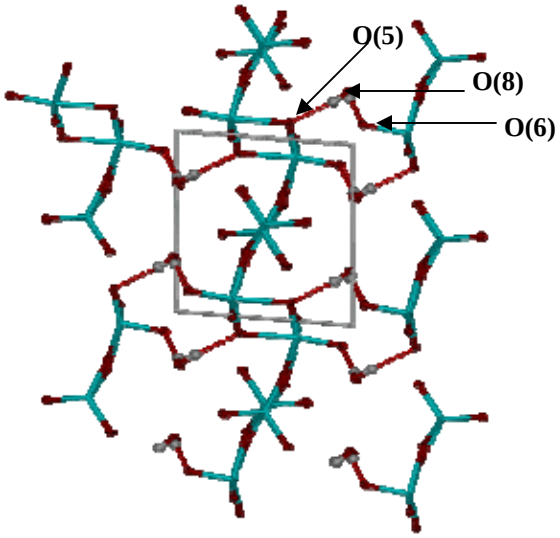

Figure 2.14a Unit cell and packing pattern of **1** viewed along the c-axis to show the hydrogen bonds.

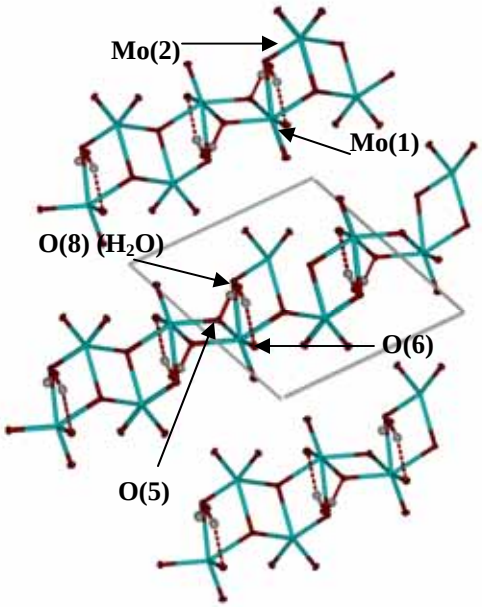

Figure 2.14b Unit cell and packing pattern of **1** viewed along the b-axis to show the hydrogen bonds and Mo_2O_7 chains.

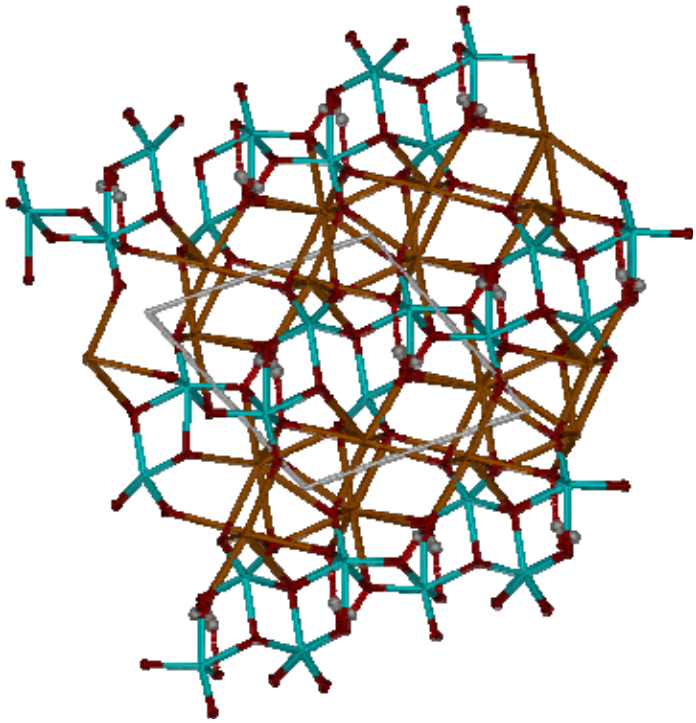

Figure 2.14c Unit cell and packing of compound **1**, viewed along the b-axis, showing the Mo_2O_7 chains with the K atoms (orange) connecting the individual chains.

Table 2.1 Selected bond lengths and angles for compound **1** with e.s.d.s in parentheses.

Bond lengths (Å)

Mo(1)-O(2)	1.728(3)	K(2)-O(4)	3.371(3)
Mo(1)-O(1)	1.737(3)	K(2)-O(6)	2.733(3)
Mo(1)-O(3)	1.803(3)	K(2)-O(8)	2.635(3)
Mo(1)-O(4)	2.023(3)	K(1)-O(1)	2.879(3)
Mo(2)-O(7)	1.731(3)	K(1)-O(2)	2.840(3)
Mo(2)-O(6)	1.738(3)		
Mo(2)-O(5)	1.818(3)		
Mo(2)-O(4)	2.051(3)		
Mo(2)-O(3)	2.220(3)		

Bond angles (°)

O(2)-Mo(1)-O(1)	106.4(1)	O(7)-Mo(2)-O(5)	89.8(1)
O(2)-Mo(1)-O(3)	105.0(1)	O(7)-Mo(2)-O(4)	91.7(1)
O(1)-Mo(1)-O(3)	104.6(1)	O(7)-Mo(2)-O(3)	158.0(1)
O(2)-Mo(1)-O(4)	118.7(1)	O(6)-Mo(2)-O(3)	90.3(1)
O(1)-Mo(1)-O(4)	132.9(1)	O(5)-Mo(2)-O(3)	87.6(1)
O(3)-Mo(1)-O(4)	77.2(1)	O(4)-Mo(2)-O(3)	68.9(1)
O(6)-Mo(2)-O(5)	101.6(1)	O(1)-K(1)-O(2)	56.6(1)
O(5)-Mo(2)-O(4)	149.5(1)	O(8)-K(2)-O(6)	108.0(1)
O(6)-Mo(2)-O(4)	97.8(1)	O(8)-K(2)-O(4)	75.5(1)
O(7)-Mo(2)-O(6)	102.9(1)	O(6)-K(2)-O(4)	54.7(1)

2.2.1.2 Isolation and structural analysis of $K_6[Mo_7O_{24}]\cdot 4H_2O$ (2)

The idea of this experiment was to isolate the rare $[Mo_{10}O_{35}]^{10-}$ polyanion with K^+ as counter ion; instead a new version of the title compound crystallized out. The reason for attempting this synthesis is the fact that only a handful of decamolybdate structures have been determined to date. According to the species distribution diagram in Figure 2.1, at a pH of 7 the concentration of this species is at a maximum. We tried the same synthesis several times, with varying concentrations of Mo, and pH values ranging between 6.80 and 7.15. Unfortunately, in most cases the well known stable hexasodium heptamolybdate species was isolated in crystalline form. We did, however, manage to isolate the hexapotassium complex of this polyanion. Although it has been synthesized before,[18] our structure shows slight differences to the one in the literature, which will be discussed later.

Compound **2** was synthesized by the reaction of MoO_3 with KOH, and HCl was used to reduce the pH to a value of 7.05. After the solution had been left undisturbed at room temperature for three days, large rectangular crystals of **2** had formed.

The molecular structure of compound **2** is represented in Figure 2.15, with the atom numbering shown. The structure was solved in the monoclinic spacegroup $P2_1/n$. The simplified structure in which the counter ions are omitted can be seen in Figure 2.16.

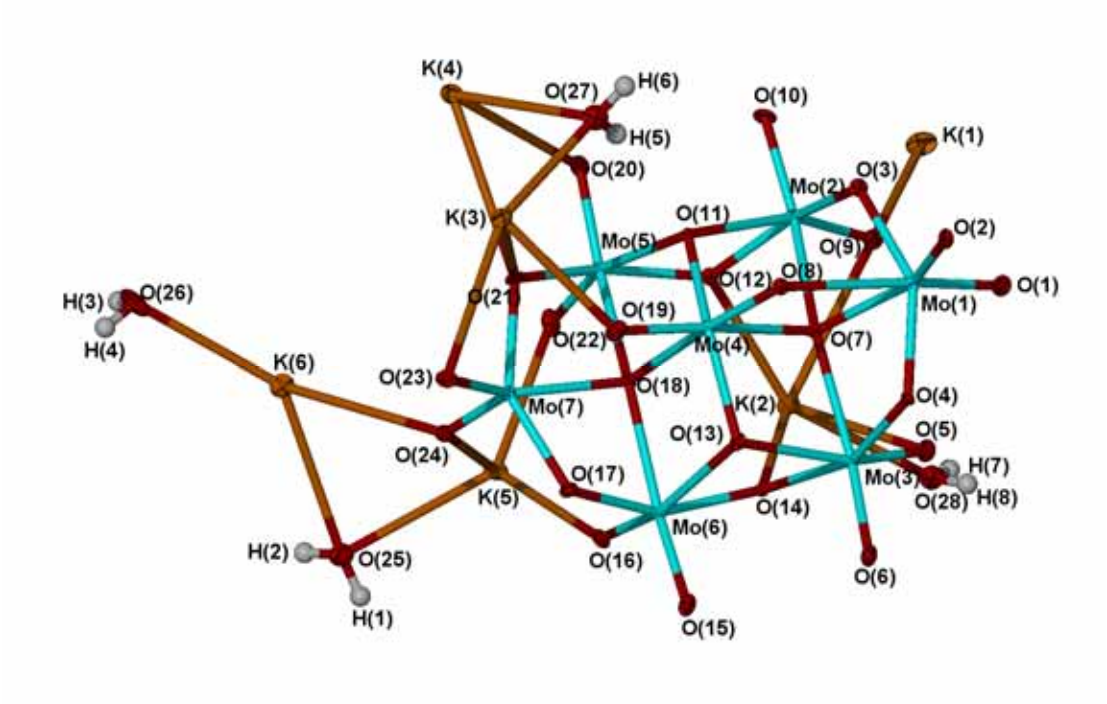

Figure 2.15 Molecular structure of **2,** showing the atom numbering scheme. Ellipsoids enclose 65 % of the electron density.

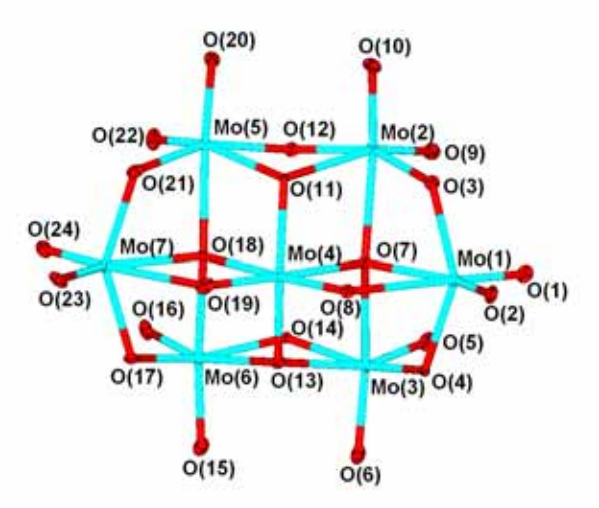

Figure 2.16 Molecular structure of **2** with the K^+ cations omitted for clarity**,** showing the atom numbering and the structure of the heptamolybdate unit.

Compound **2** consists of the classic heptamolybdate moiety: seven Mo(VI) atoms and twenty-four oxygens. Each of the metal centers is coordinated pseudo octahedrally to six surrounding oxygen atoms. There are six K^+ cations acting as counter ions in the structure, as well as four waters of crystallization per heptamolybdate unit.

The structure that was solved by Evans *et al.* in 1975[18] was isolated at a lower pH value of 6. Also, the unit cell parameters show slight deviations. In general, compound **2** exhibits the typical arrangement of the heptamolybdate unit. It contains seven MoO_6 octahedra that are condensed into a polyanion structure by edge-sharing. The bond lengths and angles of **2** show no considerable differences to those of the structure by Evans. The Mo-O bond distances of **2** range between 1.713(4) and 2.586(4) Å, which correlates reasonably well with the bond separation range reported by Evans, 1.68(5) to 2.62(4) Å. The bond angles of **2** also show no large deviations from those in the structure of Evans. The cations exhibit similar behaviour in both structures: they occupy positions between the polyanions in irregular eight- (K(1), K(5)) and nine- (K(3), K(4), K(6)) coordination with oxygens. The only notable difference between compound **2** and the compound in the literature is the presence of the seven-coordinated potassium, K(2). The K-O distances in **2** are also comparable to those in the literature, ranging from 2.628(5) to 3.423(4) Å.

Four waters of crystallization per heptamolybdate unit are present in compound **2**, forming hydrogen bonds in the structure, which could ultimately assist self-assembly in the solid state. There are six hydrogen bonds which can all be classified as of intermediate length[17] with bond separations O_x-H···O_y ranging between 2.716 and 2.932 Å (Table 2.2).

Table 2.2 Hydrogen bond lengths for compound **2**

Hydrogen bond separations (Å)	
O(25)-H(1)···O(14)	2.932
O(26)-H(3)···O(17)	2.776
O(26)-H(4)···O(16)	2.905
O(27)-H(5)···O(11)	2.767
O(27)-H(6)···O(3)	2.716
O(28)-H(7)···O(4)	2.729

In the unit cell, molecules of **2** pack in regular rows along the a-axis as shown in Figure 2.17 and 2.18 below. Figure 2.17 shows the packing of the heptamolybdate units and waters of crystallization with the potassium cations excluded so as to simplify the picture. One can clearly see the hydrogen bonds between the oxygens, bringing the polyanions in close proximity to each other. The heptamolybdate moieties pack in an interesting manner, seemingly in different orientations. Two rows of heptamolybdate units in a specific orientation are followed by two rows of heptamolybdate units rotated 90° with regard to the previous two rows. The voids formed by the anions contain the potassium atoms and waters of crystallization, as can be seen in Figure 2.18. No other significant intermolecular interactions are present.

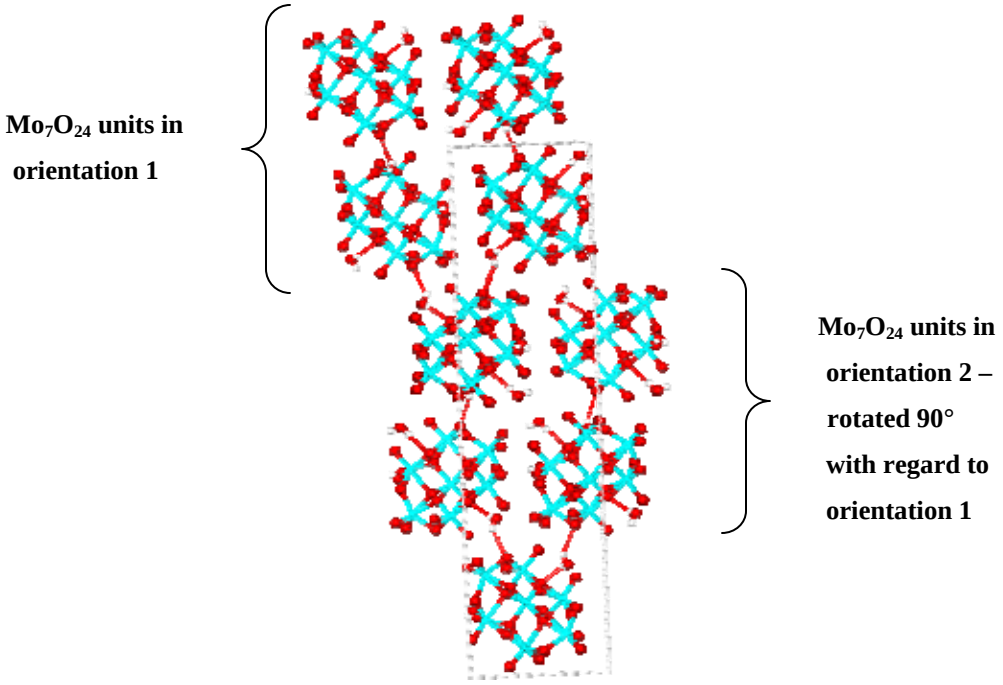

Figure 2.17 Unit cell and packing pattern of compound **2** viewed along the a-axis with the K^+ cations omitted for clarity, showing hydrogen bond formation.

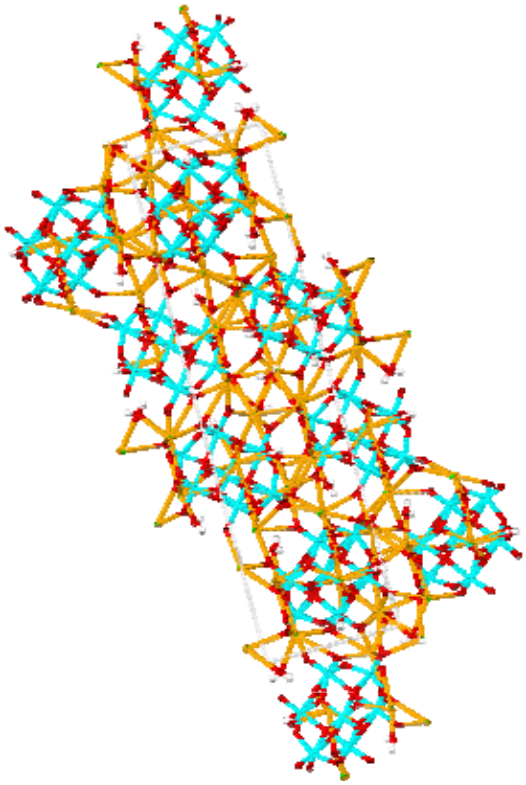

Figure 2.18 Unit cell and packing pattern of compound **2** viewed along the a-axis with the K^+ counter ions (orange) included.

2.2.1.3 Isolation and structural analysis of $[(CH_3)_3N(CH_2)_6N(CH_3)_3]_2[Mo_8O_{26}]\cdot 2H_2O$ (3)

We planned to crystallize a $[Mo_7O_{24}]^{6-}$ polyanion for the first time with $[(CH_3)_3N(CH_2)_6N(CH_3)_3]^{2+}$ acting as counter ion in isolating the complex. The species distribution diagram in Figure 2.1 indicates clearly that such crystallization is to be expected at a pH value of 6, with other species then only present in small amounts under the chosen reaction conditions. Against all expectations and illustrating the unpredictability of Mo(VI) solution chemistry, and despite the fact that the octamolybdate polyanion is only present in negligible amounts at this pH, it was isolated with the hexamethonium cation as counter ion. This result also demonstrates the influence which the type of counter ion has on the product that crystallizes.

Compound **3** was isolated by dissolving $Na_2MoO_4\cdot 2H_2O$ in a mixture of H_2O and HCl, and adding hexamethonium chloride to the solution at a pH of 6.15. The clear solution was left to crystallize at room temperature. Colourless, rectangular crystals of **3** formed after two weeks.

The molecular structure of compound **3** is represented in Figure 2.19, and selected bond lengths and angles are given in Table 3. The structure was solved in the monoclinic spacegroup $P2_1/n$.

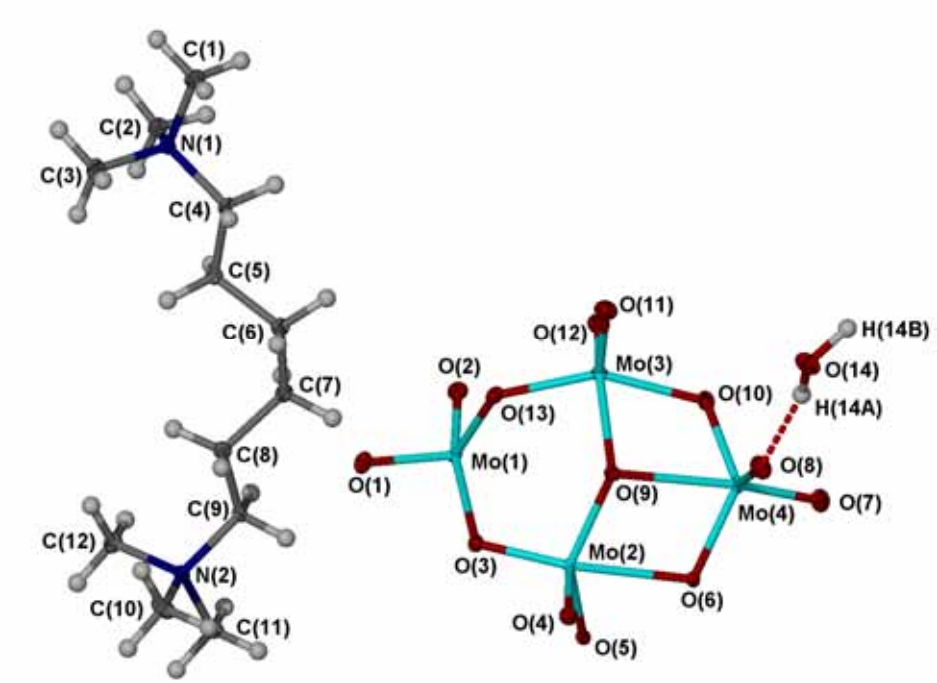

Figure 2.19 Molecular structure of the asymmetric unit of compound **3,** showing the atom numbering scheme. Ellipsoids enclose 50% of the electron density.

The asymmetric unit of compound **3** consists of four molybdenum and thirteen oxygen atoms for the polyoxoanion, one hexamethonium cation as counter ion, and one water of crystallization. Due to the presence of a C_1 center of symmetry, which generates the other half of the structure, the formulation of this compound is in fact $[Mo_8O_{26}][(CH_3)_3N(CH_2)_6N(CH_3)_3]_2 \cdot 2H_2O$.

The octamolybdate polyanion consists of eight Mo atoms and 26 oxygens. Six of the metal centers exist in an octahedral environment, and the other two are coordinated to the surrounding oxygens in a trigonal bipyramidal geometry. This proves that compound **3** is the γ-isomer of the three possible octamolybdate species, as explained earlier in this chapter.[19] The complex also has two hexamethonium cations acting as counter ions, and two waters of crystallization, coordinated to the polyanion through hydrogen bonds, which leads to stabilization of this compound.

This compound has been isolated before by Cruywagen and coworkers.[19] The bond angles and distances are all in the ranges as described by them, and will not be discussed in much detail.

The metal centers Mo(1), Mo(2) and Mo(3) are each octahedrally coordinated to six surrounding oxygen atoms, with two short, two medium and two long Mo-O bonds. Mo(4) is coordinated to the oxygen atoms surrounding the metal center in a trigonal bipyramidal manner, having two short, two medium and one long Mo-O bond. The short bond distances in compound **3** range from 1.695(1) to 1.754(1) Å, the medium bond lengths from 1.835(1) to 2.015(1) Å, and the long bond distances from 2.151(1) to 2.501(1) Å. As seen in Table 2.3, the distances for the terminal oxygen atoms are all in the short range, as is expected since this confirms the double bonding in the structure.

The terminal O-Mo-O angles range between 104.59(9) and 105.16(9)°, which is significantly larger than the normal 90° angles of octahedral and trigonal bipyramidal *cis* groups. For the three octahedrally coordinated Mo atoms, one would expect 90° angles between the six ligands coordinated to the metal atom. However, this is not the case, which illustrates the distortion of geometry this complex undergoes to form this cage-like structure. The O-Mo-O bond angles (between the single-bonded equatorial and axial Mo atoms) for Mo(1), Mo(2) and Mo(3) range from 71.56(7) to 103.54(8), which differs significantly from the expected 90° angles. For Mo(4), the bond angles between the ligands on the equatorial plane of the trigonal bipyramid, O(6), O(8) and O(10), deviate greatly from the ideal of 120°. These obtuse angles are in fact 113.62(8), 112.47(9) and 122.40(8) respectively. For the axial plane, the O(7)-Mo(4)-O(9) angle is 164.08(8), which once again differs appreciably from the typical 180° bond angle that exists in this type of geometry.

The bond distances and angles for the hexamethonium cation are all in the expected ranges and are not discussed here.

The packing of compound **3** is shown in Figures 2.20 and 2.21. When viewed along the b-axis (Fig. 2.20), one can see four octamolybdate anions packing together and forming a cavity that encapsulates four hexamethonium counter ions. Along the c-axis (Fig. 2.21) the oxygens O(7) and O(8) form stabilizing hydrogen bonds with the waters of crystallization in the voids that are formed, with the counter ions taking up the rest of the space in the cavities. The hydrogen bonds can be classified as of intermediate length (2.52–2.95 Å)[17], with O(14)-H(14B)···O(7) and O(14)-H(14A)···O(8) being 2.840 Å and 2.830 Å respectively. No other significant intermolecular interactions are noted.

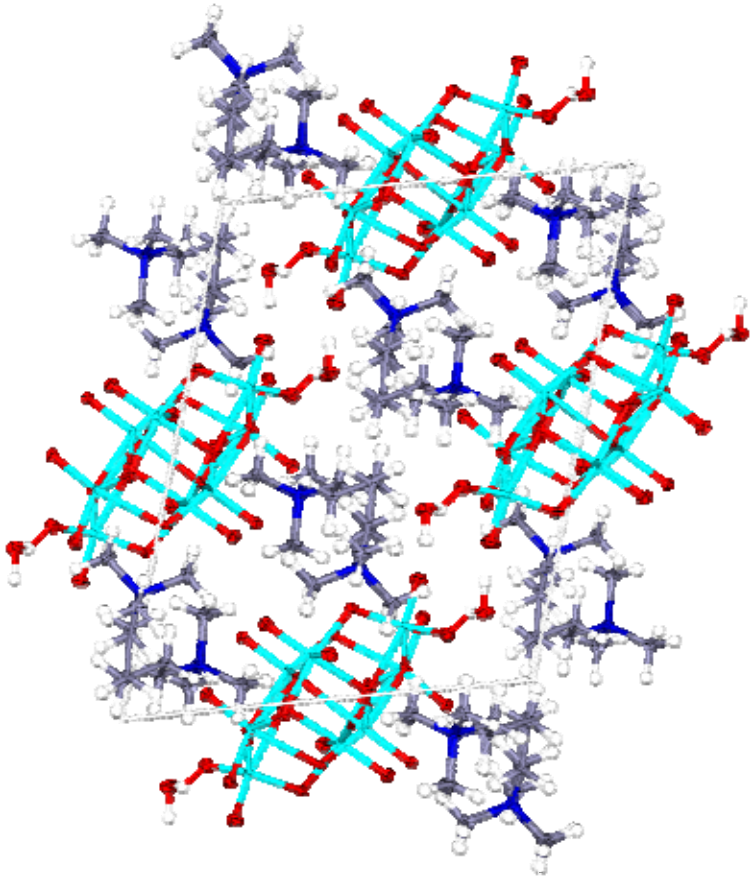

Figure 2.20 Unit cell and packing pattern of compound **3** viewed along the b-axis, showing the cavities that form and the location of the counter ion with regard to the polyanion.

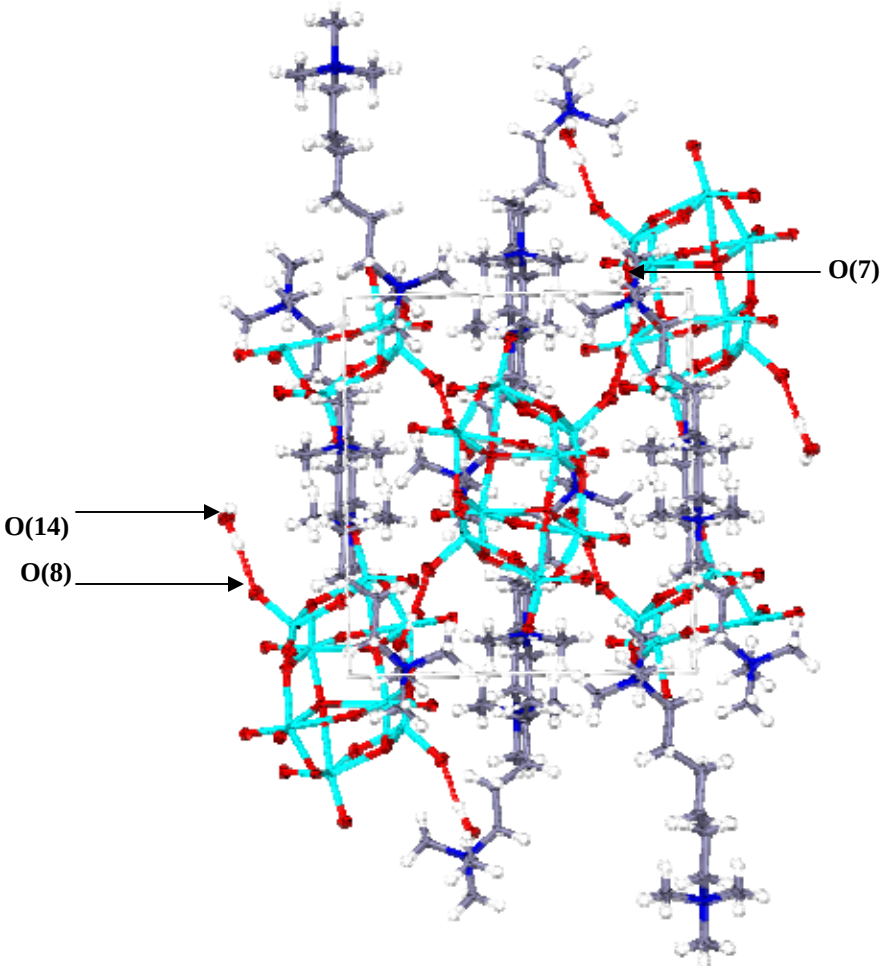

Figure 2.21 Unit cell and packing pattern of compound **3** viewed along the c-axis, showing the hydrogen bonds. O(7) is placed behind the cation and cannot be clearly shown.

Table 2.3 Selected bond lengths and angles for compound **3** with e.s.d.s in parentheses.

Bond lengths (Å)

Mo(1)-O(2)	1.700(1)	Mo(3)-O(11)	1.699(2)
Mo(1)-O(1)	1.705(1)	Mo(3)-O(12)	1.706(1)
Mo(1)-O(13)	1.907(1)	Mo(3)-O(13)	1.927(1)
Mo(1)-O(6)	2.015(1)	Mo(3)-O(10)	1.998(1)
Mo(1)-O(5)	2.222(1)	Mo(3)-O(9)	2.151(1)
Mo(1)-O(3)	2.338(1)	Mo(3)-O(5)	2.501(1)
Mo(2)-O(4)	1.695(1)	Mo(4)-O(7)	1.708(1)
Mo(2)-O(3)	1.754(1)	Mo(4)-O(8)	1.714(1)
Mo(2)-O(9)	1.899(1)	Mo(4)-O(10)	1.835(1)
Mo(2)-O(5)	1.911(1)	Mo(4)-O(6)	1.907(1)
Mo(2)-O(6)	2.259(1)	Mo(4)-O(9)	2.321(1)
Mo(2)-O(5)	2.468(1)		

Bond angles (°)

O(1)-Mo(1)-O(3)	86.56(7)	O(10)-Mo(3)-O(9)	75.36(7)
O(1)-Mo(1)-O(5)	157.24(8)	O(11)-Mo(3)-O(9)	99.50(8)
O(1)-Mo(1)-O(6)	98.43(8)	O(11)-Mo(3)-O(10)	100.38(9)
O(1)-Mo(1)-O(13)	104.15(8)	O(11)-Mo(3)-O(12)	105.16(9)
O(2)-Mo(1)-O(1)	104.59(9)	O(11)-Mo(3)-O(13)	99.59(8)
O(2)-Mo(1)-O(3)	168.86(8)	O(12)-Mo(3)-O(9)	154.17(8)
O(2)-Mo(1)-O(13)	98.44(8)	O(12)-Mo(3)-O(10)	92.56(8)
O(5)-Mo(1)-O(3)	71.79(6)	O(12)-Mo(3)-O(13)	98.47(8)
O(6)-Mo(1)-O(3)	81.80(7)	O(13)-Mo(3)-O(9)	84.69(7)
O(6)-Mo(1)-O(5)	72.21(6)	O(13)-Mo(3)-O(10)	153.75(8)
O(13)-Mo(1)-O(3)	78.33(7)	O(6)-Mo(4)-O(9)	72.51(7)
O(13)-Mo(1)-O(5)	78.76(7)	O(7)-Mo(4)-O(6)	98.60(9)
O(13)-Mo(1)-O(6)	148.75(7)	O(7)-Mo(4)-O(8)	105.1(1)
O(3)-Mo(2)-O(5)	99.29(8)	O(7)-Mo(4)-O(9)	164.08(8)
O(3)-Mo(2)-O(6)	162.42(7)	O(7)-Mo(4)-O(10)	100.96(9)
O(3)-Mo(2)-O(9)	103.54(8)	O(8)-Mo(4)-O(6)	113.62(8)
O(4)-Mo(2)-O(5)	104.55(8)	O(8)-Mo(4)-O(9)	90.78(8)
O(4)-Mo(2)-O(6)	93.06(7)	O(8)-Mo(4)-O(10)	112.47(9)
O(9)-Mo(2)-O(5)	136.98(7)	O(10)-Mo(4)-O(6)	122.40(8)
O(9)-Mo(2)-O(6)	74.15(7)		

2.2.1.4 Isolation and structural analysis of $[(CH_3CH_2)_4N]_2[W_6O_{19}]$ (4)

The idea behind this synthesis was to isolate a W(VI) complex coordinated to one or more malic acid moiety, with $[(CH_3CH_2)_4N]^+$ acting as counter ion. We decided to use a low pH of 3.27 to try and avoid the formation of polyanions, which, from our experience, generally form at pH values higher than this. However, we still isolated a hexatungstate complex. The $[W_6O_{19}]^{2-}$ ion is isomorphous to the hexamolybdate compound that has been synthesized previously by Liu *et al.*[20] with the same counter ion, but at a much lower pH value. Furthermore, the compound in the literature comprised both Mo (75%) and W (25%) in the structure. No pure tetraethylammonium hexatungstate has been isolated in the solid state until now.

Compound **4** was isolated by reacting $Na_2WO_4{\cdot}2H_2O$ with malic acid and tetraethylammonium chloride, at a pH of 3.27. The clear solution was left undisturbed at room temperature for three months, after which time small, colourless rectangular crystals of **4** formed.

The molecular structure of compound **4** is represented in Figure 2.22, and selected bond lengths and angles are given in Table 2.4. The structure was solved in the tetragonal spacegroup *P4/mnc*.

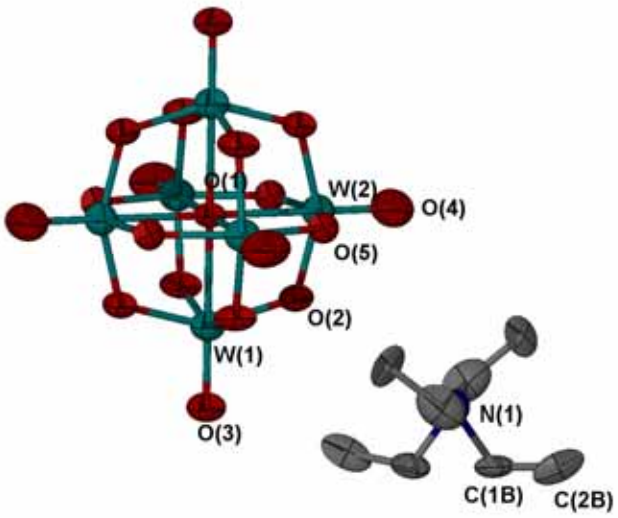

Figure 2.22 Molecular structure of **4** showing the atom numbering scheme. Ellipsoids enclose 50% of the electron density.

The asymmetric unit of compound **4** consists of two W(VI) atoms and five O atoms, and a half of the $[(CH_3CH_2)_4N]^+$ cation as counter ion. This is a very symmetric molecule, having amongst others, a 4-fold rotation axis and two 2-fold rotation axes. The symmetry operators give rise to the actual structure, which consists of six W(VI) atoms and nineteen oxygens, as well as two $[(CH_3CH_2)_4N]^+$ counter ions. All the W atoms in the $[W_6O_{19}]^{2-}$ moiety exist in a six-coordinated pseudo-octahedral arrangement. The counter ions are not coordinated to the polyanion, but rather exist in the area surrounding it.

As mentioned earlier, this structure has a molybdenum analogue, $[Mo_6O_{19}]^{2-}$. This polyanion was isolated by Huang Liu and coworkers,[20] with the same tetraethyl ammonium counter ion. The structure has many similarities to that of compound **5**, and the bond angles and distances do not differ significantly. As mentioned earlier, the Mo complex has a mixed occupancy of Mo and W, with Mo having an occupancy of 75%. The counter ions are also disordered such as ours. The $[W_6O_{19}]^{2-}$ moiety has been isolated in the past with a range of counter ions, but never with a smaller counter ion such as tetraethyl ammonium. For the most part, it has been crystallized in the presence of large cations containing phenyl rings or bulky pendant arms. The only structures similar to **4** are the two structures isolated with tetrabutyl ammonium[21] and tripropyl ammonium.[22] These structures show no significant deviations from the bond distances and angles of compound **4**.

Both W(1) and W(2) are octahedrally coordinated to six surrounding oxygens. The bond distances show that there are short, medium and long bond lengths in this structure. W(2)-O(4) and W(1)-O(3) fall in the short range (1.59(2) to 1.69(2) Å), W(2)-O(2) and W(1)-O(2) exhibit medium bond separations of 1.87(1) to 1.96(1) Å, and W(2)-O(1) and W(1)-O(1) have the longest bond distance range of 2.323(1) to 2.327(1) Å.

Ideally, the angles of the W(1) and W(2) atoms and their symmetry generated counterparts, should involve 90° angles, however, this was not found. Rather the O(1)-W(2)-(2) and O(1)-W(1)-O(2) angles are 76.5(4)° and 75.0(3)° respectively, which is dramatically more acute than the expected 90°. On the other hand, the O(2)-W(1)-O(3)

and O(4)-W(2)-O(2) angles are 105.0(3)° and 103.5(4)° respectively, which is significantly more obtuse than 90°.

The cations, which play an important role in stabilizing the structure, are two $[(CH_2CH_2)_4N]^+$ molecules. These counter ions (of which one is shown in Figure 2.22) are severely disordered and made solving this structure quite difficult. The carbon atoms in the "arms" of the counter ions ossilate/vibrate and cause disorder in the structure. The cations were thus assigned two orientations, to account for the disorder.

In the unit cell, molecules of **4** pack together as shown in Figure 2.23 and 2.24. When viewed along the c-axis, it can be seen that this highly symmetrical molecule packs in a manner which forms cavities. The tetraethylammonium counter ion molecules are encapsulated by these cavities. It is also interesting to note that although it seems that one hexatungstate anion prefers to pack in between four surrounding hexatungstates; there is in fact a hexatungstate unit packed above and one below the other four, nestling into the cavity created by these polyanions.

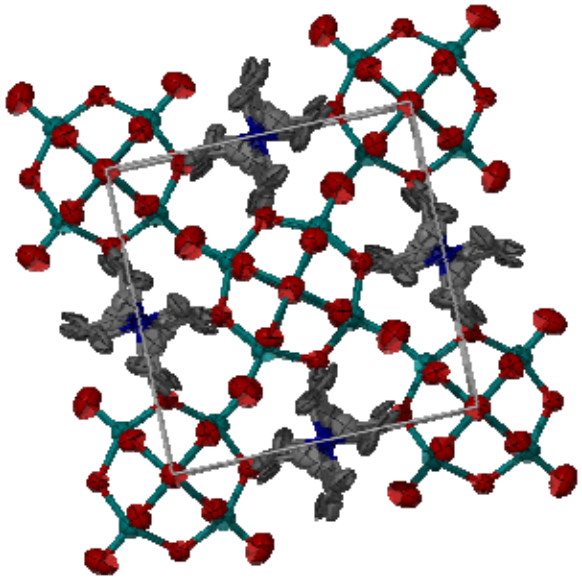

Figure 2.23 Unit cell and packing pattern of compound **4** viewed along the c-axis, illustrating the cavities created and the location of the counter ion relative to the polyanion moiety.

When viewed along the a-axis, the packing looks a bit different. Here, it can be seen that four hexatungstate molecules pack together in a layer, with the tetraethylammonium counter ions almost "embracing" them.

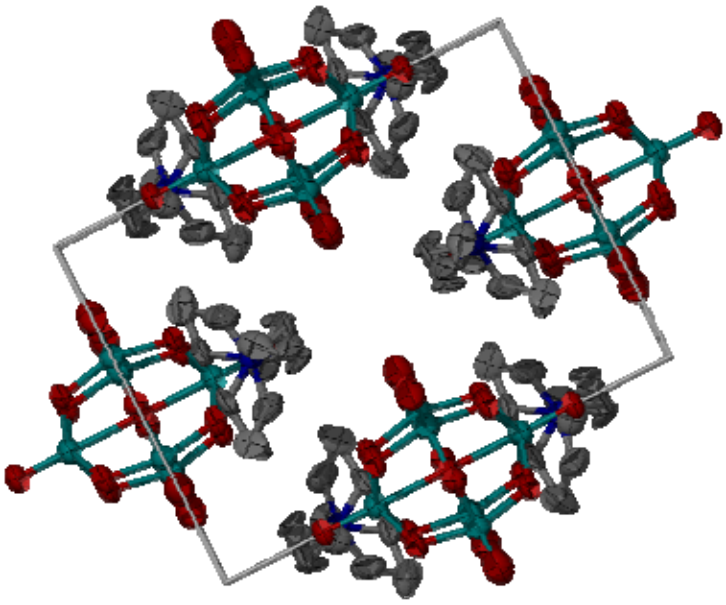

Figure 2.24 Unit cell and packing pattern of **4** viewed along the a-axis, showing the location of the counter ions.

Table 2.4 Selected bond lengths and angles for compound **4** with e.s.d.s in parentheses.

Bond lengths (Å)

W(2)-O(4)	1.59(2)	W(1)-O(3)	1.69(2)
W(2)-O(2)	1.87(1)	W(1)-O(2)	1.96(1)
W(2)-O(1)	2.327(1)	W(1)-O(1)	2.323(1)

Bond angles (°)

O(4)-W(2)-O(2)	103.5(4)	O(2)-W(1)-O(2)	86.1(1)
O(2)-W(2)-O(2)	153.0(8)	O(2)-W(2)-O(1)	76.5(4)
O(4)-W(2)-O(1)	180(1)	W(1)-O(1)-W(1)	180.0
O(2)-W(1)-O(1)	75.0(3)	W(1)-O(1)-W(2)	90.0
O(3)-W(1)-O(2)	105.0(3)	W(2)-O(1)-W(2)	90.0
O(2)-W(1)-O(2)	149.9(6)		

2.2.2 Complexes of Mo(VI) and W(VI) with carboxylic acids as ligands

In our attempts to isolate new complexes of Mo(VI) and W(VI) using the *α*-hydroxycarboxylic acids malic, tartaric and citric acid as ligands, only complexes with malic and citric acid could be isolated as single crystals. Although tartaric acid was used in several attempts, new complexes of the tartrate ligand coordinated to a metal center could not be isolated with either molybdenum or tungsten. The counter ions and compounds NH_4^+, K^+, NMe_4Cl, NEt_4Cl, NPr_4I and NBu_4Br were used in the reactions with each metal and carboxylic acid. In the preparations, the molar ratios of metal to ligand were varied from 1:1 and 1:2 to 2:1 and 2:2, and in most instances the molar ratio of metal to counter ion was 1:1. The concentration, pH and crystallization conditions of each reaction were systematically varied to attempt the crystallization of a new compound. In general the very stable species $Na_6[Mo_7O_{24}]\cdot 5H_2O$ and $Na_6[W_2O_5(cit)_2]\cdot 10H_2O$ were isolated in the solid state, although it is possible that the species which actually formed in highest concentration during the reactions did not crystallize out of solution. Still, two new complexes of Mo(VI) and W(VI) with *α*-hydroxycarboxylic acids were isolated in crystalline form. Their structural analyses are described in the next section. One known compound was also isolated, and its structure and any differences with the complex in the literature will be emphasized.

2.2.2.1 Isolation and structural analysis of $[(CH_3CH_2)_4N][MoO_3(mal)]\cdot H_2O$ (5)

We chose these reaction conditions to attempt the synthesis of a new complex of Mo(VI) with malate as ligand and $[(CH_3CH_2)_4N]^+$ as counter ion. As described earlier, malic acid can adopt bidentate and tridentate coordination modes, and this reaction formed part of a series in which we wished to investigate if certain coordination modes are preferred at certain pH values. We attempted this reaction at pH values ranging between 3 and 7, but unfortunately, in most cases either no crystals were formed, or the stable $Na_6[Mo_7O_{24}]\cdot 5H_2O$ species was isolated as single crystals. It is interesting to note, however, that according to the species distribution diagram Figure 2.1, at this pH the heptamolybdate polyanion exists almost exclusively in solution. Also, Mo tends to prefer a 1:2 metal to ligand ratio for complexes with hydroxyacids such as malic acid. Thus the

coordination of the malate and the stabilizing effect of the counter ion led to the isolation of a mononuclear Mo(VI) complex even under unfavourable conditions.

Compound **5** was synthesized by reacting $Na_2MoO_4 \cdot 2H_2O$ with HCl, malic acid and tetraethylammonium chloride, at a pH of 4.59. The solution was left to stand at room temperature, and large colourless rectangular crystals of **5** formed after two months.

The molecular structure of compound **5** is represented in Figure 2.25, and selected bond lengths and angles are given in Table 2.5. The structure was solved in the monoclinic spacegroup *C*2/c.

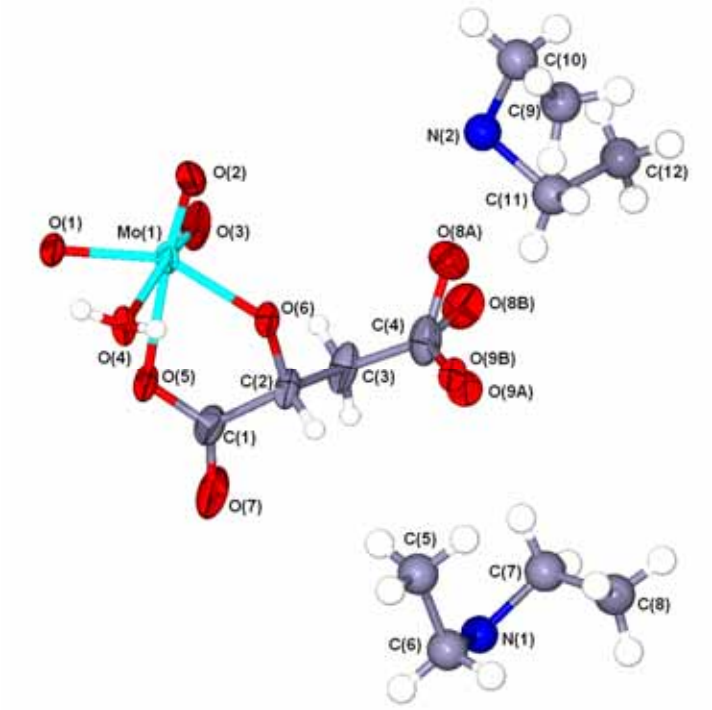

Figure 2.25 Molecular structure of compound **5** showing the atom numbering scheme. Ellipsoids enclose 50% of the electron density. Owing to disorder the counter ion atoms are not displayed as ellipsoids. The counter ion is displayed as two halves of one cation, and both O(8) and O(9) are disordered (see text).

This structure comprises a single six-coordinated Mo(VI) atom in an octahedral arrangement, coordinated bidentately to one deprotonated malic acid (malate) moiety and one tetraethyl ammonium cation, acting as counter ion for the complex, as well as one water of crystallization. The counter ion is shown in Figure 2.25 as two halves of one cation rather than one complete cation. The reason for this is that there are two counter ions lying on the edge of the unit cell with one half inside and one half outside, thus leading to only one counter ion as part of the unit cell. The counter ion is disordered: the pendant carbon "arms" of the cation ossillate and cause disorder in the structure. Therefore, the cation atoms are shown in Figure 2.25 as spheres rather than ellipsoids for clarity. The counter ion is not coordinated to the metal complex, but rather exists in the area surrounding it. The oxygen atoms of the free carboxylic group of the malate moiety are also disordered, and are thus assigned two possible occupations each.

A number of structures of molybdenum with malic acid have been isolated in the past,[23] but no 1:1 complex of Mo with malate coordinated bidentately to the metal center has been crystallized until now. An interesting structure worth noting is the tetraammonium dimolybdomalate hexahydrate complex,[23] in which two malate moieties are coordinated to a dimolybdate unit in a tetradentate mode, which is quite uncommon for malic acid.

For an octahedral environment such as that of Mo(1), one would expect Mo(1)-O(5) and Mo(1)-O(6) to have more or less the same bond distance, but in fact, this is not found. The lengths of these bonds are 2.216(5) and 1.986(4) Å respectively, which deviate quite dramatically from one another. Mo(1)-O(4) has a bond separation of 2.338(4) Å, which confirms the coordination of Mo(1) to a water molecule. The bond distance Mo(1)-O(1) exhibits a typical length for terminal oxygens, 1.897(1) Å. The distances Mo(1)-O(2) and Mo(1)-O(3), which are 1.693 and 1.704 Å respectively, clearly illustrates that these two are the double bonded O atoms.

The octahedral environment surrounding Mo(1) shows some distortion from the geometry. Typically, a molecule with this type of molecular geometry would have 90° angles between its substituents. Some of the angles in this structure, however, show

significant deviations from this. The O(3)-Mo(1)-O(1) and O(3)-Mo(1)-O(6) angles are much larger than the expected 90°, at 99.7(2)° and 97.8(2)° respectively, whereas the O(1)-Mo(1)-O(4) and O(6)-Mo(1)-O(4) angles are appreciably more acute, at 79.2(1)° and 79.4(1)° respectively. This illustrates the distortion this molecule undergoes to allow coordination to the malate unit.

The packing of compound **5** is shown in Figures 2.26a, b & c. Owing to the disorder in the structure, some atoms are not displayed as ellipsoids. When viewed along the c-axis (Fig. 2.26a), one can clearly see the dimers that form, connecting two units by oxygen bridge formation between the two metal centers. These dimers pack together forming cavities, which encapsulate the tetraethylammonium counter ions. In Figure 2.26b the cations are omitted and the hydrogen bonds connecting the dimers can be seen. Along the b-axis (Fig. 2.26c), the dimers are once again visible, and also the formation of hydrogen bonds in the cavities formed by the packing of the complex. The hydrogen bonds, although classified as intermediate (2.52-2.95 Å),[17] are nonetheless strong enough to introduce molecular recognition and direct self assembly in the solid state. The bond separations O(4)-H(1)···O(6) and O(4)-H(2)···O(5) are 2.771 and 2.806 Å respectively. No other significant molecular interactions are present.

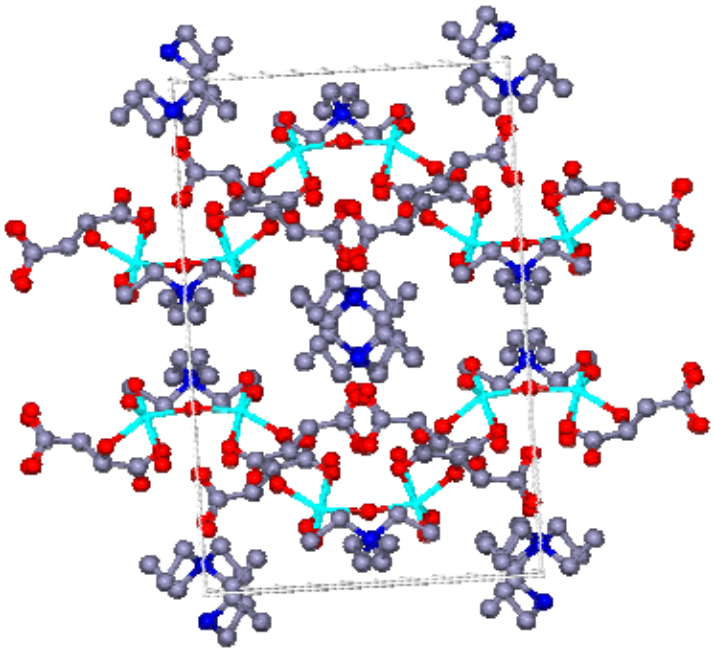

Figure 2.26a Unit cell and packing pattern of **5** viewed along the c-axis, showing the dimers and the location of the cations.

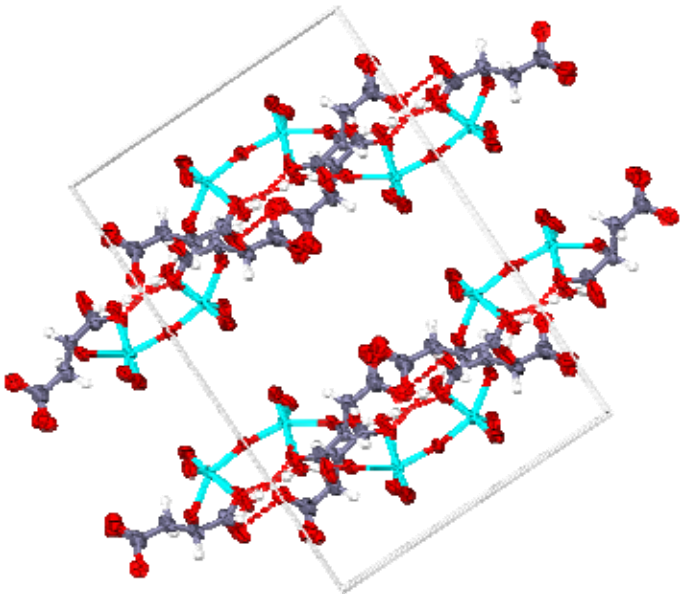

Figure 2.26b Unit cell and packing pattern of **5** viewed along the c-axis, omitting the counter ions for clarity, showing the hydrogen bonds stabilizing the structure.

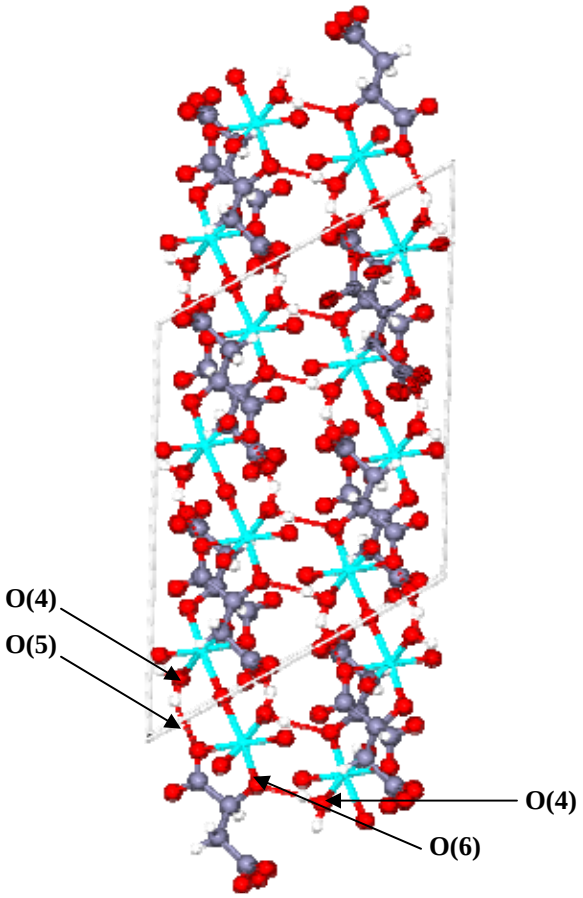

Figure 2.26c Unit cell and packing pattern of **5** viewed along the b-axis, omitting the counter ions for clarity, showing the dimers and hydrogen bonds.

Table 2.5 Selected bond lengths and angles for compound **5** with e.s.d.s in parentheses.

Bond lengths (Å)

Mo(1)-O(1)	1.897(1)	C(1)-C(2)	1.51(1)
Mo(1)-O(2)	1.693(6)	O(6)-C(2)	1.415(8)
Mo(1)-O(3)	1.704(5)	C(2)-C(3)	1.52(1)
Mo(1)-O(4)	2.338(4)	C(3)-C(4)	1.49(1)
Mo(1)-O(5)	2.216(5)	C(4)-O(8A)	1.37(1)
Mo(1)-O(6)	1.986(4)	C(4)-O(8B)	1.18(1)
C(1)-O(7)	1.238(9)	C(4)-O(9A)	1.22(3)
C(1)-O(5)	1.269(8)	C(4)-O(9B)	1.27(3)

Bond angles (°)

O(1)-Mo(1)-O(4)	79.2(1)	O(5)-Mo(1)-O(4)	77.7(1)
O(1)-Mo(1)-O(5)	83(1)	O(6)-Mo(1)-O(4)	79.4(1)
O(1)-Mo(1)-O(6)	151.7(2)	O(6)-Mo(1)-O(5)	74.5(1)
O(2)-Mo(1)-O(1)	103.6(1)	C(1)-O(5)-Mo(1)	114.4(5)
O(2)-Mo(1)-O(3)	103.7(3)	C(2)-O(6)-Mo(1)	119.1(4)
O(2)-Mo(1)-O(4)	86.9(3)	O(5)-C(1)-C(2)	116.7(6)
O(2)-Mo(1)-O(5)	161.8(3)	O(6)-C(2)-C(1)	108.6(5)
O(2)-Mo(1)-O(6)	93.6(2)	O(6)-C(2)-C(3)	111.2(7)
O(3)-Mo(1)-O(1)	99.7(2)	O(8B)-C(4)-O(9A)	115(1)
O(3)-Mo(1)-O(4)	169.3(3)	O(8B)-C(4)-O(9B)	127(1)
O(3)-Mo(1)-O(5)	91.7(3)	O(9A)-C(4)-O(8A)	120(1)
O(3)-Mo(1)-O(6)	97.8(2)	O(9B)-C(4)-O(8A)	111(1)

2.2.2.2 Isolation and structural analysis of $Na_6[Mo_2O_5(cit)_2]$ (6)

With this synthesis we planned to isolate a new Mo(VI) complex with citrate as ligand, and possibly Na^+ cations as counter ions. As described earlier, citric acid can adopt many coordination modes, from bidentate to tetradentate. Once again this reaction formed part of our study to investigate the influence which reaction conditions could have on the coordination of the ligand and the type of species that crystallizes. We attempted the same reaction several times, each time varying either the metal to ligand ratios, pH of the solution, concentration of the ligand or changing the starting reagent. In most instances either no crystals were isolated, or the stable $Na_6[Mo_7O_{24}]\cdot 5H_2O$ species formed. However, after many attempts, one of the reactions (see experimental section 2.4.2.6) proved to be successful, and we could isolate a new compound of Mo(VI) with the ligand. Interestingly, even though Mo(VI) normally prefers a 1:2 metal to ligand ratio in its complexes with citrate, a 2:2 complex was in fact isolated.

Compound **6** was synthesized by reacting $Na_2MoO_4{\cdot}2H_2O$ with citric acid and tetraethylammonium chloride in a slightly acidic aqueous solution. The solution was left undisturbed at room temperature, and large colourless crystals of **6** formed after five months.

The molecular structure of compound **6** is represented in Figure 2.27, and selected bond lengths and angles are given in Table 2.6. The structure was solved in the triclinic spacegroup *P*$\bar{1}$. A simplified representation of its molecular structure in which the counter ions are omitted can be seen in Figure 2.28.

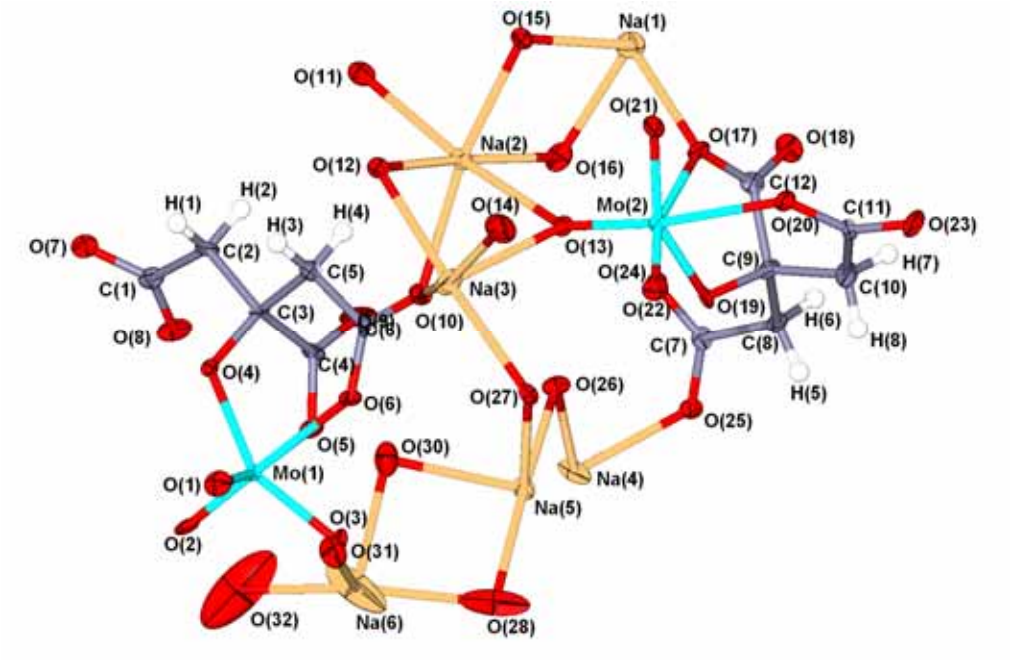

Figure 2.27 Molecular structure of compound **6** showing the atom numbering scheme. Ellipsoids enclose 50% of the electron density.

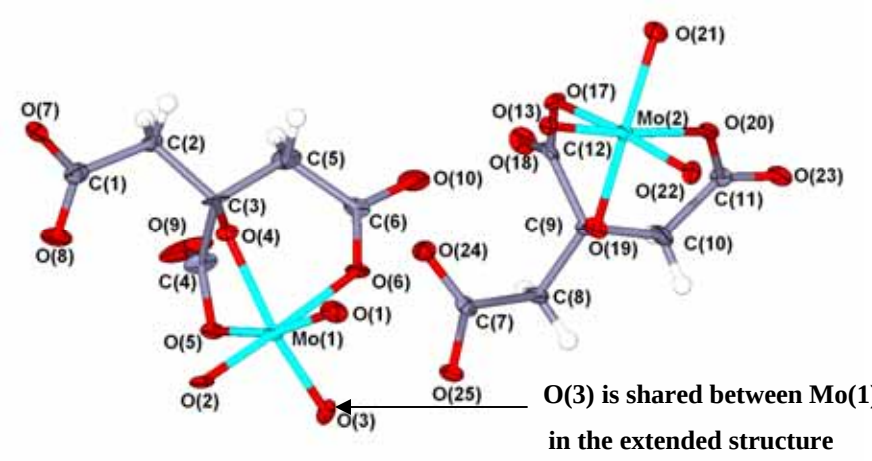

Figure 2.28 Molecular structure of compound **6** with the Na^+ counter ions omitted for clarity. Ellipsoids enclose 60% of the electron density.

The structure of compound **6** is represented in Figures 2.27 and 2.28 as two separate Mo(VI) centers coordinated each to one citrate moiety. In the unit cell, no sharing of atoms between these two Mo units can be seen. However, when looking at the extended structure, it becomes clear that this compound is in fact a Mo(VI) dimer (Mo_2O_5) coordinated to two citrate ligands. This will become apparent when looking at the packing diagrams of **6** later in this section (Fig. 2.29a & b).

The simplest unit of compound **6** comprises two Mo(VI) atoms, both in an octahedral environment, as well as two citrate moieties and six Na^+ counter ions. As mentioned above, the compound is in fact a dimer, with an oxygen bridge between the two octahedrally coordinated metal centers. Each metal atom is coordinated to two terminal oxygen atoms, the oxygen bridge between them and one citrate unit. The citrate acts as a tridentate ligand, coordinating through the oxygen atoms of one deprotonated hydroxyl group and two deprotonated carboxylate groups, forming five- and six-membered rings with the metal. In the extended structure (Fig. 2.29a) it can be seen that the six Na^+ counter ions are in fact all six-coordinate, except for Na(1) and Na(4), which are five-coordinate.

A few related structures of compound **6** have been isolated in the past, including its tungsten analogue, $Na_6[W_2O_5(cit)_2]\cdot 10H_2O$, which was isolated in 1992 by Cruywagen *et al.*.[24] This structure shows some similarities to compound **6**, with small differences in bond lengths and angles, as would be expected for the different metals. However, the Mo structure has not been characterized until now. Also, it is worth noting that compound **6** was isolated without any waters of crystallization. As for Mo(VI) structures, a number of similar complexes are known, the most relevant in this instance being the two compounds by Zhou and coworkers,[25,26] namely tetrapotassium-bis(hydrogencitrate)-tetraoxo-dimolybdate tetrahydrate and tetrasodium-dipotassium-bis(citrato)-bis(dioxo-molybdenum(VI)) pentahydrate. The latter complex differs from compound **6** not only in composition: the oxygen bridge between the two molybdenum atoms are at an angle of 154°, whereas the oxygen bridge in **6** is a straight Mo-O-Mo bond. This straight oxygen bridge is also seen in the tetrapotassium compound by Zhou. The bond lengths and angles in the two literature compounds show some great similarities to that of compound **6**. Still, no pure sodium salt of the Mo(VI)-citrate dimer has been isolated until now.

In the octahedral environment of Mo(1), the substituents O(1), O(3), O(4) and O(5) could form an equatorial plane, with O(2) and O(6) occurring axial to this plane. The bond distances for the terminal oxygens, Mo(1)-O(1) and Mo(1)-O(2), are 1.718(5) and 1.729(5) Å respectively, which is typical of Mo-O double bonds.[16] The bond separation Mo(1)-O(3) is, however, 1.868(1) Å, which is significantly larger than the average values for terminal Mo-O bonds.[16] This could be explained by the fact that the structure of compound **6** is a dimer, with O(3) being the bridging oxygen, which is confirmed when looking at the packing diagram later in this section (Fig. 2.29). When looking at Mo(2), the same tendency in bond distances is obvious. The bond lengths for the double bonded oxygens Mo(2)-O(13) and Mo(2)-O(22) are 1.724(5) and 1.698(5) Å respectively, whereas the bond separation Mo(2)-O(21) is again appreciably longer at 1.884(1) Å. The Mo-O bond distances for the coordinated oxygens of the citrate unit (O(4), O(5), O(6), O(17), O(19) and O(20)) are all in the ranges as seen in related compounds.[25,26] Furthermore, it is worth noting that the *trans* lengthening effect, as described by Cruywagen[24] for the tungsten analogue of compound **6**, is clearly demonstrated by these

bond distances. This *trans* lengthening effect, which is caused by the terminal oxygen ligands lying *trans* to the coordinated oxygen in the organic ligand, has been seen with many complexes of W(VI) and Mo(VI) with carboxylates. The C-C, C-O and C-H bond distances show no significant deviations from those in related structures.[25,26] For the counter ions, the Na-O separations are in the range of 2.310(6) to 2.661(8) Å, which correlates well with those found by Cruywagen *et al.* in the tungsten analogue, 2.32(1) to 2.81(1) Å.[24]

One would expect the angles between the oxygens coordinated to the metal centers to ideally be either 90° or 180°. However, some of these angles show severe distortions from the octahedral geometry, as can be seen by referring to Table 2.6 at the end of this section. For Mo(1), the only angle resembling that of an octahedral environment is the O(2)-Mo(1)-O(5) angle which is 92.1(2)°. All the other angles show deviations of 4° to 30° from the expected 90° or 180° angles. The same tendency can be seen for Mo(2), but in this instance two angles close to 90° are found, with O(13)-Mo(2)-O(17) and O(22)-Mo(2)-O(20) being 92.2(2)° and 88.2(2)° respectively. The other angles again differ from the ideal values by 4° to 27°. A possible reason for this is that the chelate rings of the citrate largely maintain their "normal" bond lengths and angles,[24,25,26] and thus to prevent too much strain on the chelate rings, pseudo-octahedral geometry is adopted.

The packing of compound **6** is shown in Figures 2.29a & b. When viewed along the a-axis, one can clearly see the dimers which form *via* oxygen bridge formation. The charges on the dimers are then balanced by the presence of the well-ordered Na^+ counter ions in the cavities which form when the dimers pack together. In Figure 2.29b, the packing of compound **6** is shown without the counter ions, to emphasize the way in which the dimers pack. It seems the Mo_2O_5 units pack in rows with different orientations. Every second row has the same orientation, showing a rotation of approximately 45° with regard to the first row. No hydrogen bonds are present in this structure, and no other significant intermolecular interactions are noted.

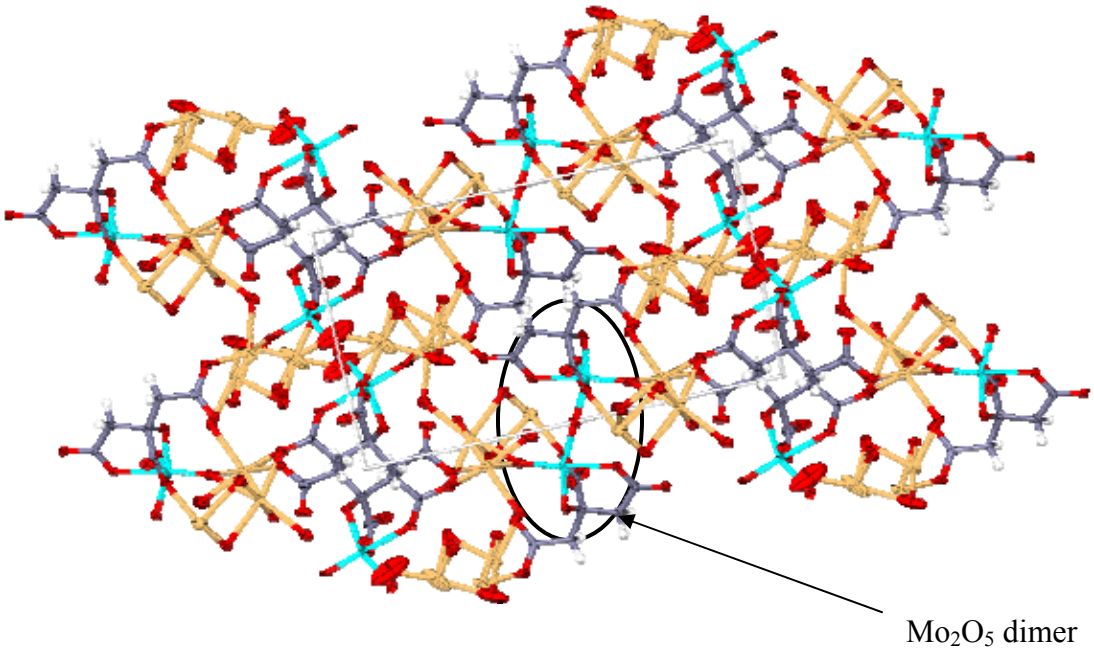

Figure 2.29a Unit cell and packing pattern of **6** viewed along the a-axis, showing the dimers and the location of the Na^+ counter ions (orange).

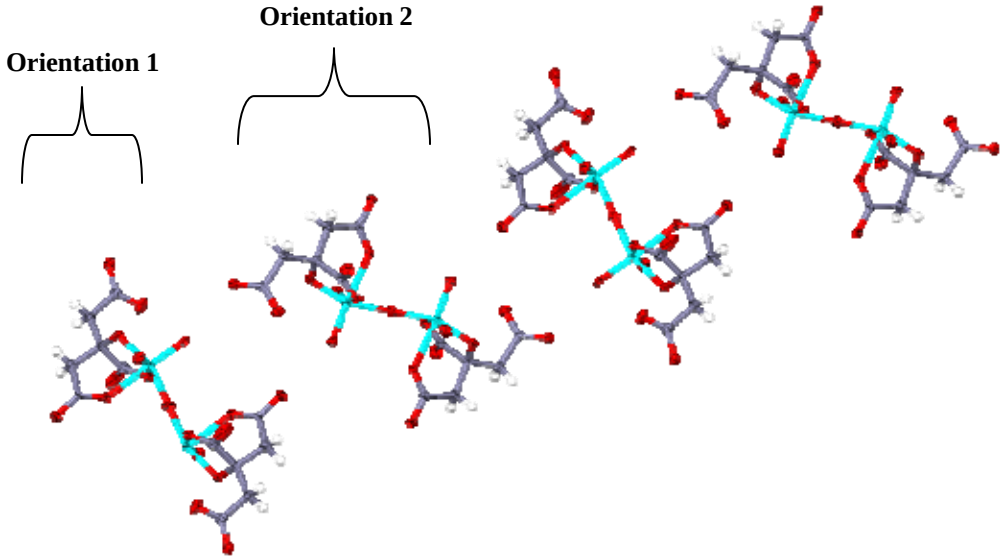

Figure 2.29b Packing pattern of compound **6** with the counter ions omitted, accentuating the structure of the dimers. Orientation 2 shows a 45° rotation with regard to orientation 1.

Table 2.6 Selected bond lengths and angles for compound **6** with e.s.d.s in parentheses.

Bond lengths (Å)

Mo(1)-O(1)	1.718(5)	Mo(2)-O(13)	1.724(5)
Mo(1)-O(2)	1.729(5)	Mo(2)-O(17)	2.227(5)
Mo(1)-O(3)	1.868(1)	Mo(2)-O(19)	1.970(5)
Mo(1)-O(4)	1.955(5)	Mo(2)-O(20)	2.257(5)
Mo(1)-O(5)	2.183(5)	Mo(2)-O(21)	1.884(1)
Mo(1)-O(6)	2.277(5)	Mo(2)-O(22)	1.698(5)

Bond angles (°)

O(1)-Mo(1)-O(2)	102.6(3)	O(13)-Mo(2)-O(17)	92.2(2)
O(1)-Mo(1)-O(3)	101.0(1)	O(13)-Mo(2)-O(19)	98.2(2)
O(1)-Mo(1)-O(4)	95.2(2)	O(13)-Mo(2)-O(20)	168.8(2)
O(1)-Mo(1)-O(5)	163.7(2)	O(13)-Mo(2)-O(21)	99.8(1)
O(1)-Mo(1)-O(6)	86.5(2)	O(17)-Mo(2)-O(20)	76.8(1)
O(2)-Mo(1)-O(3)	100.7(1)	O(19)-Mo(2)-O(17)	73.9(2)
O(2)-Mo(1)-O(4)	99.1(2)	O(19)-Mo(2)-O(20)	81.1(1)
O(2)-Mo(1)-O(5)	92.1(2)	O(21)-Mo(2)-O(17)	84.9(1)
O(2)-Mo(1)-O(6)	170.9(2)	O(21)-Mo(2)-O(19)	152.6(1)
O(3)-Mo(1)-O(4)	150.9(1)	O(21)-Mo(2)-O(20)	77.2(1)
O(3)-Mo(1)-O(5)	82.9(1)	O(22)-Mo(2)-O(13)	103.1(2)
O(3)-Mo(1)-O(6)	77.5(1)	O(22)-Mo(2)-O(17)	162.2(2)
O(4)-Mo(1)-O(5)	75.2(1)	O(22)-Mo(2)-O(19)	94.7(2)
O(4)-Mo(1)-O(6)	79.6(1)	O(22)-Mo(2)-O(20)	88.2(2)
O(5)-Mo(1)-O(6)	78.8(2)	O(22)-Mo(2)-O(21)	101.1(1)

2.2.2.3 Isolation and structural analysis of $[(CH_3)_3N(CH_2)_6N(CH_3)_3][Mo_2O_7(cit)]$ (7)

The aim of this synthesis was to isolate a Mo(VI) citrate complex, comparable to compound **6** and under identical reaction conditions, but using a different counter ion. We investigated the effect that the presence of a larger counter ion, the hexamethonium cation, would have on the ease of crystallization and also on the type of complex which would form during crystallization. It is worth noting that, whereas compound **6** took five months to crystallize, compound **7** was obtained after only six weeks, which could possibly be ascribed to the presence of the large counter ion. Also, compound **6** has the typical formation of a Mo(VI) dimer which consists of two metal centers connected by an oxygen bridge, whereas compound **7** exhibits an unusual structure: an oxygen-bridged dimer of two dimolybdate moieties. This result indicates that the chosen counter ion could have an influence on the type of species that forms.

Compound **7** was synthesized by reacting $Na_2MoO_4 \cdot 2H_2O$ with citric acid and hexamethonium chloride in a slightly acidic, aqueous solution. The solution was left undisturbed at room temperature for six weeks, after which time large colourless crystals of **7** had formed.

The molecular structure of compound **7** is represented in Figure 2.30 and selected bond lengths and angles are given in Table 2.7. The structure was solved in the monoclinic spacegroup *C*2/c.

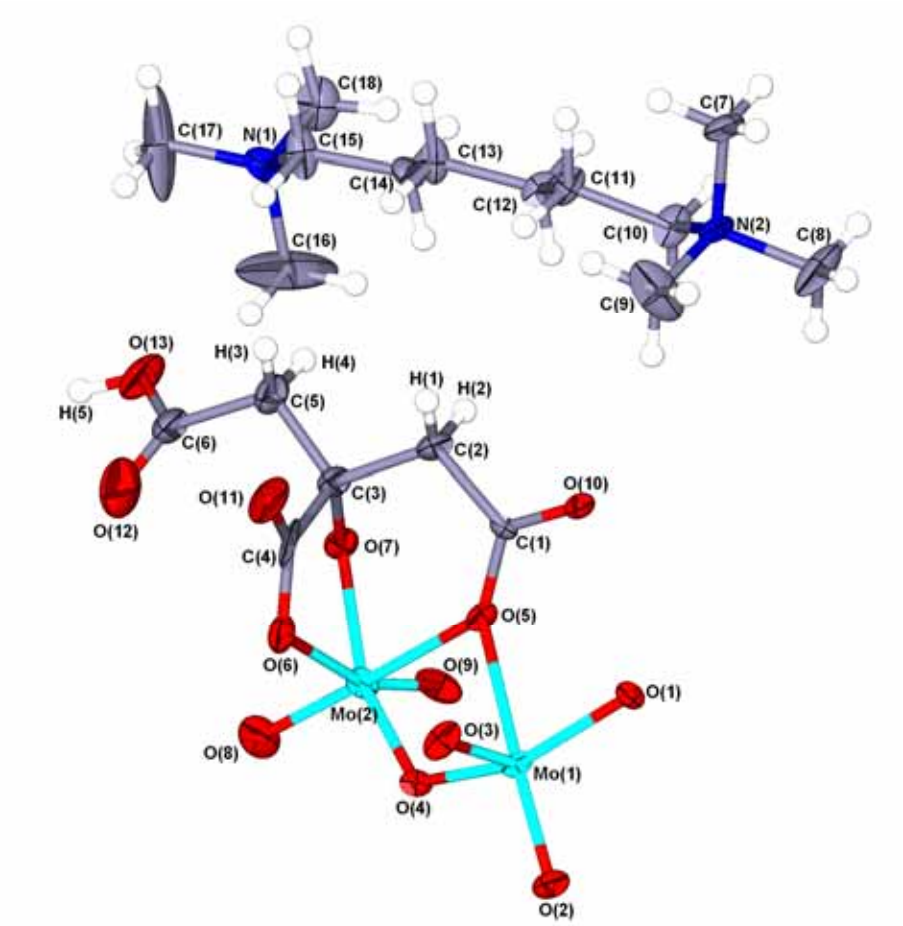

Figure 2.30 Molecular structure of compound **7** showing the atom numbering scheme. Ellipsoids enclose 55 % of the electron density.

As briefly mentioned above, the asymmetric unit of compound **7** comprises two octahedrally coordinated Mo(VI) atoms as a dimolybdate unit, $[Mo_2O_7]$, coordinated to one deprotonated citrate moiety with a hexamethonium counter ion. The actual structure of this unit is a dimer consisting of two dimolybdate moieties connected by an oxygen bridge, with one deprotonated citric acid ligand coordinated tridentately to each dimolybdate, as well as two hexamethonium cations that exist in the area around it. The structure of the dimer coordinated to the citrates is shown in Figure 2.31a, and the structure of the dimer alone is represented in Figure 2.31b. From these figures, one can see that the extended structure exhibits an intriguing feature, i.e. that the deprotonated citrate becomes tetradentate in terms of the tetranuclear metal unit. The second oxygen of the carboxyl group (O(10)) is coordinated to the first Mo atom in the second dimolybdate unit. Similarly, another coupling occurs between the first dimolybdate and the citrate of the second Mo_2 moiety. This then gives rise to two tetradentate citrate units in the structure. It should be noted that there is some residual electron density in the structure which could not be solved. This electron density was calculated by using SQUEEZE in the Platon program,[27] and was then assigned to an unknown number of water molecules. Unfortunately this means that any hydrogen bonds which would exist between the Mo(VI) unit and the surrounding waters of crystallization cannot be specified in this instance.

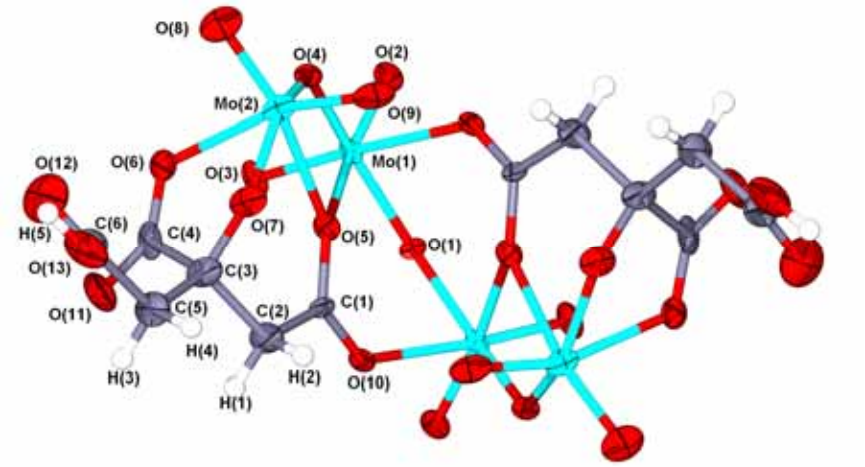

Figure 2.31a Extended structure of compound **7** showing the oxygen-bridged dimer of dimolybdates. The counter ions are omitted for clarity. Ellipsoids enclose 55% of the electron density.

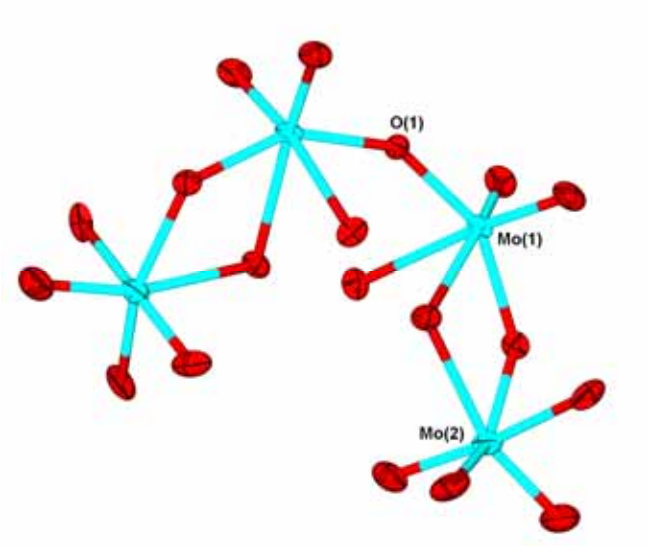

Figure 2.31b Extended structure of compound **7** showing the oxygen-bridged dimer of dimolybdates. The counter ions are omitted for clarity. Ellipsoids enclose 55% of the electron density.

Compound **7** has been isolated before by Nassimbeni *et al.*[28] In their structure, they were able to locate the water molecules, all twelve of them occurring in the channels which form during molecular assembly of the compound, as can be seen in the packing diagrams later on in this section (Fig. 2.32a & b). The bond lengths and angles of compound **7** compare very well with those of the structure by Nassimbeni. No significant differences between the two structures could be found. Compound **7** also has some similarities to compound **1** (see Section 2.2.1.1). Compound **1** is also a dimolybdate, but in compound **7** the two dimolybdates are oxygen-bridged and also coupled by two of the ligands. The bond lengths exhibited by **1** are comparable to those of **7**, but the bond angles of **1** deviate much more from the ideal 90° and 180° angles of an octahedral environment than those in **7**, possibly due to differences in the extended structures. Compound **7** also shows a close resemblance to compound **6** (see Section 2.2.2.2), the only difference being the counter ion and the structure of the dimer: where compound **6** has the typical dimeric structure of two separate metal centers bonded *via* an oxygen bridge, compound **7** consists of two dimolybdate units connected by, amongst others, a single oxygen bridge. Nevertheless, the structures of the asymmetric units of

these compounds exhibit similar tendencies in bond lengths and also comparable bond angles.

Both Mo(1) and Mo(2) exist in an octahedral environment. Even though it initially seems as though Mo(1) is five-coordinate (Fig. 2.30), it follows from the extended structure (Fig. 2.31a) that Mo(1) becomes six-coordinate by sharing an oxygen of the citrate unit of Mo(2), as discussed above. For Mo(1), two short, two medium, and two long Mo-O bonds are present. The bond distances Mo(1)-O(2) and Mo(1)-O(3) are short at 1.710(5) and 1.718(5) Å respectively, indicating double bonds. The atomic separations Mo(1)-O(1) and Mo(1)-O(4) are of medium length at 1.900(2) and 1.926(6) Å, involving the bridging oxygen atoms of the dimer and the dimolybdate moiety respectively. Thus the latter distances are somewhat larger. The Mo(1)-O(5) bond length is appreciably longer than Mo(1)-O(4) at 2.316(5) Å. The former forms part of the citrate moiety. The citrate unit forms five- and six-membered rings with the metal, and these chelate rings cannot distort significantly to accommodate coordination to the dimolybdate, thus the Mo-O atomic separations increase to relieve strain on the chelate rings. The Mo(1)-O(10) distance (with O(10) being the carboxylic oxygen in the symmetry generated Mo unit in the extended structure of compound **7**) is 2.305(5) Å, and this longer bond length could also be explained by the fairly rigid chelate rings. For Mo(2), once again two short, two medium and two long bond separations can be seen. The Mo(2)-O(8) and Mo(2)-O(9) separations are short, being 1.690(7) and 1.716(6) Å respectively, which indicates that they represent double bonds. The medium bond separations are the Mo(2)-O(4) and Mo(2)-O(7) distances at 1.899(5) and 1.967(6) Å, with O(4) being the bridging oxygen of the dimer, and O(7) forming part of the citrate unit. On the longer end, singular the bond distances Mo(2)-O(5) and Mo(2)-O(6) at 2.333(6) and 2.217(6) Å respectively.

Both Mo(1) and Mo(2) show some great deviations from the ideal octahedral angles (Table 2.7), with only one angle, O(8)-Mo(2)-O(6), near 90° at 89.2(3)°. The atoms O(3), Mo(1) and O(10) form a bond angle of 170.4(2)°, which seems much smaller than the 180° angle in an ideal octahedral arrangement. For O(1), O(2), O(4) and O(5), the angles between them and the metal range from 70.3(2)° to 103.1(3)°. For Mo(2), the O(5)-

Mo(2)-O(8) angle is 162.6(3)°, also deviating greatly from the ideal 180°. The O(4), O(6), O(7) and O(9) atoms exhibit angles with the metal center ranging from 70.4(2)° to 105.0(3)°.

The packing of compound **7** viewed along the a-axis (Fig. 2.32a) indicates that the dimers pack in rows with the citrate units directed outwards. An open channel exists between each row of dimers, and there are also cavities formed by the structure of the dimer. It is suspected that the waters of crystallization would occur in these cavities, in the same way as in the complex by Nassimbeni *et al.*[28] Along the b-axis (Fig. 2.32b), one can clearly see the dimer formation and the location of the counter ions. Also, the channels that form during packing become apparent. As mentioned above, the waters of crystallization would most probably occur in these cavities.

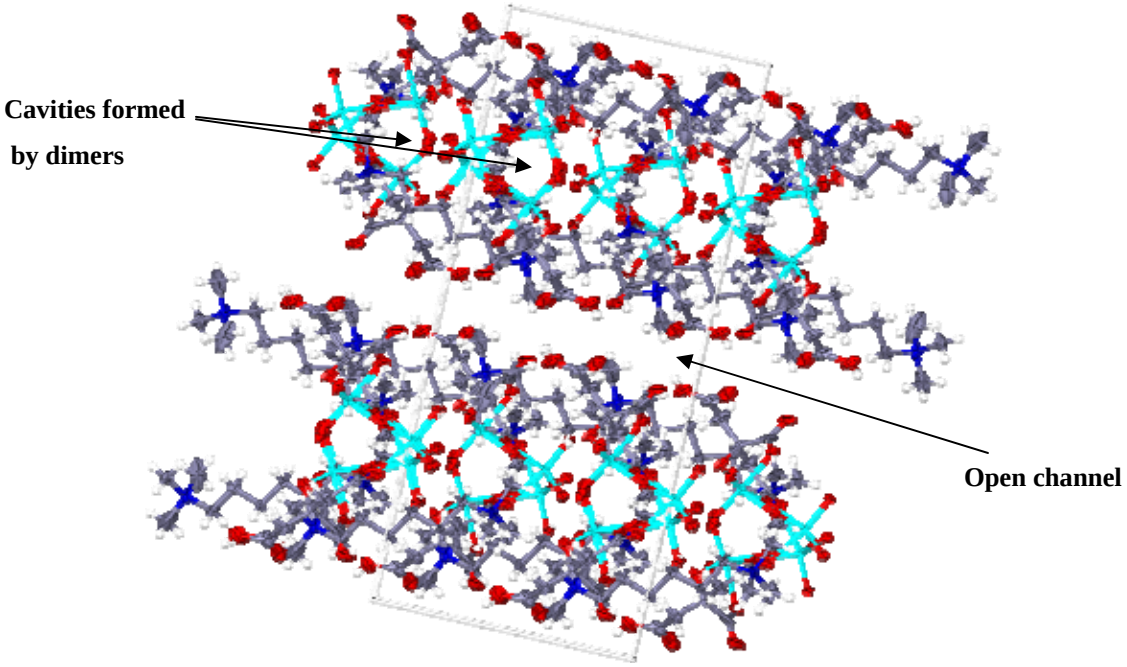

Figure 2.32a Packing of compound **7** along the a-axis, showing the channels and cavities which form upon assembly.

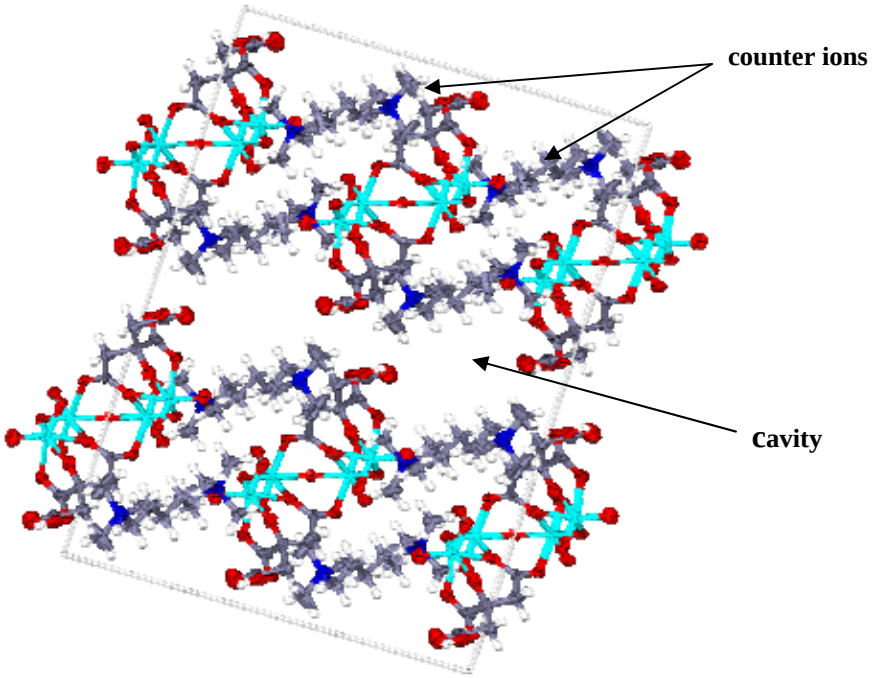

Figure 2.32b Packing of **7** along the b-axis, showing the dimer formation and the location of the counter ions.

Table 2.7 Selected bond lengths and angles for compound **7** with e.s.d.s in parentheses.

Bond lengths (Å)

Mo(1)-O(1)	1.900(2)	Mo(2)-O(4)	1.899(5)
Mo(1)-O(2)	1.710(5)	Mo(2)-O(5)	2.333(6)
Mo(1)-O(3)	1.718(5)	Mo(2)-O(6)	2.217(6)
Mo(1)-O(4)	1.926(6)	Mo(2)-O(7)	1.967(6)
Mo(1)-O(5)	2.316(5)	Mo(2)-O(8)	1.690(7)
Mo(1)-O(10)	2.305(5)	Mo(2)-O(9)	1.716(6)

Bond angles (°)

O(1)-Mo(1)-O(4)	149.5(3)	O(6)-Mo(2)-O(5)	75.1(2)
O(1)-Mo(1)-O(5)	82.8(2)	O(7)-Mo(2)-O(5)	78.6(2)
O(2)-Mo(1)-O(1)	102.2(3)	O(7)-Mo(2)-O(6)	74.9(3)
O(2)-Mo(1)-O(3)	103.1(3)	O(8)-Mo(2)-O(4)	101.7(3)
O(2)-Mo(1)-O(4)	99.5(3)	O(8)-Mo(2)-O(5)	162.6(3)
O(2)-Mo(1)-O(5)	162.1(2)	O(8)-Mo(2)-O(6)	89.2(3)
O(3)-Mo(1)-O(1)	98.4(2)	O(8)-Mo(2)-O(7)	105.0(3)
O(3)-Mo(1)-O(4)	97.3(3)	O(8)-Mo(2)-O(9)	103.6(3)
O(3)-Mo(1)-O(5)	93.0(2)	O(9)-Mo(2)-O(4)	102.0(3)
O(3)-Mo(1)-O(10)	170.4(2)	O(9)-Mo(2)-O(5)	93.3(2)
O(4)-Mo(1)-O(5)	70.3(2)	O(9)-Mo(2)-O(6)	162.5(3)
O(4)-Mo(2)-O(5)	70.4(2)	O(9)-Mo(2)-O(7)	90.1(3)
O(4)-Mo(2)-O(6)	86.6(2)		
O(4)-Mo(2)-O(7)	147.1(2)		

2.3 Conclusions and possible future work

From the beginning of this study, it was clear that the isolation of new species of Mo(VI) and W(VI) would not be easy. These metals show a great tendency to condense into polyanions, and unfortunately they condense into well-known structures more often than not. Only a few of the many experiments we did proved to be successful in crystallizing new compounds of Mo(VI) and W(VI). What made this study so particularly complex is the unpredictability of the behaviour of these metals. Merely a small adjustment in concentration, pH or counter ion would result in the formation of a completely different species. Although this made the study very complicated, it also made it so much more challenging and interesting. Regarding future work, it is obvious that the chemistry of Mo(VI) and W(VI) is far from completely understood and definitely not near the limit of its possibilities. One would need to examine the influence of pH, counter ion and concentration on the resulting product, but by taking smaller steps. For instance, by varying the pH by miniscule amounts and keeping the rest of the reaction conditions constant, and *vice versa*, one might be able to get a clearer picture of the species formation of these metals.

2.4 Experimental

2.4.1 General procedures and instruments

All the reactions were done at room temperature in distilled water, unless otherwise noted. The chemicals MoO_3, $Na_2MoO_4{\cdot}2H_2O$, $Na_2WO_4{\cdot}2H_2O$, $[(CH_3)_4NCl]$, NH_4OH and tartaric acid (Merck), $[(CH_3CH_2)_4NCl]$, $[(CH_3CH_2CH_2)_4NI]$, DMF, malic acid and citric acid (Sigma-Aldrich) and $[(CH_3)_3N(Cl)(CH_2)_6(Cl)N(CH_3)_3]$ (Fluka) were purchased and used without further purification. Crystallographic data sets for all compounds were collected on a Bruker SMART Apex CCD diffractometer with graphite monochromated Mo-Kα radiation (λ = 0.71073 Å). Data reduction was carried out with standard methods from the software package Bruker SAINT. The crystal structures were solved and refined using SHELX-97 within the X-seed environment. Figures were generated with X-seed and POV-Ray for Windows, with the displacement ellipsoids at the probability level specified in the text.

2.4.2 Preparations and procedures

2.4.2.1 Isolation of $K_2[Mo_2O_7]{\cdot}H_2O$ (1)

In 100 ml of water 14.4 g (0.100 mol) MoO_3 was stirred for 30 minutes. KOH pellets were added to the solution whilst stirring and heating, until all the MoO_3 had dissolved and a clear solution had formed. Tetramethylammonium chloride (2.74 g, 0.0250 mol) was added and the solution was stirred for 2 hours. The pH at this time was measured as 12.80. Concentrated HCl was added to the solution with constant monitoring of the pH, until a pH of 7.19 was reached. The solution was covered and left to stand undisturbed at room temperature. Clear, colourless hexagonal crystals of **1** formed after ten days.

2.4.2.2 Isolation of $K_6[Mo_7O_{24}]{\cdot}4H_2O$ (2)

In 100 ml of water 14.4 g (0.100 mol) MoO_3 was stirred for 30 minutes. KOH pellets were added to the stirring solution whilst being heated, until all the MoO_3 had been dissolved. The resulting clear solution was stirred for 2 hours. At this point the pH was measured as 7.33. Concentrated HCl was added to the solution with constant monitoring of the pH, until the pH reached a value of 7.05. The solution was left undisturbed and

covered at room temperature for three days, at which time large, colourless, rectangular crystals of **2** formed.

2.4.2.3 Isolation of $[(CH_3)_3N(CH_2)_6N(CH_3)_3][Mo_4O_{13}]\cdot H_2O$ (3)

To a stirring solution of 6.05 g (0.0250 mol) $Na_2MoO_4\cdot 2H_2O$ in 50 ml water was added 2.00 ml concentrated HCl until all the solids had been dissolved. The clear solution was stirred for 2 hours, and the pH was determined as 6.15. Small amounts of hexamethonium chloride, to a total mass of 6.83 g (0.0250 mol), was added slowly to the solution, but the pH remained unchanged. The clear solution was stirred for another hour, then covered and left to stand undisturbed at room temperature. Small, colourless rectangular crystals of **3** formed after two weeks.

2.4.2.4 Isolation of $[(CH_3CH_2)_4N][W_6O_{19}]$ (4)

To a solution of 0.830 g (0.00250 mol) $Na_2WO_4\cdot 2H_2O$ and 2.00 ml concentrated HCl, 0.700 g (0.00520 mol) (S-)malic acid was added and stirred for 30 minutes. Tetraethyl-ammonium chloride (1.00 g, 0.0600 mol) was added to the resulting clear solution, and stirred for an hour whilst being heated to 80°C. After cooling, 10 ml DMF was added, and the solution was stirred for a few more minutes. The pH was measured to be 3.27. The solution was covered and left at room temperature for three months, after which time small, colourless crystals of **5** formed.

2.4.2.5 Isolation of $MoO_3(mal)[(CH_3CH_2)_4N]\cdot H_2O$ (5)

In 50 ml of water 1.20 g (0.00500 mol) $Na_2MoO_4\cdot 2H_2O$ and 2.00 ml HCl was stirred for 30 minutes. The pH of the solution was measured as 5.93. Tetraethylammonium chloride (0.900 g, 0.00540 mol) was added and the solution was stirred for another 30 minutes. Malic acid (1.35 g, 0.0100 mol) was added, and the solution was stirred for a further 60 minutes. A pH of 4.59 was measured. The solution was then covered and left at room temperature for two months, after which time large colourless crystals of **8** had formed.

2.4.2.6 Isolation of $Na_6[Mo_2O_5(cit)_2]$ (6)

In 20 ml of water, 0.605 g (0.00250 mol) $Na_2MoO_4 \cdot 2H_2O$, 2.00 ml concentrated HCl and 0.530 g (0.00280 mol) citric acid was stirred for 1 hour. $10cm^3$ DMF was added dropwise to the solution, and stirred for a few more minutes. The solution turned a light yellow colour, and it was covered and left to stand undisturbed at room temperature. The yellow colour intensified as evaporation occurred. Clear colourless crystals of **6** formed after five months.

2.4.2.7 Isolation of $[(CH_3)_3N(CH_2)_6N(CH_3)_3][Mo_2O_7(cit)]$ (7)

To a solution of 0.605 g (0.00250 mol) $Na_2MoO_4 \cdot 2H_2O$ and 2.00 ml concentrated HCl in 20 ml of water was added 0.530 g (0.00280 mol) citric acid. The clear solution was stirred for 1 hour, after which time 0.420 g (0.00150 mol) hexamethonium chloride was added. The solution was then stirred for another 30 minutes. 10 ml DMF was added dropwise to the solution and it was left uncovered at room temperature. The colourless solution turned light yellow after a few days. Hexagonal colourless crystals of **7** formed after six weeks.

Table 2.8 Crystal data and structure refinement parameters of compounds **1** and **2**

	1	**2**
Empirical formula	$Mo_2K_2O_8H_2$	$Mo_7K_6O_{28}H_8$
M_r	444.09	1362.24
Temp. (K)	100(2)	100(2)
Wavelength (Å)	0.71073	0.71073
Crystal system	triclinic	monoclinic
Space group	P_{-1}	$P2_1/n$
a (Å)	7.580(3)	8.1096(6)
b (Å)	7.613(3)	35.434(3)
c (Å)	8.427(3)	9.9765(7)
α (°)	63.699(5)	90
β (°)	66.823(5)	111.387(1)
γ (°)	84.049(5)	90
Volume (Å^3)	399.3(2)	2669.4(3)
Z	2	4
d_{calcd} (g/cm^3)	3.693	3.390
Absorption coefficient (μ, mm^{-1})	4.229	4.228
Absorption correction	none	none
F(000)	418	2560
Crystal size (mm)	0.15 x 0.12 x 0.10	0.25 × 0.10 × 0.03
θ-range for data collection (°)	2.93 to 26.49	2.27 to 26.39
No. of reflections collected	4137	15593
No. independemt reflections	1578	5455
Refinement method	Full-matrix least-squares on F^2	Full-matrix least-squares on F^2
Data / restraints / parameters	1578 / 8 / 118	5455 / 34 / 362
Goof on F_2	1.054	1.033
Final *R* indices [$I > 2\sigma(I)$]	*R1* = 0.0237	*R1* = 0.0381
	wR2 = 0.0489	*wR2* = 0.0723
R-indices (all data)	*R1* = 0.0264	*R1* = 0.0480
	wR2 = 0.0509	*wR2* = 0.0753

Table 2.9 Crystal data and structure refinement parameters of compounds **3** and **4**

	3	**4**
Empirical formula	$Mo_8O_{28}N_4C_{24}H_{64}$	$W_6N_2O_{19}C_{16}H_{40}$
M_r	1624.31	1603.60
Temp. (K)	100(2)	100(2)
Wavelength (Å)	0.71073	0.71073
Crystal system	monoclinic	tetragonal
Space group	$P2_1/n$	$P_{4/mnc}$
a (Å)	12.2468(9)	10.7939(8)
b (Å)	12.8696(10)	10.7939(8)
c (Å)	15.6889(12)	14.274(2)
α (°)	90.00	90
β (°)	106.5210(10)	90
γ (°)	90.00	90
Volume (Å^3)	2370.7(3)	1663.1(3)
Z	2	2
d_{calcd} (g/cm^3)	2.276	3.202
Absorption coefficient (μ, mm^{-1})	2.135	20.725
Absorption correction	none	none
F(000)	1592	1428
Crystal size (mm)	0.08 x 0.06 x 0.04	0.15 × 0.13 × 0.07
θ-range for data collection (°)	1.87 to 26.39	2.37 to 26.39
No. of reflections collected	13503	8892
No. independemt reflections	4839	888
Refinement method	Full-matrix least-squares on F^2	Full-matrix least-squares on F^2
Data / restraints / parameters	4839 / 3 / 303	888 / 2 / 72
Goof on F_2	1.060	1.046
Final R indices [$I > 2\sigma(I)$]	$R1$ = 0.0212	$R1$ = 0.0695
	$wR2$ = 0.0487	$wR2$ = 0.1979
R-indices (all data)	$R1$ = 0.0233	$R1$ = 0.0745
	$wR2$ = 0.0495	$wR2$ = 0.2060

Table 2.10 Crystal data and structure refinement parameters of compounds **5** and **6**

	5	**6**
Empirical formula	$Mo_2N_2O_{17}C_{24}H_{50}$	$Mo_2Na_6O_{30}C_{12}H_8$
M_r	830.54	962.00
Temp. (K)	100(2)	273(2)
Wavelength (Å)	0.71073	0.71073
Crystal system	monoclinic	triclinic
Space group	*C*2/c	*P*î
a (Å)	15.293(6)	9.011(1)
b (Å)	20.239(8)	9.882(1)
c (Å)	12.473(5)	17.493(2)
α (°)	90.00	89.375(2)
β (°)	120.039(7)	85.092(2)
γ (°)	90.00	86.050(2)
Volume ($Å^3$)	3342(2)	1548.3(4)
Z	4	2
d_{calcd} (g/cm^3)	1.651	2.064
Absorption coefficient (μ, mm^{-1})	0.826	1.009
Absorption correction	none	none
F(000)	1712	940
Crystal size (mm)	0.12 x 0.10 x 0.07	0.08 x 0.11 x 0.12
θ-range for data collection (°)	1.84 to 26.50	1.17 to 28.30
No. of reflections collected	9684	17057
No. independemt reflections	3446	6905
Refinement method	Full-matrix least-squares on F^2	Full-matrix least-squares on F^2
Data / restraints / parameters	3446 / 17 / 236	6905 / 0 / 454
Goof on F_2	1.136	1.190
Final *R* indices [$I > 2\sigma(I)$]	*R1* = 0.0722	*R1* = 0.0584
	wR2 = 0.1677	*wR2* = 0.0759
R-indices (all data)	*R1* = 0.0877	*R1* = 0.1490
	wR2 = 0.1759	*wR2* = 0.2109

Table 2.11 Crystal data and structure refinement parameters of compound **7**

	7
Empirical formula	$Mo_2N_2O_{12.5}C_{18}H_{35}$
M_r	671.36
Temp. (K)	293(2)
Wavelength (Å)	0.71073
Crystal system	monoclinic
Space group	*C*2/c
a (Å)	19.679(5)
b (Å)	11.747(3)
c (Å)	26.836(7)
α (°)	90.00
β (°)	92.135(4)
γ (°)	90.00
Volume (Å^3)	6199(3)
Z	8
d_{calcd} (g/cm^3)	1.439
Absorption coefficient (μ, mm^{-1})	0.861
Absorption correction	none
F(000)	2728
Crystal size (mm)	0.07 x 0.09 x 0.12
θ-range for data collection (°)	1.52 to 26.41
No. of reflections collected	16511
No. independemt reflections	6250
Refinement method	Full-matrix least-squares on F^2
Data / restraints / parameters	6250 / 1 / 322
Goof on F_2	1.173
Final *R* indices [$I > 2\sigma(I)$]	*R1* = 0.0849
	wR2 = 0.2005
R-indices (all data)	*R1* = 0.0958
	wR2 = 0.2060

1. Pope MT. Isopolyanions and Heteropolyanions. **In**: Wilkinson G (ed.), *Comprehensive Coordination Chemistry: The Synthesis, Reactions, Properties & Applications of Coordination Compounds,* Vol. 3, Pergamon Press, Oxford, 1987; 1023-1034.
2. Cruywagen JJ. *Adv. Inorg. Chem.* 2000; **49**: 127-182.
3. Cotton FA, Wilkinson G, Murillo CA, Bochmann M. *Advanced Inorganic Chemistry*. John Wiley & Sons, inc., New York, 1999.
4. Sykes AG. Molybdenum: The Element and Aqueous Solution Chemistry. **In**: Wilkinson G (ed.), *Comprehensive Coordination Chemistry: The Synthesis, Reactions, Properties & Applications of Coordination Compounds*, Vol. 3, Pergamon Press, Oxford, 1987; 1229-1261.
5. Cruywagen JJ, Esterhuysen MW, Heyns JBB. *Inorg. Chim. Acta* 2003; **348**: 205-211.
6. Niven ML, Cruywagen JJ, Heyns JBB. *J. Chem. Soc. Dalton Trans.* 1991: 2007-2011.
7. Dori Z. Tungsten. **In**: Wilkinson G (ed.), *Comprehensive Coordination Chemistry: The Synthesis, Reactions, Properties & Applications of Coordination Compounds*, Vol. 3, Pergamon Press, Oxford, 1987; 973-981.
8. Hlaibi M, Chapelle S, Benaissa M, Verchere J. *J. Inorg. Chem.* 1995; **34**: 4434-4440.
9. Pedrosa De Jesus JD. Hydroxy acids. **In**: Wilkinson G (ed.), *Comprehensive Coordination Chemistry: The Synthesis, Reactions, Properties & Applications of Coordination Compounds,* Vol. 2, Pergamon Press, Oxford, 1987; 461-483.
10. Cruywagen JJ, Rohwer EA, Van de Water RF. *Polyhedron* 1997; **16**: 243-251.
11. Cruywagen JJ, Kruger L, Rohwer EA. *J. Chem. Soc. Dalton Trans.* 1997: 1925-1929.
12. Zhang H, Zhao H, Jiang Y, Hou S, Zhou Z, Wan H. *Inorg. Chim. Acta* 2003; **351**: 311-318.
13. Cruywagen JJ, Heyns JBB, Rohwer EA. *J. Chem. Soc. Dalton Trans.* 1990: 1951-1956.
14. Gatehouse BM, Jozsa AJ. *J. Solid State Chem.* 1987; **71**: 34-39.
15. Grzywa M, Lasocha W, Surga W. *J. Solid State Chem.* 2007; **180**: 1590-1594.
16. Orpen AG, Brammer L. *J. Chem. Soc. Dalton Trans.* 1989: S1-S83.
17. Aullon G, Bellamy D, Brammer L, Bruton EA, Orpen AG. *Chem. Commun.* 1998: 653-654.
18. Evans HT, Gatehouse BM, Leverett P. *J. Chem. Soc. Dalton Trans.* 1975: 505-514.
19. Cruywagen JJ, Kruger L, Rohwer EA. *J. Chem. Soc. Dalton Trans.* 1991: 1727-1731.
20. Liu H, Xi L, Huang XY, Chen WD, Huang JS. *Chinese J. Struct. Chem* 1995; **14**: 78.
21. Hou HW, Ye X, Xin X, Wang Z, Liu S, Huang J. *Acta Cryst. Sect. C: Cryst. Struct. Commun.* 1995; **51**: 2013-2015.
22. Lehtonen A, Sillanpaa R. *J. Chem. Soc. Dalton Trans.* 1995: 2701.
23. Porai-Koshits MA, Aslanov LA, Ivanova GV, Polynova TN. *Russian J. Struct. Chem.*; **9**: 475.
24. Cruywagen JJ, Saayman LJ, Niven ML. *J. Cryst. Spectrosc.* 1992; **22**: 737-740.
25. Zhou Z, Wan H, Tsai K. *J. Inorg. Chem.* 2000; **39**: 59.
26. Zhou Z, Wan H, Tsai K. *Polyhedron* 1997; **16**: 75.
27. Spek AL. *J. Appl. Crystallogr.* 2003; **36**: 7-13.
28. Nassimbeni LR, Niven ML, Cruywagen JJ, Heyns JBB. *J. Cryst. Spectrosc. Res.* 1987; **17**: 373.

Chapter 3

Synthesis and structural study of new Au(I,III) and Pt(IV) complexes

Abstract

Platinum and gold chemistry has been of interest for many decades, not only due to their versatility in chemical reactions but also for their potential in cancer treatment and other medicinal fields. In this study, we attempted to isolate new and useful Pt(IV) and Au(III) complexes with unique ligands that have not been used before in coordination chemistry. Most of the reactions proved to be fruitless or yielded inconclusive results. Nevertheless, a new complex of Pt(IV) with a sulphur ligand has been isolated, $PtCl_2(S_3C_8H_7)_2$ (**9**). Also, a known compound of gold having mixed valencies of +1 and +3 has been synthesized, $[Au(I)Cl(S(CH_2C_6H_5)_2)][Au(III)Cl_3(S(CH_2C_6H_5)_2]$ (**8**), but its structure was analyzed more extensively than previously reported.

3.1 Introduction and aim of this study

3.1.1 Background

Platinum

Quite unusually for transition metal chemistry, platinum complexes exist mostly in the oxidation states 0, 2 or 4. Although all the transition elements exhibit a range of oxidation states, platinum is one of only a few metals that has three oxidation states that differ by two electrons each. This property has led to the existence of a wide range of oxidative addition chemistry in the oxidation states 0 and 2. Platinum is a third row transition metal, thus the large values of the ligand field lead to low spin, kinetically inert d^6 complexes of Pt(IV) with hexacoordinate structures, and low spin kinetically inert d^8 complexes of Pt(II) with square-planar tetracoordinate geometry. [1]

Platinum compounds are widely used in medicine as anticancer agents. Of these complexes, cisplatin (Fig. 3.1) is the most well-known. Although it has now been replaced by other drugs such as carboplatin and oxaliplatin, it still serves as a benchmark for determining anti-cancer activity. Cisplatin is highly effective in the treatment of ovarian and testicular cancer, as well as in the treatment of bladder, head and neck tumors. It is believed that the ability of platinum complexes to kill tumor cells is a direct result of their ability to form various types of adducts with DNA.[2]

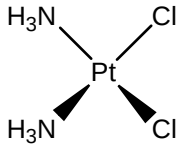

Figure 3.1 Structure of *cis*-diamminedichloroplatinum(II), or cisplatin.

Since cisplatin and its later generation successors are administered intravenously, it may react with many compounds (especially those containing sulphur) before reaching the DNA. This side mechanism is believed to be the reason for the resistance some tumors have shown to platinum-based drugs, the inactivation of these drugs and their severe side-effects. In general, sulphur-containing biomolecules can be highly reactive towards cisplatin, which often results in inactivation of the drug. [2]

Some mixed platinum complexes with dithiocarbamate derivatives (Fig. 3.2) have been studied in the past[3] to try and synthesize complexes that have lower nephrotoxicity. Renal toxicity results from the high affinity of Pt(II) for protein-sulphur sites. Thus, by coordinating the dithiocarbamate to platinum, thereby coordinating the metal to two sulphur atoms, it is believed that this may prevent the reaction of the complex with the proteins.[3] The dithiocarbamates selectively remove platinum from the enzyme-thiol complexes by nucleophilic attack of the chelating sulphur atoms on the platinum ion. More importantly, they selectively protect normal tissue without inhibiting the antitumor effect of cisplatin. [4]

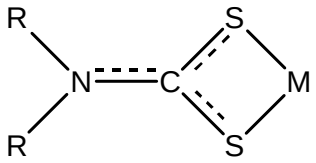

Figure 3.2 Structure of a dithiocarbamate metal complex.

The high affinity of certain metals for sulphur can be clearly seen from the large variety of metal sulfides existing in nature. Sulphur has low lying, unoccupied 3d-orbitals that are available for bonding. This might explain the affinity of the 'soft' metals for sulphur, but it it believed that it is actually the high polarizability of the electrons on the sulphur atoms that is responsible for this affinity and therefore the great number of structures that exist and the reactivity of these metal complexes with sulphur-containing ligands. [5]

Dithio-ligands can generally quite easily be oxidized to carbon disulfides, resulting in ligands that contain the fragment as seen in Figure 3.3a, where x =1, 2 or more. The bicovalent sulphur atoms provide two donor sites and can thus act as a bidentate ligand. With x = 2, seven-membered rings can form with certain metals (see Fig. 3.3b). Reverse reactions, where the carbon disulfides are reduced and S-S bond breaking takes place, can also happen. [5]

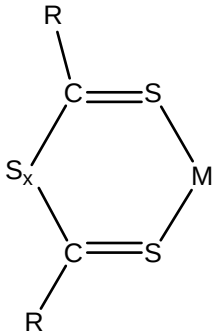

Figure 3.3a Structure of a CS_2 ligand coordinated to a metal centre

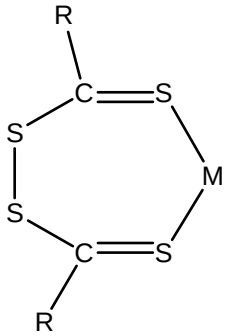

Figure 3.3b Showing the seven-membered ring which forms when x = 2

The interest in the chemical and biochemical properties of platinum complexes with thiocarbonyl donors is the result of the discovery that sulphur ligands can be used as detoxicant agents against metal-containing drugs, as mentioned above. For a long time, mostly dithiocarbamates have been investigated for their efficiency as inhibitors of the nephrotoxicity caused by cisplatin and related drugs. Other ligands are currently being investigated for potential anticancer properties, and the focus remains on sulphur and its role in the process.[4]

Gold

Gold can exist in any oxidation state ranging from -1 to 5. Of these, only Au(0), Au(I) and Au(III) are stable in aqueous and thus biological environments. Generally, Au(I) complexes are thermodynamically more stable than Au(III) complexes. Since most Au(III) complexes are strong oxidation agents and can easily be reduced to Au(I), they are mostly toxic.[6]

Gold has been used for its medical properties for many ages. It was first discovered to be useful in the treatment of tuberculosis, which ultimately led to the discovery of its application as treatment for rheumatoid arthritis. The compounds used at the beginning were mostly Au(I) complexes. It was during this time that chrysotherapy (medical treatment with gold-based drugs) became an accepted and integral part of modern medicine as we know it.[6] Gold drugs have been used for many other related diseases, such as psoriatic arthritis, palindromic rheumatism and discoid lupus erythmatosus. It has also proved useful in the treatment of some skin disorders such as urticaria and psoriasis.[6]

Gold(III) has raised medical interest in the last few decades because it is isoelectronic to Pt(II). Au(III) and Pt(II) are both d^8 ions, and adopt a square-planar configuration. Therefore it has been speculated that Au(III) complexes might have a similar antitumour activity to that of cisplatin. However, only very few reports exist regarding the use of Au(III) in medicine, probably because of its high reactivity compared to Pt(II) complexes, and also because, as mentioned earlier, Au(III) complexes are usually toxic.[6]

The design and testing of Au complexes for antitumour activity over the last few decades have been based on three strategies: firstly, the analogies between the square-planar complexes of Pt(II) and Au(III) were investigated; secondly, an analogy to the immunomodulatory effects of Au(I) antiarthritic agents was sought, and lastly, complexation of Au(I) and Au(III) with some known antitumour agents were investigated to attempt the synthesis of new compounds with higher activity.[7]

Since the mammalian environment is usually reducing, compounds containing Au(III) may be reduced to Au(I) and metallic Au. However, it has been postulated that by selection of the right ligand-donor set, the Au(III) state can be stabilized.[8] The majority of Au(I) complexes feature gold coordinated to soft ligand atoms such as sulphur or phosphorus. However, Au(III) complexes mostly contain hard donor atoms such nitrogen and oxygen.[8] As mentioned earlier, four-coordinate, square-planar Au(III) complexes could resemble the Pt(II) complex cisplatin. Therefore, screening of Au(III) complexes for antitumour activity has been ongoing for the past 30 years. This interest has risen over the last decade, as illustrated by the number of recent papers on this subject.[8]

Gold-based complexes often exhibit antimicrobial activity, and there is a growing need for new antimicrobial agents. Although mostly Au(I) complexes are tested, a few Au(III) complexes have shown potential.[6] Au(III) complexes have also shown some antiviral activity. It has even been suggested that Au compounds might have anti-HIV activity. Especially the Au(III) compound [$HAuCl_4$] has potential for inhibiting the effectiveness of HIV-1. [6]

A wide variety of ligands can form stable complexes with Au(III) and, therefore, Au(III) exhibits a range of physical and chemical properties. This is useful because, with the right combination of ligands, one can form complexes with any charge between -1 and +3. This modulation of charge by ligand exchange reactions can greatly influence the hydrophilicity and lipophilicity of Au(III) complexes.[9] The exchange of monodentate ligands bound to Au(III) is generally rapid and proceeds *via* an associative mechanism

that involves a five-coordinate Au(III) transition state or intermediate. The reactions of Au(III) are typically much faster than their Pt(II) analogues. Although a five-coordinate intermediate forms during the reaction, very few stable five-coordinate Au(III) complexes exist and it is therefore believed that this is rather a transition state than an intermediate species. [9]

Au(III) is a powerful oxidant, as mentioned earlier. It is capable of oxidizing thiols to disulfides or even higher oxidation states, and thioethers to sulfoxides. It is this property of Au(III) that makes it so useful in its role in immunological side reactions and chrysotherapy. [9] Au(III) also has the ability to alter protein residues, especially those containing sulphur in its side chains, and this ability may have important implications for the immunological effects of gold-based therapy.[9]

In the past decade, much interest has been focused on the synthesis of Au(I) derivatives containing sulphur or phosphorous ligands. Especially dithiocarbamates (see Fig. 2, previous section) have been studied extensively in the past for their antimicrobial activity and action against metal poisoning. It is also an interesting ligand because of its ability to act as a bidentate ligand with formation of four-membered chelates. [10]

A number of complexes containing Au(III) coordinated to sulphur and selenium donor atoms have been reported to date. In some instances, the Au(III) is easily reduced to Au(I), and sometimes the Au(III) centre may catalyze the hydrolysis of the ligand.[11] 1,2-Dithiol-ligands can produce a range of stable square-planar complexes of Au(III), some of which are of interest in the field of biochemistry. Dithiocarbamates and related complexes of Au(III) have also been studied extensively. The chemistry of Au with ligands containg sulphur and other soft donor atoms is of growing interest and may play an important part in the field of medicine in the future.[11]

3.1.2 Particular aims of the study

In this part of the study, we planned to synthesize new complexes of Pt(IV) and Au(III) with ligands containing soft donor atoms such as sulphur, selenium and phosphorous (Fig. 3.4 a, b & c). New ligands containing these atoms were synthesized, coordinated to the metal centers, and any interesting behaviour of these ligands was recorded. Furthermore, single crystals were grown and the structure of a new Pt(IV) complex with ligand **I** was determined. A previously known complex of Au with mixed valencies of +1 and +3 was also isolated, but under different reaction conditions than before and all the connectivities as well as the extended crystal structure were unequivocally determined.

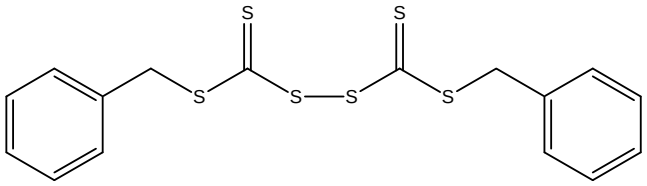

Figure 3.4a $S_6C_8H_{14}$ (**I**)

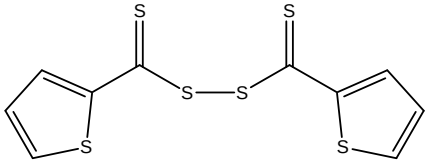

Figure 3.4b $S_6C_{10}H_6$ (**II**)

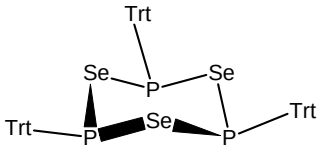

Figure 3.4c $P_3Se_3(Trt)_3$ (**III**) (Trt = $C_{19}H_{15}$)

3.2 Results and discussion

3.2.1 Synthesis and structural analysis of $[Au(I)Cl(S(CH_2C_6H_5)_2)][Au(III)Cl_3(S(CH_2C_6H_5)_2)]$ (8)

With this synthesis we planned to isolate new compounds of Au^{III} with the trithio-carbonate ligands **I** and **II**, which both offer a range of possibilities for coordination to a metal center such as Au^{III}. We attempted several conversions and varied starting reagents, reaction times, solvents and crystallization techniques. However, only one complex of a Au center to the sulphur ligand could be obtained in pure crystalline form. We expected to isolate a compound with one or more Au^{III} centers coordinated in different ways to the donor atoms in the ligand, however, we crystallized a halogen-bridged, mixed valence complex of $Au^{I,III}$ with the trithio-carbonate ligand **I**, which was greatly rearranged during the reaction: a CS_2 fragment was released from the ligand to furnish, by rearrangement of **I,** dibenzylsulphide, $S(CH_2C_6H_5)_2$.

At first, we thought that this was a pure Au^{III} compound, but it soon became clear that if the electron density is allocated to outer chlorine atoms from nearby molecules, they would be much too close to one another to justify such an assumption. Thus we discovered the product to be a mixed valence compound. We then attempted to solve the crystal structure of compound **8** in such a manner as to include both Au^{I} and Au^{III} molecules in the unit cell, but unfortunately this was not possible. Instead, we modelled the structure under the assumption that, in the extended structure, the compound exists as alternating Au^{I} and Au^{III} centers with one or three coordinated chloride ligands respectively. The structure was thus solved as a Au^{III} metal center with one fully occupied Cl atom, and two Cl atoms with half occupancy to account for the presence of the Au^{I} centers.

Compound **8** was synthesized by reacting $AuCl(SC_4H_8)$ with ligand **I** in CH_2Cl_2 for three hours (Fig. 3.5). After removal of the solvent, a light brown powder remained that was recrystallized from CH_2Cl_2, as described in the experimental section (3.4.2.1). Clear, colourless crystals of **8** formed after 6 weeks.

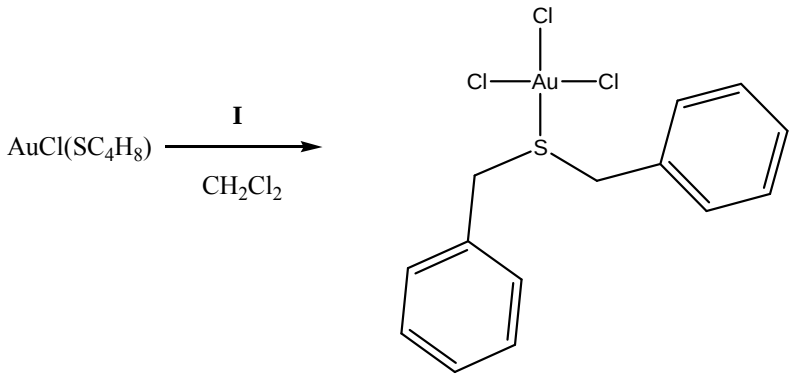

Figure 3.5 Reaction scheme for the formation of compound **8**

The molecular structure of compound **8** is represented in Figure 3.6, and selected bond lengths and angles are given in Table 3.1. The structure was solved in the monoclinic spacegroup $P2_1/c$.

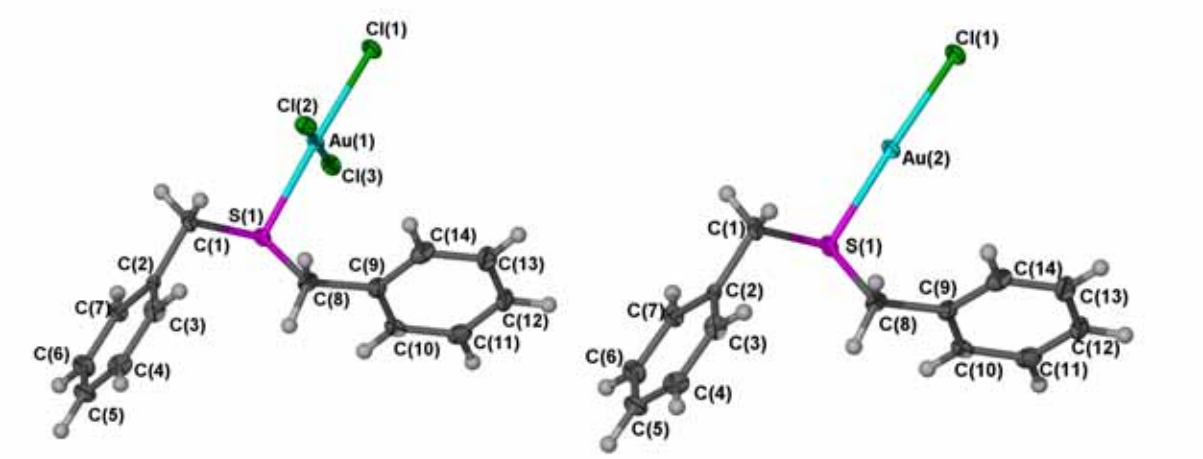

Figure 3.6 Molecular structures of compound **8**, showing the atom numbering scheme. Ellipsoids enclose 50% of the electron density.

As mentioned earlier, the monomeric units in the crystals of compound **8** comprise of both Au^{I} and Au^{III} chlorides coordinated to identical metal sulphide ligands, which generated from the rearranged ligand **I**. The Au^{I} atom Au(2) exists in a linear arrangement, and the Au^{III} center Au(1) has a square-planar environment. Compound **8**

thus exists as a mixed oxidation state compound affording a chain of Au^{I} and Au^{III} centers, as seen in Figure 3.7.

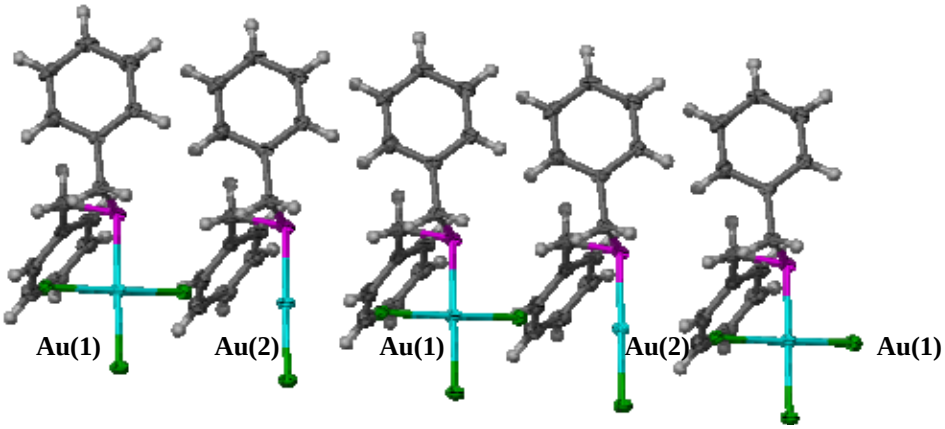

Figure 3.7 The formation of a chain of alternating Au^{I} and Au^{III} centers.

A similar compound has been reported previously by Tanino and coworkers in 1988.[12] They used the same metal starting reagent, but they used dibenzyl sulphide as ligand, and chose different reaction conditions. Also, in their report,[12] a clear exposition of the crystal structure of the compound is not given. We now report the packing diagram of this compound (Fig. 3.8). The bond lengths and angles reported by Tanino do not differ significantly from that of compound **8**.

The bond distances Au(1)-Cl(1), Au(1)-Cl(2) and Au(1)-Cl(3) are 2.284(1), 2.324(3) and 2.242(3) Å respectively. These bond lengths correlate well with those found by Tanino *et al.,* which vary between 2.26 to 2.32 Å. Similarly, the bond separation Au(1)-S(1) is 2.291(1) Å, which is rather close to the Au-S bond distance in the previously reported structure (2.311 Å). The bond lengths for the phenyl groups are all in the expected ranges.[13]

With Au(2) in its linear environment, the ideal Cl(1)-Au(2)-S(1) angle would be 180°, and it is in fact 177.71(5)°. The Au^{III} metal center Au(1) is coordinated to its surrounding donor atoms in a square-planar geometry and thus the ideal angles between its

substituents would be 90°. The Cl-Au-Cl angles in the one complex of **8** range between 87.67(8)° and 91.00(8)°. The C(2)-C(1)-S(1) and C(9)-C(8)-S(1) angles are 110.4(4) and 111.0(4)° respectively. The bond angles for the phenyl groups are all in expected ranges.

The packing of compound **8** can be viewed along the a-axis in Figure 3.8. Two chains of Au^{I}-Au^{III} units pack in close proximity to one another. The distance between Au^{I} and Au^{III} in the main chain is 5.610 Å, and the distance between two different Au^{I}-Au^{III} chains in the packed structure is 3.756 Å. No significant intermolecular interactions are noted.

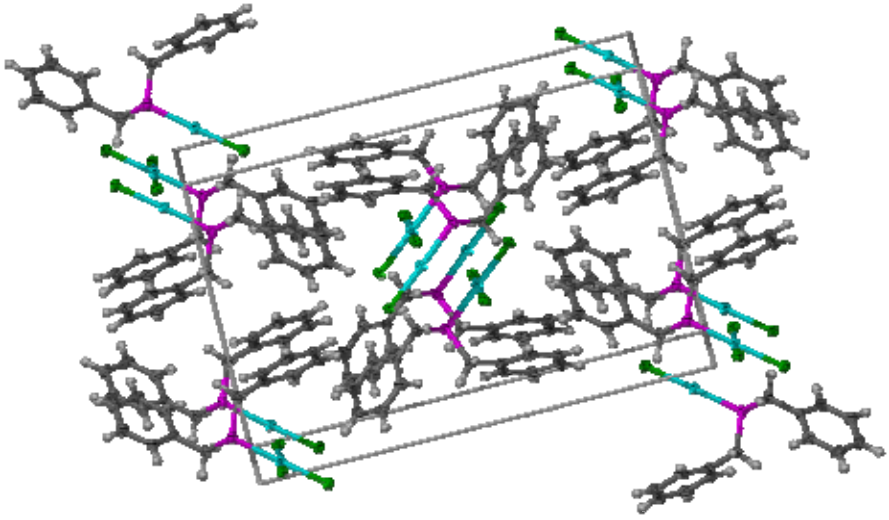

Figure 3.8 Packing of compound **8** viewed along the a-axis.

Table 3.1 Selected bond lengths and angles for compound **8** with e.s.d.s in parentheses.

Bond lengths (Å)

Au(1)-Cl(1)	2.284(1)	C(4)-C(5)	1.365(9)
Au(1)-Cl(2)	2.324(3)	C(5)-C(6)	1.370(8)
Au(1)-Cl(3)	2.242(3)	C(7)-C(6)	1.376(8)
Au(1)-S(1)	2.291(1)	C(9)-C(8)	1.505(8)
S(1)-C(1)	1.830(6)	C(9)-C(10)	1.369(9)
S(1)-C(8)	1.835(6)	C(9)-C(14)	1.392(8)
C(2)-C(1)	1.507(8)	C(10)-C(11)	1.388(8)
C(2)-C(3)	1.391(8)	C(12)-C(11)	1.374(9)
C(2)-C(7)	1.381(8)	C(13)-C(12)	1.38(1)
C(3)-C(4)	1.380(8)	C(14)-C(13)	1.388(8)

Bond angles (°)

Cl(1)-Au(1)-Cl(2)	91.00(8)	C(6)-C(7)-C(2)	120.4(5)
Cl(3)-Au(1)-Cl(1)	90.69(8)	C(7)-C(2)-C(3)	118.8(5)
Cl(3)-Au(1)-Cl(2)	174.7(1)	C(7)-C(2)-C(1)	120.7(5)
Cl(1)-Au(1)-S(1)	177.71(5)	C(8)-S(1)-Au(1)	104.1(2)
Cl(3)-Au(1)-S(1)	87.67(8)	C(9)-C(8)-S(1)	111.0(4)
S(1)-Au(1)-Cl(2)	90.49(8)	C(9)-C(10)-C(11)	120.2(6)
C(1)-S(1)-C(8)	100.1(3)	C(10)-C(9)-C(8)	121.1(6)
C(1)-S(1)-Au(1)	106.6(2)	C(10)-C(9)-C(14)	119.9(6)
C(2)-C(1)-S(1)	110.4(4)	C(11)-C(12)-C(13)	120.9(6)
C(3)-C(2)-C(1)	120.5(5)	C(12)-C(13)-C(14)	119.3(6)
C(4)-C(3)-C(2)	120.0(6)	C(12)-C(11)-C(10)	119.7(6)
C(4)-C(5)-C(6)	119.9(6)	C(13)-C(14)-C(9)	120.0(6)
C(5)-C(4)-C(3)	120.5(6)	C(14)-C(9)-C(8)	119.0(6)
C(5)-C(6)-C(7)	120.4(6)		

3.2.2 Synthesis and structural analysis of $PtCl_2(S_3C_8H_7)_2(CH_2Cl_2)_{1.5}$ (9)

This synthesis formed part of two planned syntheses to isolate new complexes of Pt(II) coordinated to the trithio-ligands $S_6C_{16}H_{14}$ (**I**) and $S_6C_{10}H_6$ (**II**). We went about this using different starting reagents and solvents, as well as crystallization techniques. Although colour changes occurred during the reactions and TLC's showed no unreacted starting material, all complexes with **II** seemed to show traces of decomposition within ten to twenty minutes of reaction with the metal fragment. The resulting products were insoluble in most solvents, and NMR analysis proved either inconclusive as to whether or not a reaction did take place, or the sample decomposed before the NMR had been

recorded. Even though **II** differs only slightly from **I**, the latter proved to be much more successful and stable than the former. Although **I** disintegrated during the reaction, a new complex of Pt(IV) with the formed ligand was crystallized.

Compound **9** was synthesized by reacting $PtCl_2(COD)$ with ligand **I** in CH_2Cl_2 (Fig. 3.9). The fine, white product was precipitated by the addition of diethyl ether to the solution. After removal of the solvents, a light yellow powder remained which was then recrystallized from CH_2Cl_2, as described in the experimental section (3.4.2.2). Small, colourless crystals of **9** formed after 2 months.

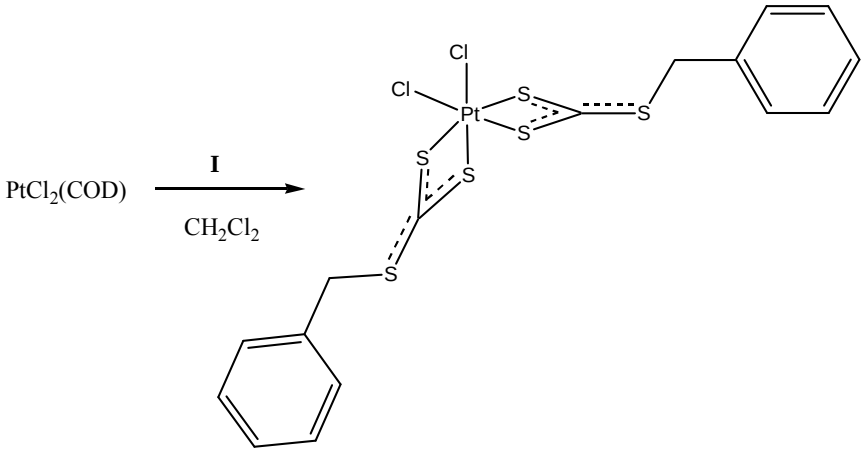

Figure 3.9 Reaction scheme for the synthesis of compound **9**.

The molecular structure of compound **9** with the CH_2Cl_2 molecules excluded is represented in Figure 3.10, and selected bond lengths and angles are given in Table 3.2. The structure was solved in the monoclinic spacegroup *C*2/c.

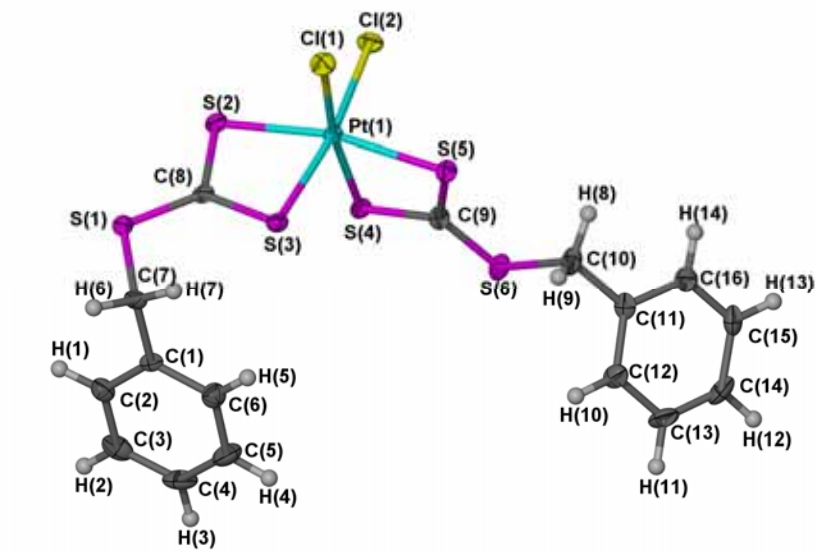

Figure 3.10 Molecular structure of compound **9**, showing the atom numbering scheme. Ellipsoids enclose 50% of the electron density.

Compound **9** comprises a single Pt(IV) atom coordinated to two Cl atoms and four sulphur atoms of ligand **I**. From Figure 3.10 it is obvious that the S-S bond in **I** was cleaved homolytically during the reaction, resulting in the formation of two identical neutral fragments, each containing an R-SCS_2 unit (Fig. 3.11); these fragments then oxidatively add in a bidentate fashion to the metal center. One and a half CH_2Cl_2 molecules are present per asymmetric unit. Although not shown in Figure 3.10, their location will become clear in the packing diagram (Fig. 3.14) described later in this section.

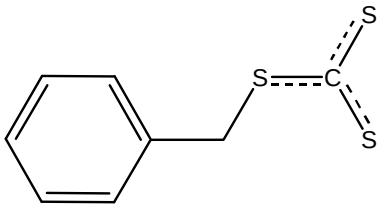

Figure 3.11 The fragment which forms upon homolytic cleavage of the S-S bond in ligand **I**.

No complexes of platinum with the R-SCS_2 fragment have been isolated to date. The only structures showing resemblances to compound **9** are a series of complexes by Aucott

and coworkers, such as bis(trimethylphosphine)-(thiocarbonato-S,S')-platinum and bis(dimethyl(phenyl)phosphine)-(thiocarbonato-S,S')-platinum (Fig. 3.12).[14] These compounds have only one SCS_2 fragment such as those in compound **9**, and they all have a terminal C=S double bond (Fig. 3.13a), whereas in compound **9**, this S atom is single-bonded to C and also to a CH_2-C_6H_5 fragment (Fig. 3.13b). The bond distances and angles in the structures by Aucott show no significant differences to those in **9**, but will be discussed in more detail later in this section.

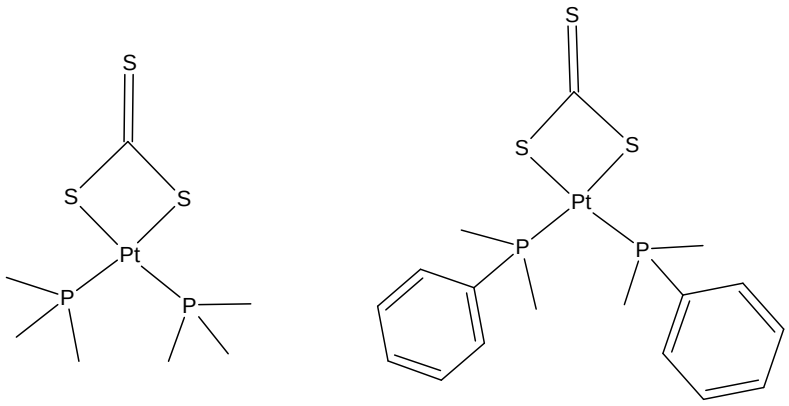

Figure 3.12 Related complexes by Aucott and coworkers.[14]

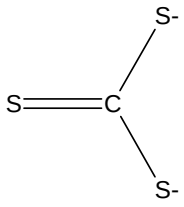

Figure 3.13a The SCS_2 ligand present in the structures by Aucott

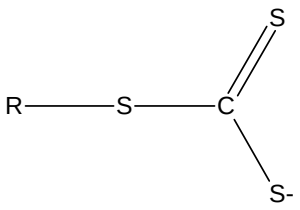

Figure 3.13b The R-SCS_2 fragment in compound **9** (R = CH_2-C_6H_5)

As mentioned earlier, Pt(1) is surrounded by six donor atoms. The bond separations Pt(1)-Cl(1) and Pt(1)-Cl(2) are 2.350(2) and 2.351(2) Å respectively and compare very well with the known average terminal Pt-Cl bond length of 2.324 Å.[13] In the two identical chelate rings, no significant deviations from the structures isolated by Aucott and coworkers could be found. The bond distances Pt(1)-S(2), Pt(1)-S(3), Pt(1)-S(4) and

Pt(1)-S(5) are all in the range of 2.319(2) to 2.367(2) Å, exhibiting much the same Pt-S separations as in the structures by Aucott, which have Pt-S bond lengths of between 2.342 and 2.354 Å.[14] For the coordinated CS_2 fragment, the C-S bond lengths are practically identical, ranging from 1.695(9) to 1.708(9) Å, which is comparable to Aucott's values, 1.655 to 1.756 Å. One would expect a slight change in the bond distances of C(8)-S(1) and C(9)-S(6), due to the bicovalent character of the sulphur atom. However, these separations are almost exactly the same as the CS_2 bonds, at 1.707(9) and 1.695(9) Å respectively. This implies delocalization of electron density in the complete -S-CS_2 fragment. Worth noting is the difference in bond distances for the other two C-S bonds, S(1)-C(7) and S(6)-C(10), which are appreciably larger at 1.838(9) and 1.834(9) Å respectively.

The angle between the two chlorine atoms and the metal, Cl(1)-Pt(1)-Cl(2), is 91.95(8)°, which, according to the CCDC database, is a normal value for a -S_2Pt(Cl)Cl complex such as this, which generally has average Cl-Pt-Cl angles of 92.65°. The S-Pt-Cl angles in the related compounds by Aucott[14] are in the range of 87.59° to 89.21°, deviating somewhat from the angles found in compound **9**, which are between 92.39(8)° and 96.37(8)°. This small difference could be explained by the fact that, in the complexes reported by Aucott,[14] only one SCS fragment is coordinated to the metal center, whereas in compound **9**, there are two fragments which forms four-membered chelate rings with the Pt(IV) center. These chelate rings are probably strained, which ultimately leads to distortion of the angles in the structure. The angles S(3)-Pt(1)-S(2) and S(4)-Pt(1)-S(5) are *ca* 74°, which agrees well with the angles found by Aucott, 73.29° and 73.80°. The C-S-Pt angles in the structures by Aucott range between 87.59° to 89.27°, correlating very well with these angles in compound **9**, between 86.3(3)° and 87.7(3)°. The outer S-C-S angles in **9** are between 120.1(5)° and 128.0(6)°, which compares well with the structures by Aucott that have average angles of 127.66°.[14] The inner S-C-S angles of the chelate rings in compound **9** have values of 111.9(5)° and 112.1(5)°, once again in accordance with the average value of the angles in the structures by Aucott, 110.56°.[14]

The packing of compound **9** along the b-axis is represented in Figure 3.14. From this diagram it is clear that, in the unit cell, two molecules of **9** pack closely together. These two molecules are surrounded by cavities which form during assembly and the dichloromethane molecules are encapsulated within these spaces. No significant intermolecular interactions are present.

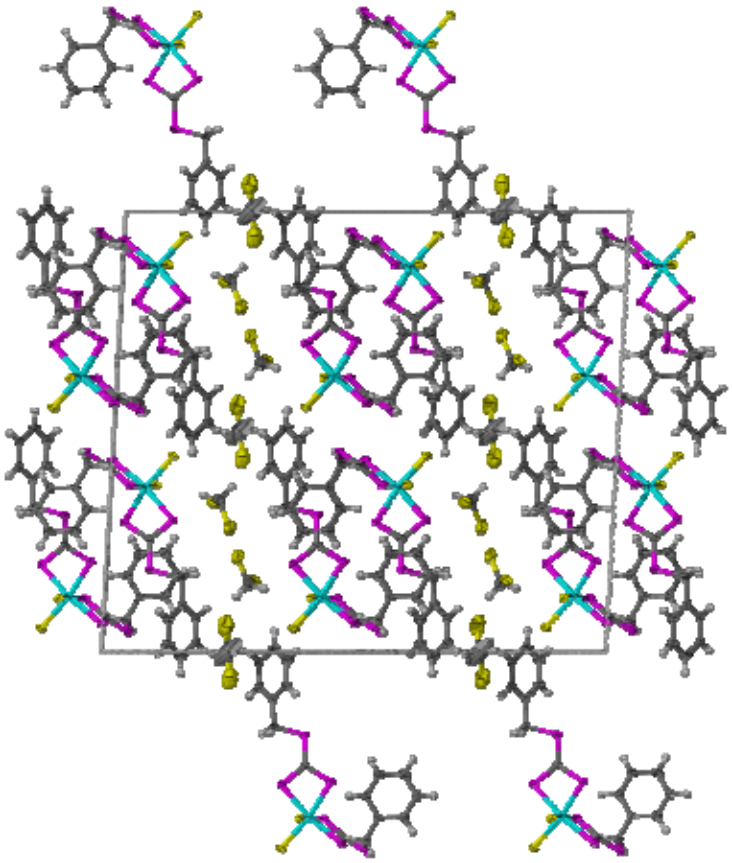

Figure 3.14 Packing of compound **9** along the b-axis, accentuating the location of the solvent molecules in the cavities which form during assembly.

Table 3.2 Selected bond lengths and angles for compound **9** with e.s.d.s in parentheses.

Bond lengths (Å)

Pt(1)-Cl(1)	2.350(2)	S(2)-C(8)	1.702(9)
Pt(1)-Cl(2)	2.351(2)	S(3)-C(8)	1.704(9)
Pt(1)-S(2)	2.360(2)	S(4)-C(9)	1.708(9)
Pt(1)-S(3)	2.327(2)	S(5)-C(9)	1.695(9)
Pt(1)-S(4)	2.319(2)	S(6)-C(9)	1.695(9)
Pt(1)-S(5)	2.367(2)	S(6)-C(10)	1.834(9)
S(1)-C(8)	1.707(9)	C(1)-C(7)	1.50(1)
S(1)-C(7)	1.838(9)	C(10)-C(11)	1.51(1)

Bond angles (°)

Cl(1)-Pt(1)-Cl(2)	91.95(8)	S(6)-C(9)-S(4)	120.1(5)
Cl(1)-Pt(1)-S(2)	93.10(8)	S(6)-C(9)-S(5)	128.0(6)
Cl(1)-Pt(1)-S(5)	96.37(8)	C(1)-C(7)-S(1)	111.9(6)
Cl(2)-Pt(1)-S(2)	95.52(8)	C(2)-C(1)-C(7)	120.6(8)
Cl(2)-Pt(1)-S(5)	92.39(8)	C(2)-C(3)-C(4)	121(1)
S(3)-Pt(1)-Cl(1)	90.26(8)	C(3)-C(2)-C(1)	120(1)
S(3)-Pt(1)-Cl(2)	169.54(8)	C(4)-C(5)-C(6)	121(1)
S(4)-Pt(1)-Cl(1)	170.34(8)	C(5)-C(4)-C(3)	119(1)
S(4)-Pt(1)-Cl(2)	88.92(8)	C(5)-C(6)-C(1)	120(1)
S(2)-Pt(1)-S(5)	167.45(8)	C(6)-C(1)-C(2)	118.8(9)
S(3)-Pt(1)-S(2)	74.15(8)	C(6)-C(1)-C(7)	120.6(8)
S(3)-Pt(1)-S(5)	97.53(8)	C(8)-S(1)-C(7)	104.3(4)
S(4)-Pt(1)-S(2)	96.40(8)	C(9)-S(6)-C(10)	102.9(4)
S(4)-Pt(1)-S(3)	90.62(8)	C(11)-C(10)-S(6)	104.6(6)
S(4)-Pt(1)-S(5)	73.98(8)	C(12)-C(11)-C(16)	118.0(9)
C(8)-S(2)-Pt(1)	86.3(3)	C(12)-C(11)-C(10)	121.1(9)
C(8)-S(3)-Pt(1)	87.4(3)	C(13)-C(12)-C(11)	121.2(9)
C(9)-S(4)-Pt(1)	87.7(3)	C(13)-C(14)-C(15)	120(1)
C(9)-S(5)-Pt(1)	86.4(3)	C(14)-C(13)-C(12)	120(1)
S(2)-C(8)-S(1)	120.7(5)	C(15)-C(16)-C(11)	121(1)
S(2)-C(8)-S(3)	112.1(5)	C(16)-C(11)-C(10)	120.9(9)
S(3)-C(8)-S(1)	127.1(5)	C(16)-C(15)-C(14)	120(1)
S(5)-C(9)-S(4)	111.9(5)		

3.3 Conclusions and possible future work

We hoped to discover a whole series of new complexes of Pt(IV) with sulphur ligands that are generally used in polymerization reactions. All of these ligands differ only by a small amount with regard to one another, and it was thus planned to isolate a range of complexes with these ligands and test their properties and anti-cancer activity. Unfortunately, only one compound with a sulphur ligand (**I**) could be isolated as single crystals. We attempted reactions with another ligand (**II**) but it cannot be said with certainty that the conversion did in fact take place. However, we are pleased with the synthesis of the Pt(IV) complex since it is the first of its kind, and we hope to continue research regarding this and other similar ligands.

With gold as metal center for coordination reactions, the idea was to synthesize a complex of this metal with an unusual P-Se heterocycle (ligand **III**). Due to the inability of the final compound to crystallize and the fact that NMR could not prove its conversion beyond any doubt, it cannot be said with certainty that the reaction was successful. We then decided to shift our focus towards the same sulphur ligands that we used with platinum, and we could isolate a previously reported compound of Au(I,III) with the rearranged ligand **I**. Even though this was not what we planned, it was still an interesting compound to study, especially when it became clear that the compound in the literature was not clearly illustrated from a chemist's point of view. Future work in this regard includes continued efforts to crystallize the suspected Au compound with the P-Se heterocycle, as well as varying reaction conditions to try and isolate a different compound of gold with the sulphur ligands.

3.4 Experimental

3.4.1 General procedures and instruments

Reactions were carried out under argon using standard Schlenk- and vacuum-line techniques, unless otherwise stated. All glassware was dried at 110°C and cooled under vacuum before use. *n*-Pentane, *n*-hexane, diethyl ether and tetrahydrofuran (THF) were distilled under nitrogen from sodium benzophenone ketyl, and dichloromethane from CaH_2. [AuCl(tht)] was prepared as described in the literature.[15] Crystallographic data sets for all compounds were collected on a Bruker SMART Apex CCD diffractometer with graphite monochromated Mo-Kα radiation (λ = 0.71073 Å). Data reduction was carried out with standard methods from the software package Bruker SAINT. The crystal structures were solved and refined using SHELX-97 within the X-seed environment. Figures were generated with X-seed and POV-Ray for Windows, with the displacement ellipsoids at the probability level specified in the text.

3.4.2 Preparations and procedures

3.4.2.1 Synthesis of

$[Au(I)Cl(S(CH_2C_6H_5)_2)][Au(III)Cl_3(S(CH_2C_6H_5)_2]$ (8)

In 10 ml of CH_2Cl_2, 0.104 g (0.260 mmol) $S_6C_{16}H_{14}$ (**I**) and 0.347 g (1.10 mol) $AuCl(SC_4H_8)$ was dissolved and then stirred for 3 hours. The colour of the solution changed immediately from bright yellow to light orange. A TLC in *n*-hexane was done at the beginning, and again after 3 hours to ensure that all starting reagents reacted. The CH_2Cl_2 was removed *in vacuo*, and the remaining brown solid was triturated 5 times with *n*-pentane, each time removing any remaining solvent *in vacuo*, to ensure that all CH_2Cl_2 had been removed. After the last vacuum removal the solid was left to dry *in vacuo* for a further 2 hours. Yield: **0.197 g** (66.3 %)

Crystallization of the compound was attempted by dissolving it in a minimum amount of CH_2Cl_2 (which turned out to be quite a lot of solvent due to the insolubility of the product). It was then covered with a thin layer of *n*-pentane, and put in the fridge for a few weeks, but with no results. In the end, the crystallization method that we found most

successful was to dissolve the compound in a minimum amount of CH_2Cl_2 in an NMR tube. This was then put inside a Schlenk tube with a small volume of *n*-pentane, and it was cooled down. A crystal suitable for single crystal X-ray analysis grew after 6 weeks.

3.4.2.2 Synthesis of $PtCl_2(S_3C_8H_7)_2$ (9)

In 80 ml of distilled H_2O, 5.00 g (12.0 mmol) K_2PtCl_4 was dissolved, and 55 ml *n*-propanol, 10 ml 1,5-cyclooctadiene (COD), as well as 0.0750 g (0.400 mmol) $SnCl_2$ was added. The resulting brownish mixture was stirred for 48 hours, at which time the solution was almost colourless, and a whitish precipitate had formed. The solid was filtered, washed with 50 ml distilled H_2O as well as 10 ml absolute ethanol, then left to dry at room temperature for 3 days. Yield $PtCl_2$(COD): **3.93 g** (87.6 %).

To a solution of 0.104 g (0.280 mmol) $PtCl_2$(COD) in 15 ml CH_2Cl_2 was added 0.110 g (0.280 mmol) of ligand **I** and then stirred for 2 hours. The clear yellow solution that formed was concentrated *in vacuo* to approximately 2 ml, at which time 15 ml freshly distilled diethyl ether was added. A fine white powder formed. The solvents were removed *in vacuo*, and the light yellow solid was dried *in vacuo* for a further 2 hours. Yield: **0.153 g** (82.21%)

3.4.2.3 Attempted synthesis of $PtCl_2(S_6C_{10}H_6)$

To a solution of 0.10 g (0.28 mmol) $PtCl_2$(COD) in 15 ml CH_2Cl_2 was added 0.089 g (0.28 mmol) of ligand **II** ($S_6C_{10}H_6$). The colour of the solution changed from light yellow to red. The solution was stirred for 2 hours, after which time it was evaporated to a volume of about 3 ml. Diethyl ether (15 ml) was added and a reddish solid formed. The solvent was removed *in vacuo* and left to dry at the vacuum pump for 3 hours. The product which formed showed traces of decomposition, so it was decided to try another starting reagent.

In 10 ml of distilled H_2O, 0.10 g (0.24 mmol) K_2PtCl_4 was dissolved and stirred for 30 minutes, followed by the addition of 0.085 g (0.27 mmol) of **II** in 10 ml acetone. The solution was stirred for 48 hours, during which time the colour changed from a red

solution to a very dark brown suspension. The solvents were removed *in vacuo*, and the solid was washed twice with diethyl ether. The product was then dissolved in CH_2Cl_2 and the black solid which formed was filtered off. Once again the solvent was removed and the remaining product was left to dry *in vacuo* for 3 hours. The product was dark brown, almost black, and seemed to show traces of decomposition.

The reaction was repeated, but this time the solution was only stirred for 2 hours, at which time the solution had changed colour from red to reddish brown. The solvent was removed *in vacuo,* and the solid washed twice with CH_2Cl_2 and twice with diethyl ether. The solid turned a light red-brown colour, and it was left to dry *in vacuo* for 2 hours. Yield: **0.128 g** (87.7 %).

We attempted crystallization of the product by dissolving a small amount of the compound in CH_2Cl_2 in a crystallization tube and layering it with *n*-pentane. This was then put in the fridge. Unfortunately, this proved to be an unsuccessful method. We attempted crystallization again, with various other crystallization methods, but with no success.

3.4.2.4 Synthesis of ligand I, $S_6C_{16}H_{14}$

This ligand was prepared by a modified method of the one described by Weber *et al.*[16] In 50 ml of water, 7.3 g (0.13 mol) KOH was dissolved and stirred until the solution had cooled. To this solution, 12.4 g (0.10 mol) of benzyl mercaptan was added dropwise and stirred until all solids had dissolved, whereafter 2 drops of Aliquat 336 was added. Next, 7.6 g (0.10 mol) carbon disulfide was added and the solution was stirred for 30 minutes. *p*-Tosyl chloride (9.6 g, 0.050 mol) was dissolved in 50 ml acetone and added to the previous solution and stirred for one hour, during which time a bright yellow solid formed. The mixture was left to evaporate in the fumehood for 2 hours to remove the excess acetone. The remaining yellow solid was filtered and washed with distilled water, and the product was recrystallized from hot acetone and left in the fridge overnight to crystallize. The light yellow crystals which formed were filtered and washed with hexane and left to dry at room temperature for a few hours. Yield: **6.02 g** (30.1 %).

Table 3.3 Crystal data and structure refinement parameters of compounds **8** and **9**

	8	**9**
Empirical formula	$AuCl_2SC_{14}H_{14}$	$PtS_6Cl_5C_{17.5}H_{17}$
M_r	482.18	792.01
Temp. (K)	100(2)	100(2)
Wavelength (Å)	0.71073	0.71073
Crystal system	monoclinic	monoclinic
Space group	$P2_1/c$	$C2/c$
a (Å)	5.610(1)	24.176(3)
b (Å)	19.874(4)	7.7718(9)
c (Å)	13.241(3)	27.593(3)
α (°)	90.00	90.00
β (°)	93.700(4)	93.205(2)
γ (°)	90.00	90.00
Volume (Å^3)	1473.2(5)	5176 (1)
Z	4	8
d_{calcd} (g/cm^3)	2.174	2.033
Absorption coefficient (μ, mm^{-1})	10.469	6.428
Absorption correction	none	none
F(000)	908	3048
Crystal size (mm^3)	0.20 × 0.10 × 0.08	0.09 × 0.08 × 0.06
θ-range for data collection (°)	1.85 to 26.40	1.69 to 26.40
No. of reflections collected	8457	14652
No. independemt reflections	2997	5273
Refinement method	Full-matrix least-squares on F^2	Full-matrix least-squares on F^2
Data / restraints / parameters	2575 / 0 / 173	4968 / 0 / 267
Goof on F_2	1.053	1.315
Final *R* indices [$I > 2\sigma(I)$]	*R1* = 0.0336	*R1* = 0.0575
	wR2 = 0.0660	*wR2* = 0.1208
R-indices (all data)	*R1* = 0.0425	*R1* = 0.0610
	wR2 = 0.0686	*wR2* = 0.1221

1. Roundhill DM. *Comprehensive Coordination Chemistry: The Synthesis, Reactions, Properties & Applications of Coordination Compounds*, Vol. 5, Pergamon Press, Oxford, 1987; 353
2. Brabec V, Kasparkova J. *Drug Resist. Update* 2002; **5**: 147-161.
3. Marzano C, Trevisan A, Giovagnini L, Fregona D. *Toxicol. in Vitro* 2002; **16**: 413-419.
4. Fregona D, Giovagnini L, Ronconi L et al. *J. Inorg. Biochem.* 2003; **93**: 181-189.
5. Cras JA, Willemes J. *Comprehensive Coordination Chemistry: The Synthesis, Reactions, Properties & Applications of Coordination Compounds*, Vol. 2, Pergamon Press, Oxford, 1987; 517-591
6. Fricker SP. Medicinal chemistry of gold compounds. **In**: Patai S, Rappoport Z (eds.), *The chemistry of organic derivates of gold and silver*. John Wiley & Sons, Ltd, 1999; 641-659.
7. Shaw III CF. *Chem. Rev.* 1999; **99**: 2589-2600.
8. Tiekink ERT. *Crit. Rev. Oncol. Hematol.* 2002; **42**: 225-248.
9. Shaw III CF. The Biochemistry of Gold. **In**: Schmidbaur H (ed.), *Progress in Chemistry, Biochemistry and Technology*. John Wiley & Sons, Ltd, 1999; 260-298.
10. Ronconi L, Maccata C, Barreca D, Saini R, Zancato M, Fregona D. *Polyhedron* 2005; **24**: 521-531.
11. Puddephatt RJ. *Comprehensive Coordination Chemistry: The Synthesis, Reactions, Properties & Applications of Coordination Compounds*, Vol. 5, Pergamon Press, Oxford, 1987; 863-897
12. Tanino H, Takahashi K, Tajima M, Kato M, Yao T. *J. Phys. Rev. B* 1988; **38**: 8327-8335.
13. Orpen AG, Brammer L. *J. Chem. Soc. Dalton Trans.* 1989: S1-S83.
14. Aucott SA, Slawin AMZ, Woollins JD. *Polyhedron* 2000; **19**: 499.
15. Haas A, Helmbrecht J, Niemann U. Handbuch der Präparativen Anorganischen Chemie. **In**: Brauer G (ed.), Ferdinand Enke Verlag, Stuttgard 1978; 1014.
16. Weber WG, McLeary JB, Sanderson RD. *Tetrahedron Lett.* 2006; **47**: 4771-4774.